Spatial Information Technology for Intelligent Watershed Reservoir

Dr. Tien-Yin Chou

jimmy@gis.tw

Director/Lifetime Distinguished Professor, GIS Research Center, Feng Chia University, Taiwan

Chair, Open Geospatial Consortium (OGC) Asia Forum

Secretary-General, Asia-Pacific Federation for Information Technology in Agriculture (APFITA)

Real World – Complex Information...

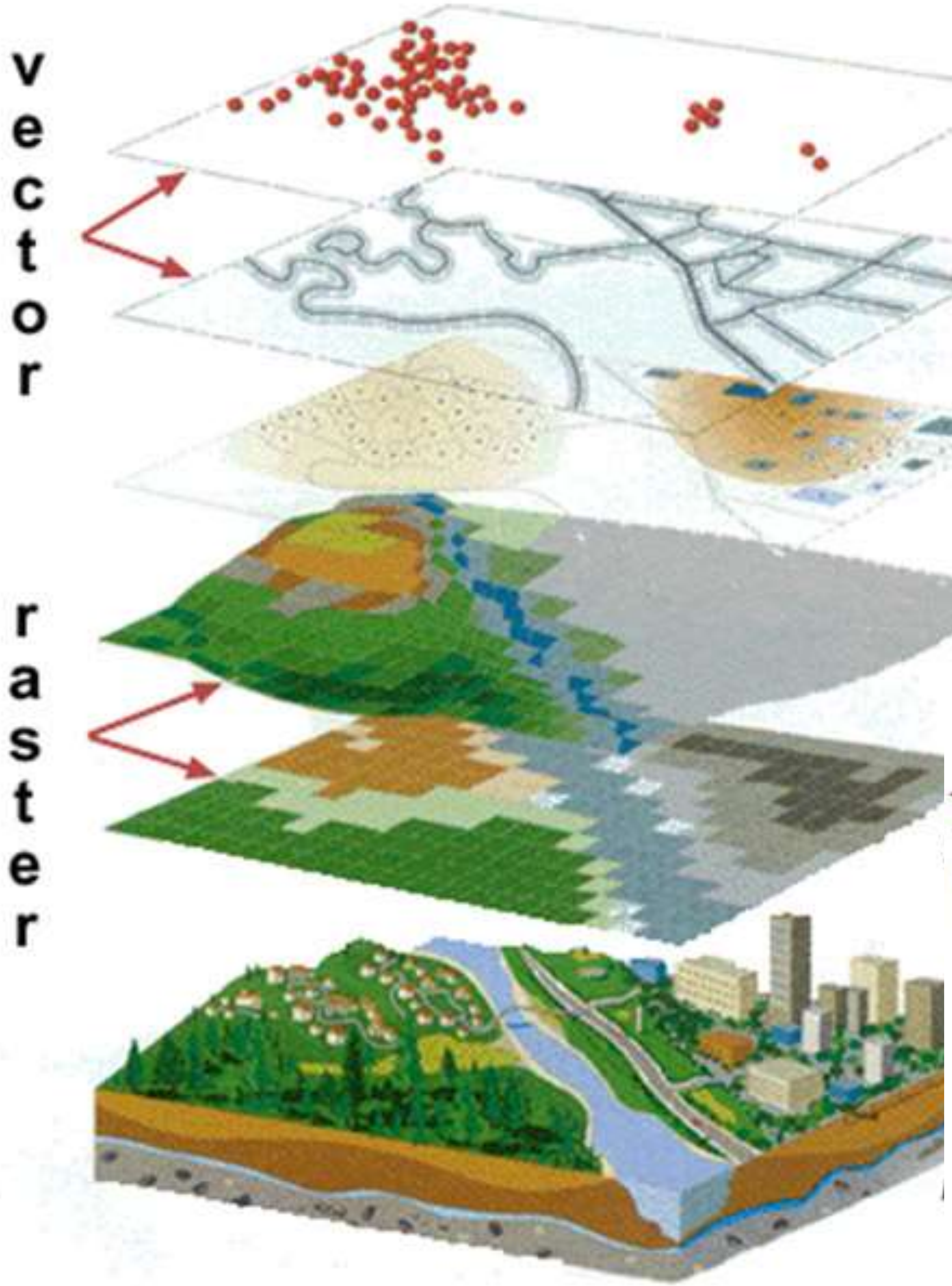

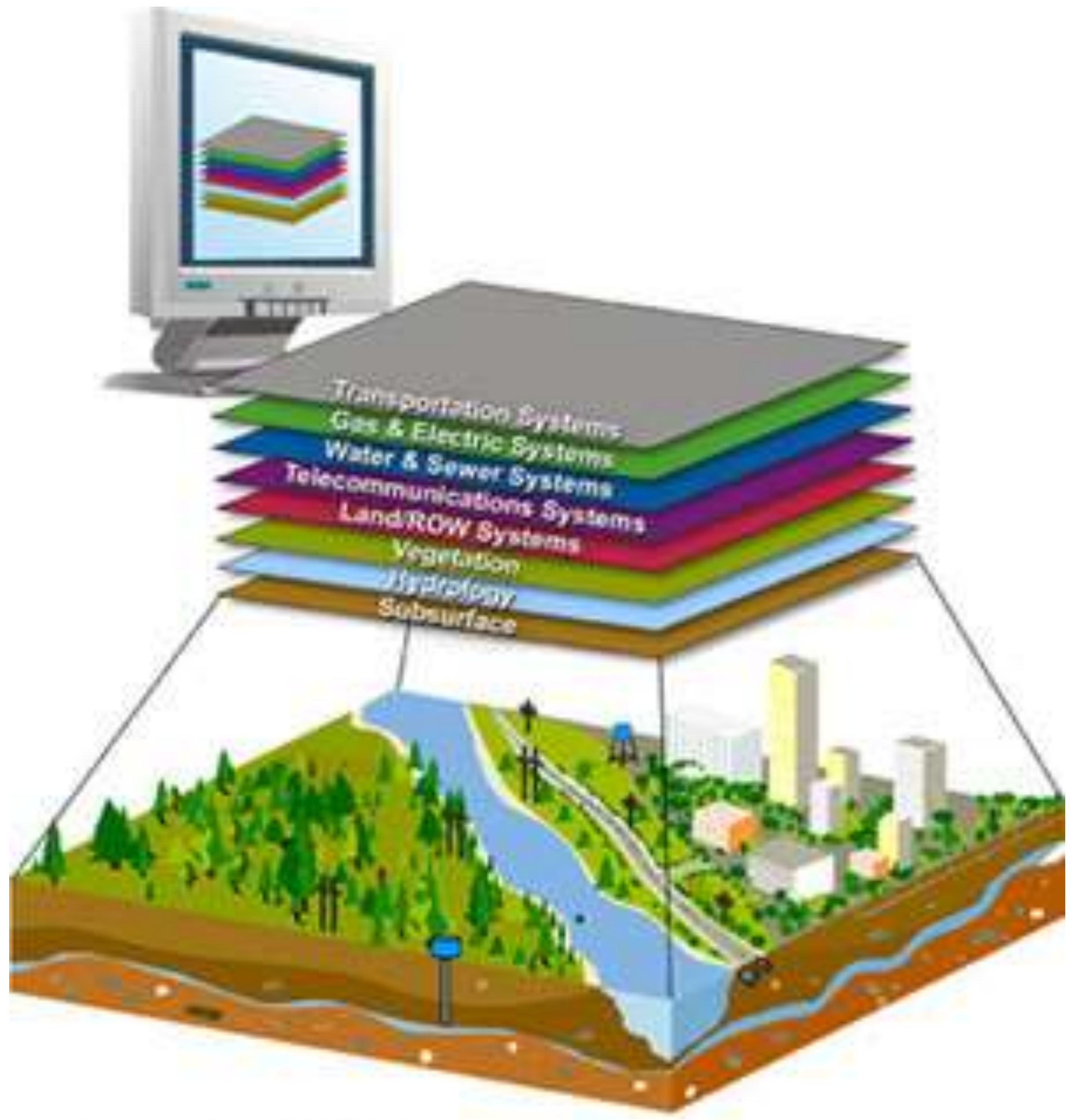

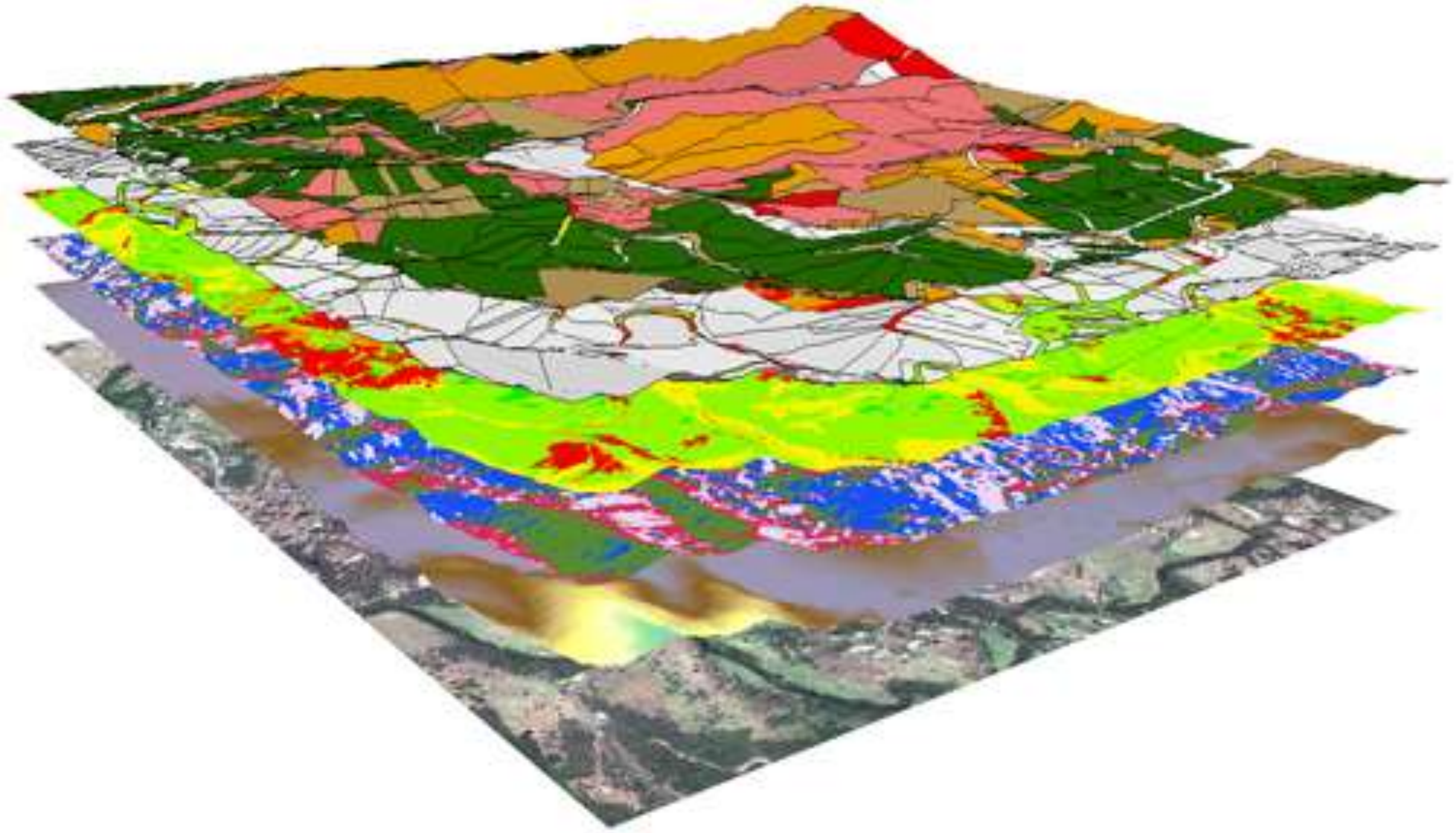

Multi-Scale & Multi-Dimensional

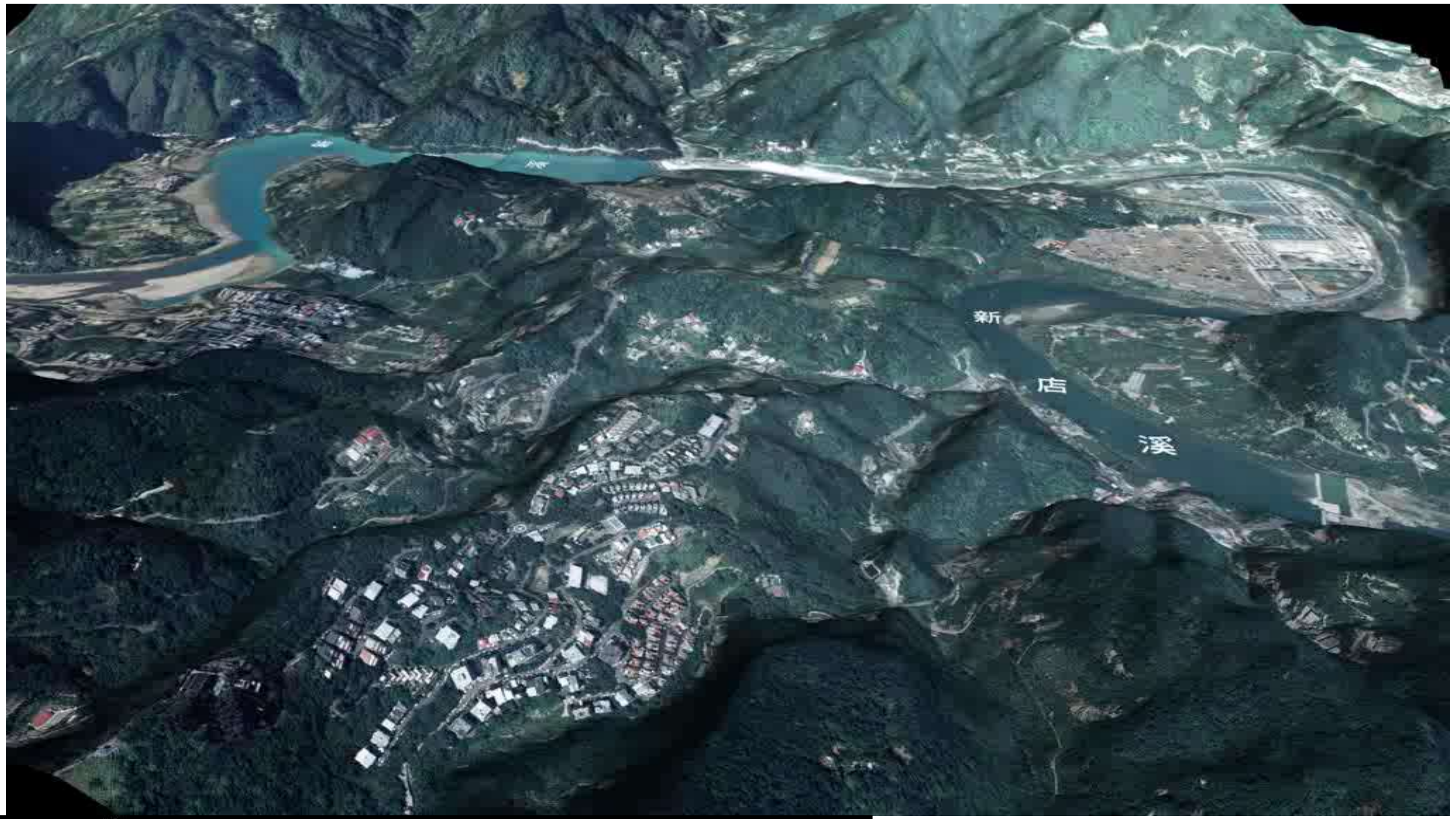

What we've concerned

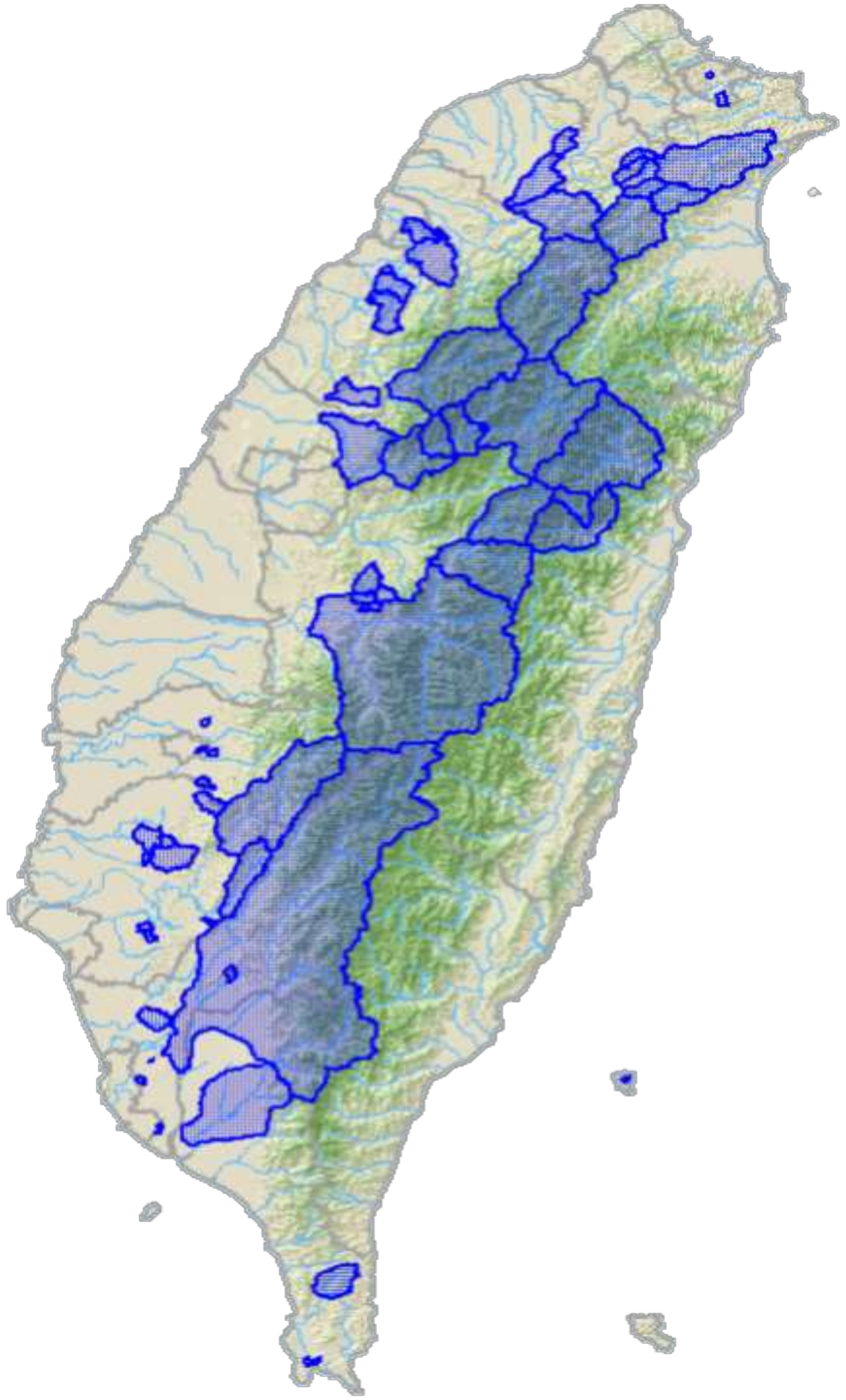

- Environmental monitoring
  - Most area in Taiwan is fragile and sensitive.
  - Various equipment used to detect and monitor all kinds of environmental characteristics

Smart AIoT

Slope Land Disaster Monitoring and Decision-Making

Sensors

>Sensor Web Enablement

>Wireless Sensor Network

>OGC SensorThings API

Satellite
Fiber optic
5G/4G
LoRa
NB-IoT
MicroWave

LoRa

Emergency Operation Center

Alert

Cross-platform information integration application

Debris flow / Sediment / Ecosystem
Landslide / Bridge

Disaster prevention monitoring

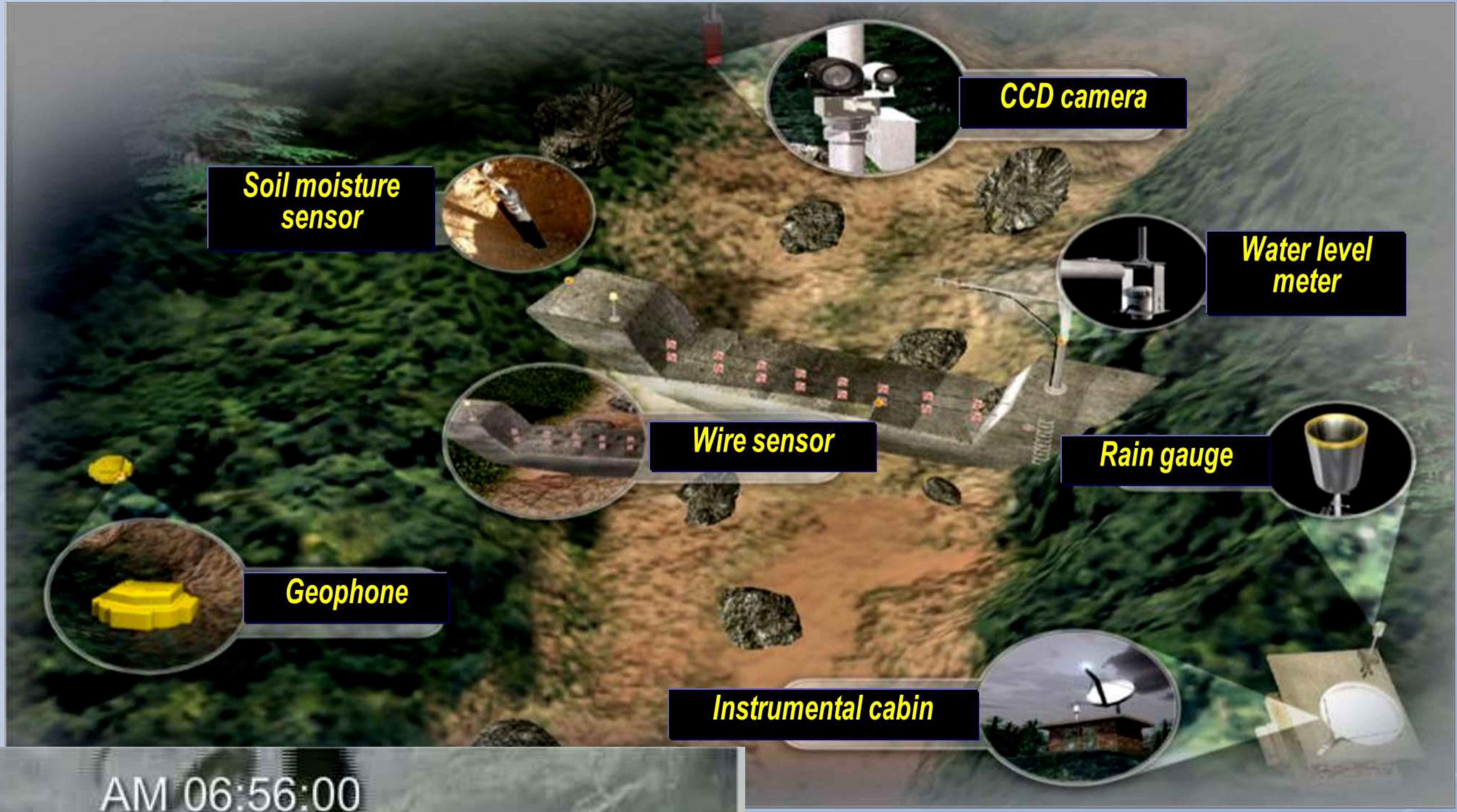
CCD camera
Soil moisture sensor
Water level meter
Wire sensor
Rain gauge
Geophone
Instrumental cabin

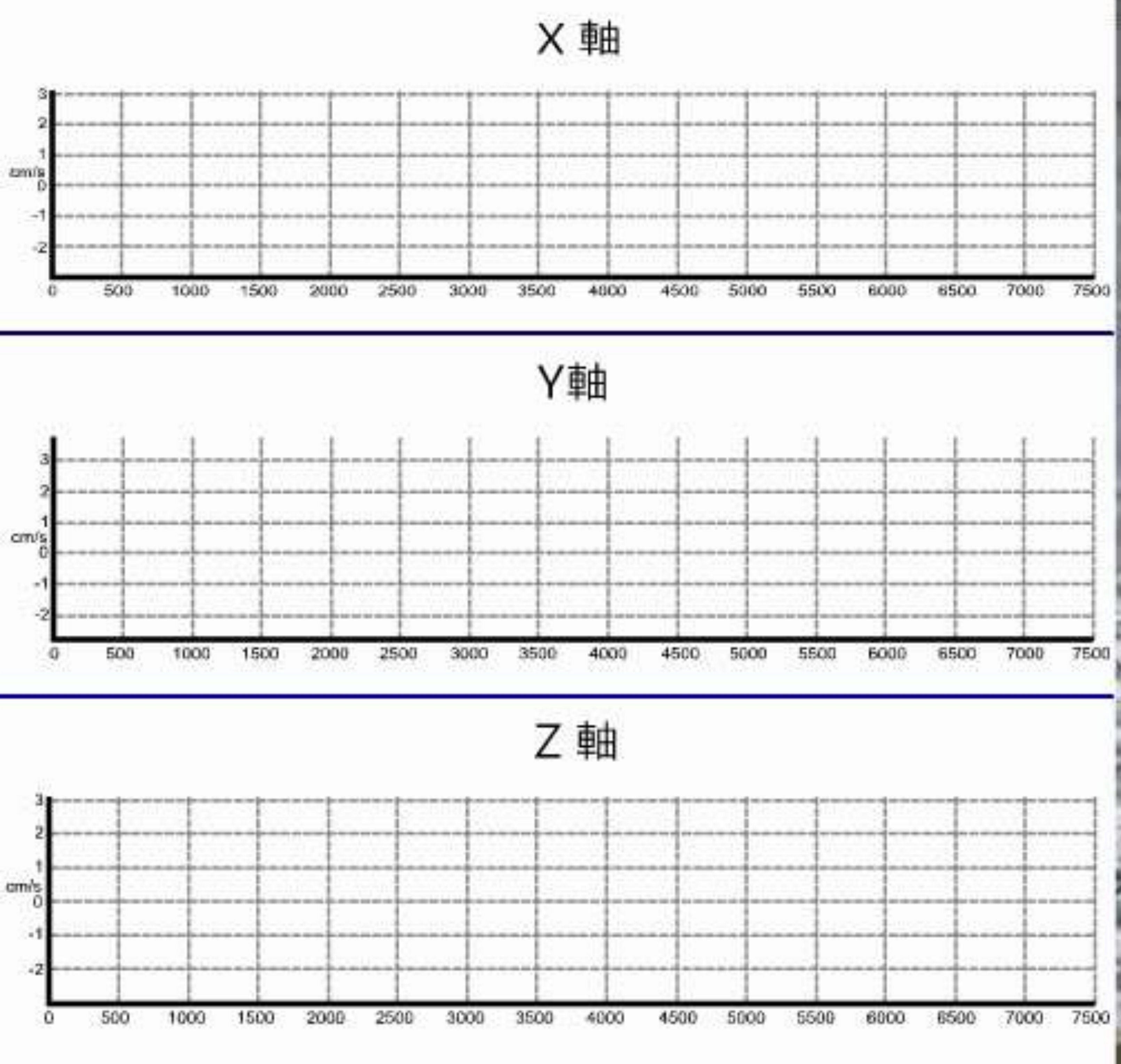
X 軸
Y軸
Z 軸
cm/s


AM 06:56:00
水土保持局

Slope Land Disaster Management Scenario, OGC Disaster Pilot

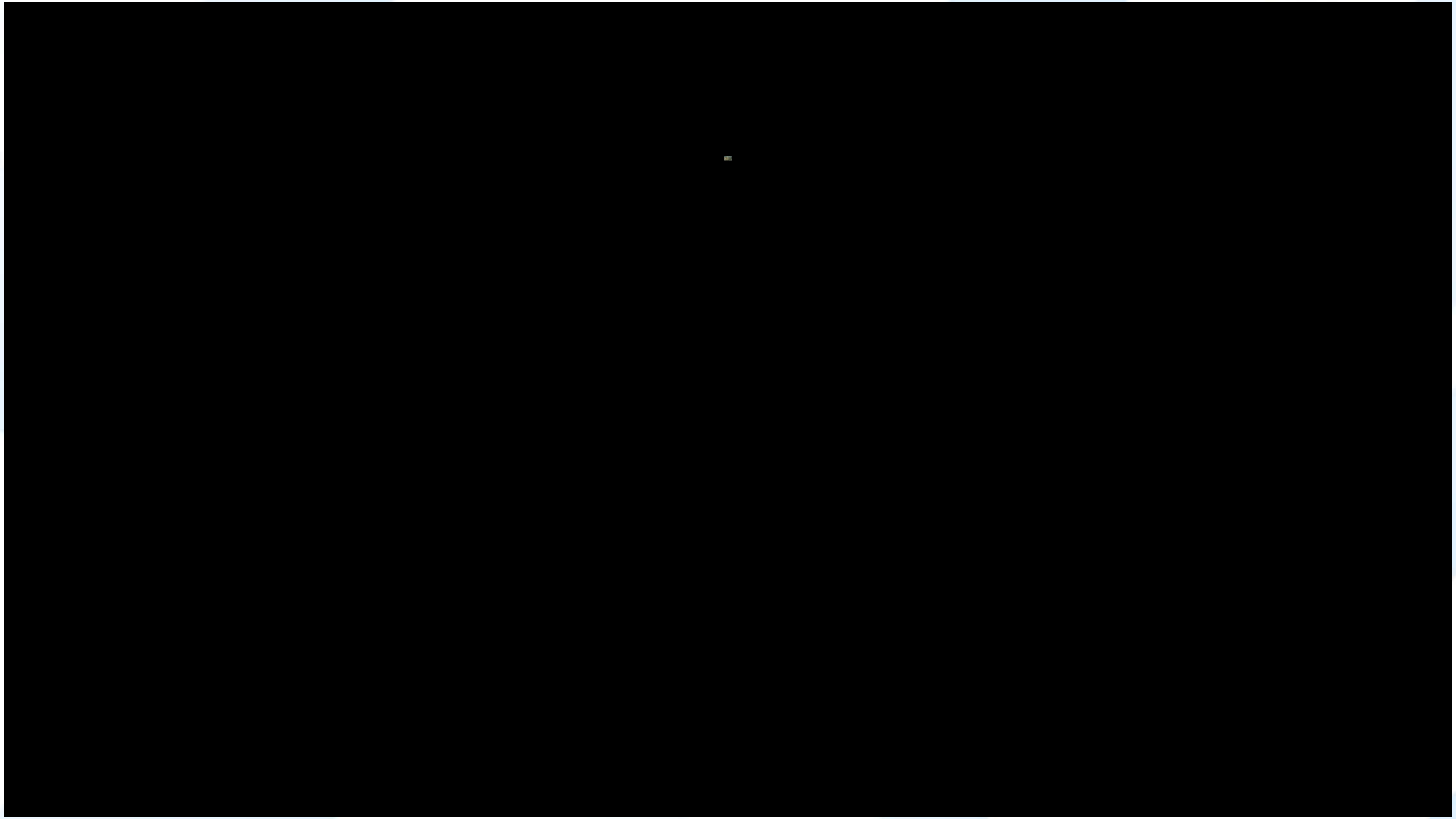

Water Resources Monitoring and Management

Smart AIoT

Intelligent Cloud-based IoT Water Information Platform

By integrating diversified data from cloud-based IoT network, the platform perform the stereoscopic water information assessment and big data analysis, providing significant elements for decision-making.

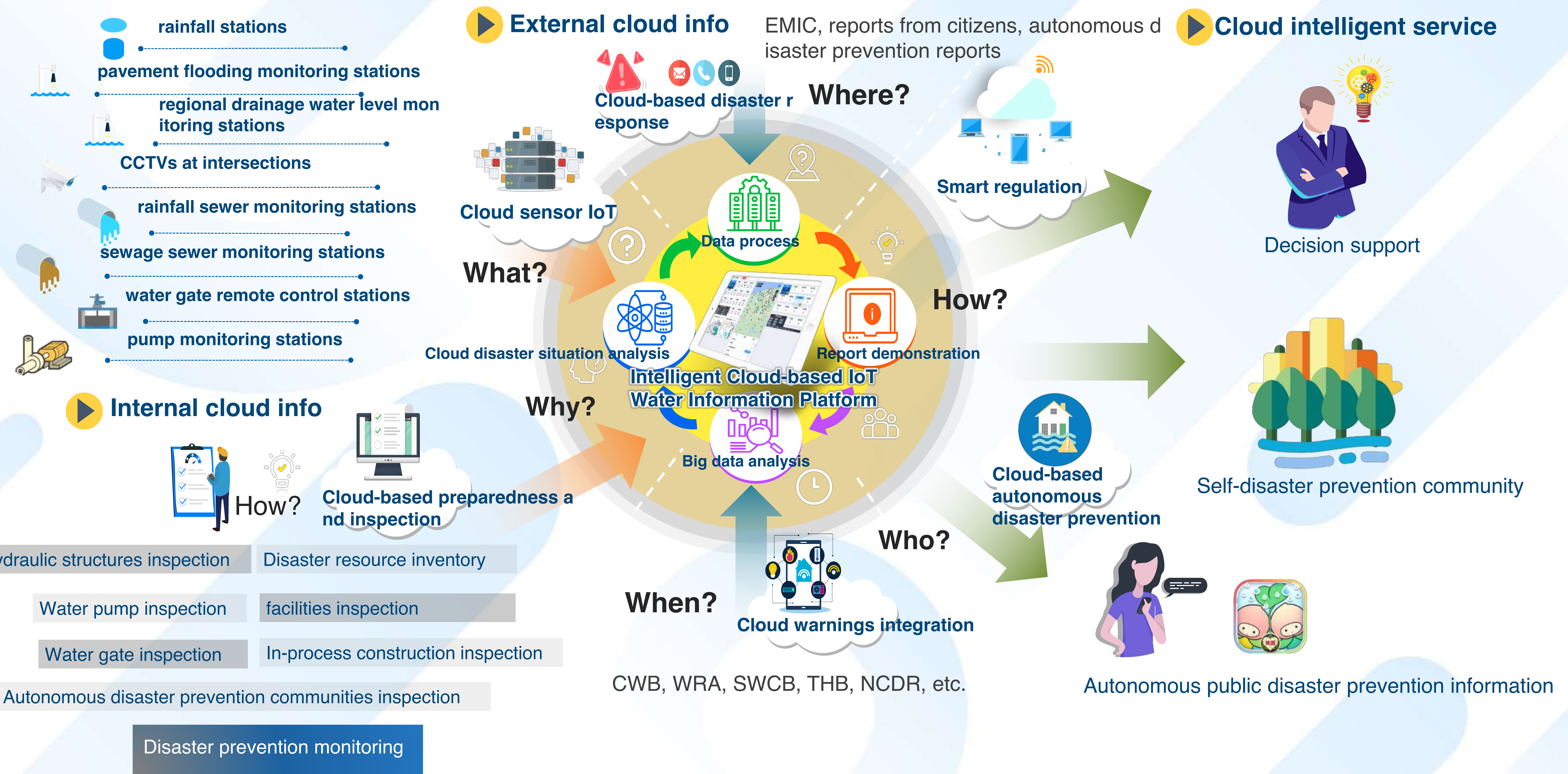

River Basin Monitoring

Security for equipments

Vehicles monitoring on the river bed

illegal quarrying monitoring

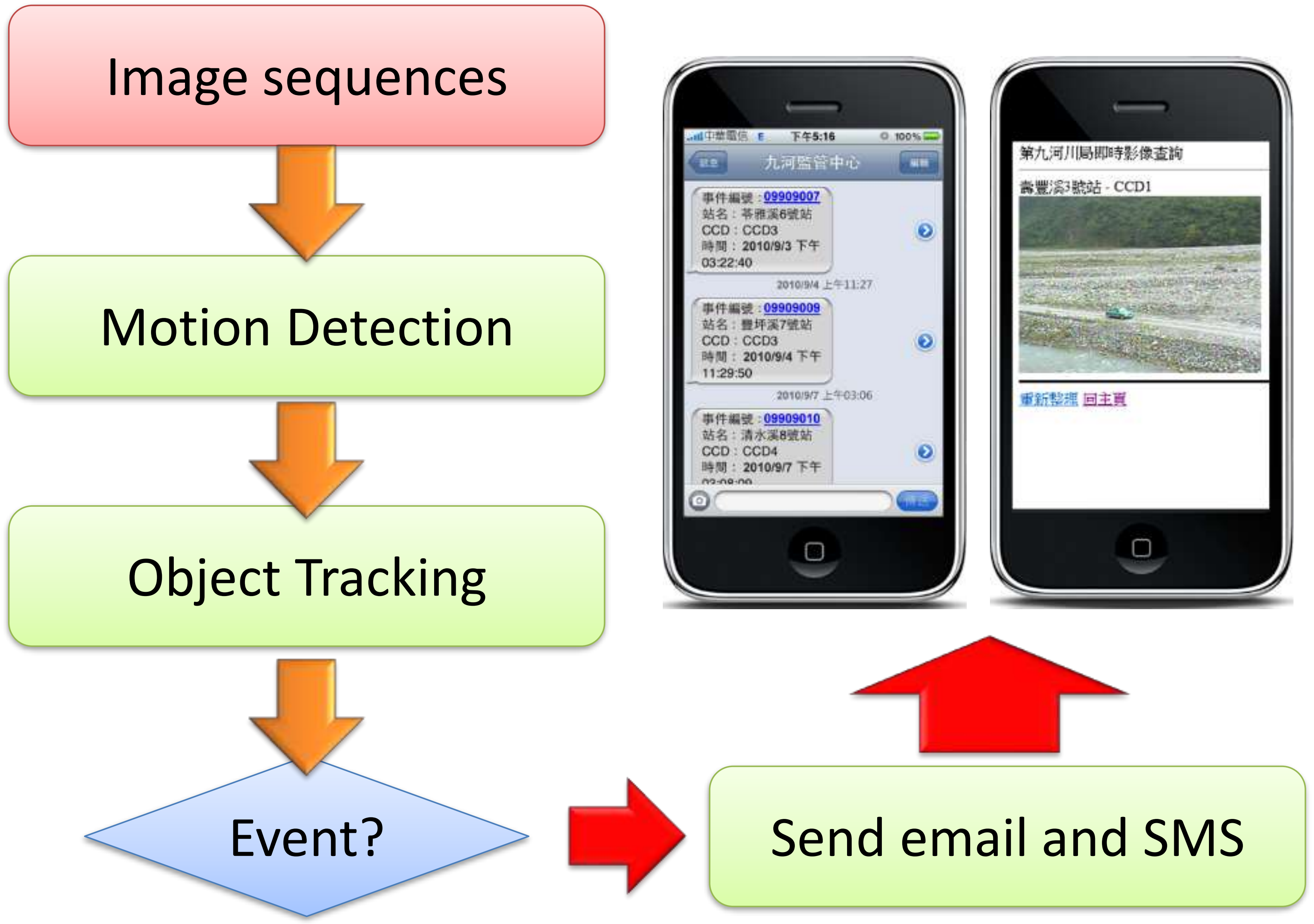

Supplementary Monitoring System

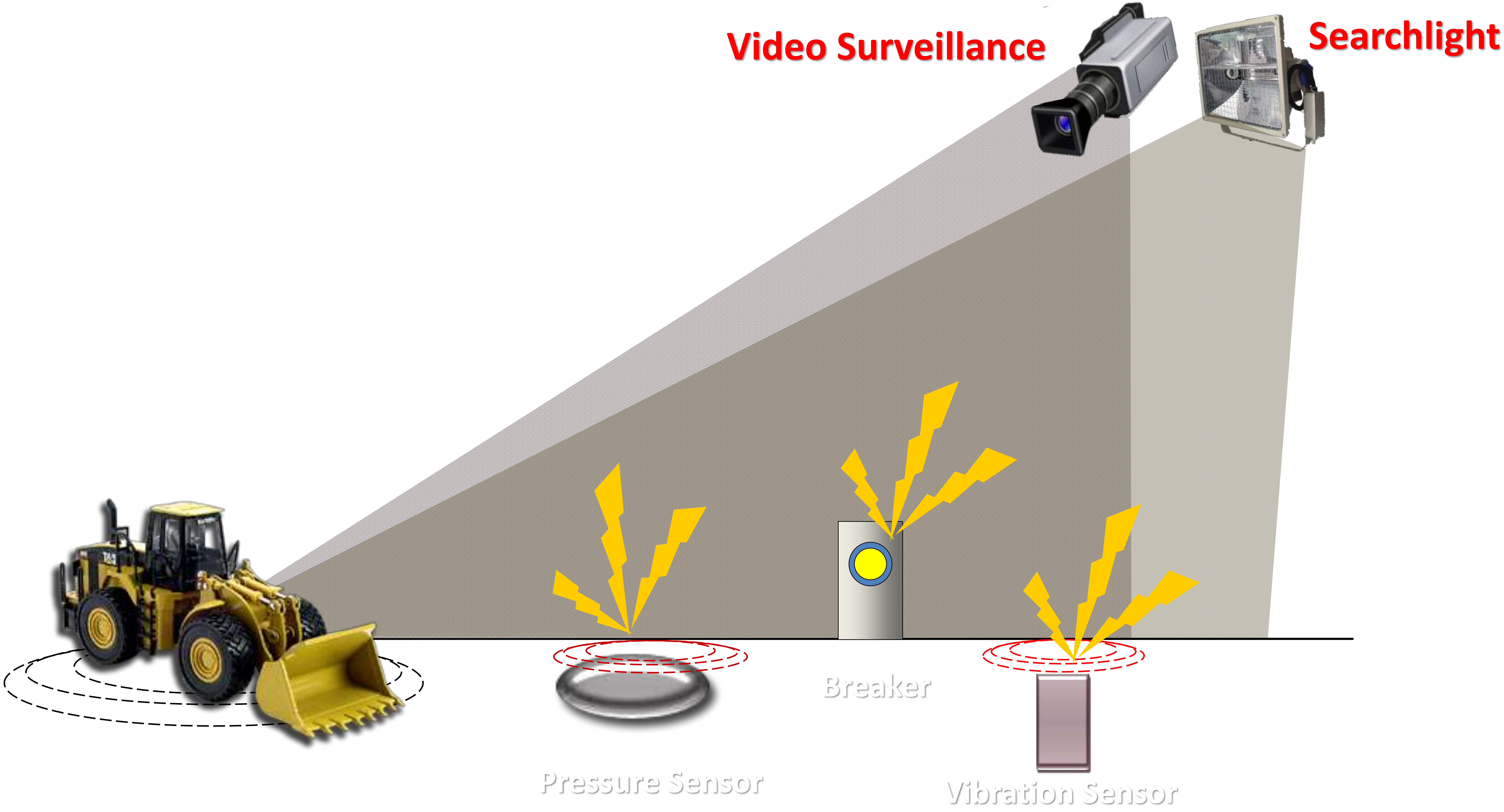

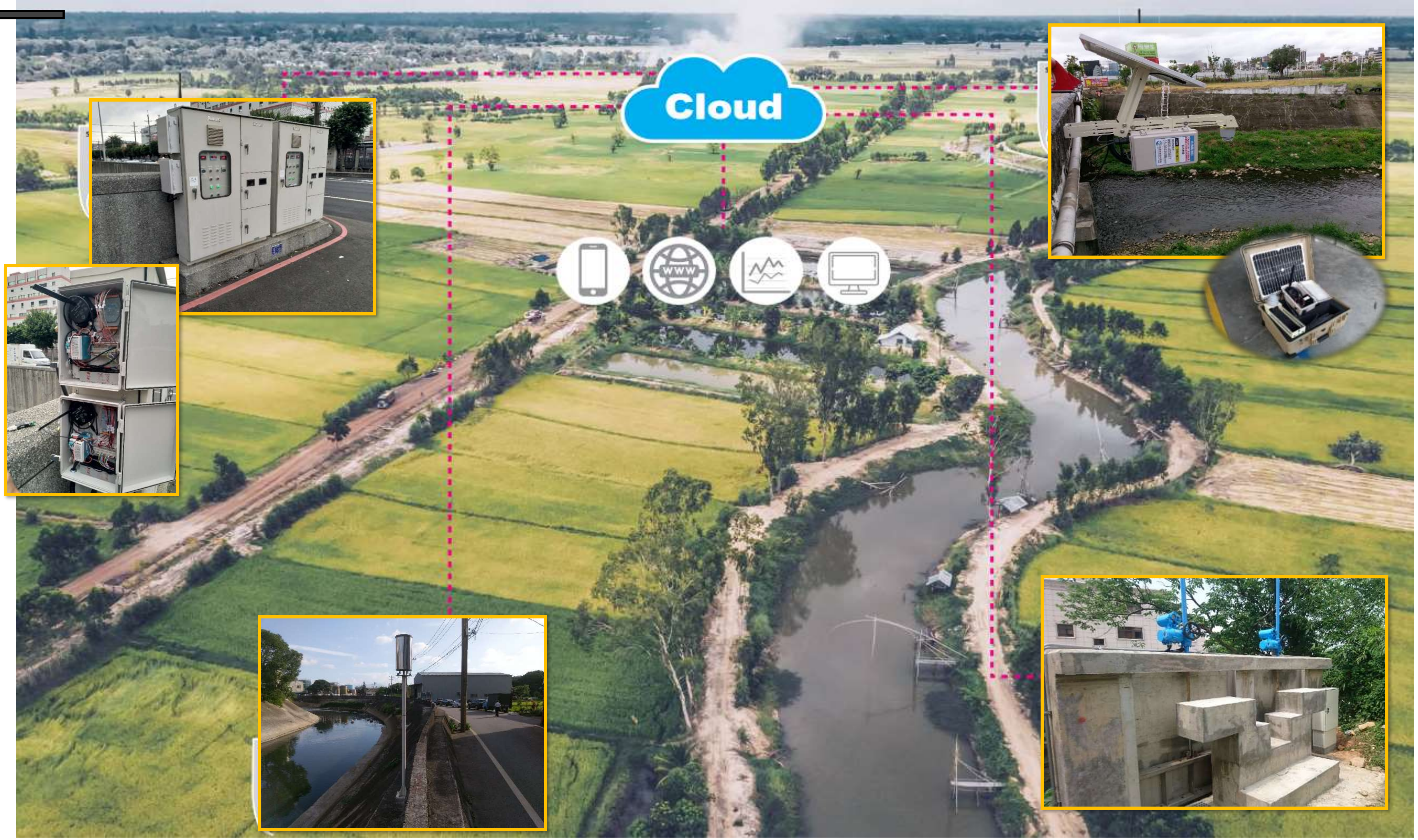
Cloud

Common Alerting Protocol Platform

The Common Alerting Protocol uniforms the structure of the disaster alerts, accelerating the exchange of disaster mitigation information between authorities and maximizing the effectiveness of disaster response.

AIoT of Smart Cities

Total solutions: GIS, smart disaster mitigation, smart governance, decision-making support, innovative application

Customized Sensors

The main structure of AIoT

AI training mode

Structure
Water

Provide a full range of integrated solutions

Floods

Why?

On 13th August 2019, it once rained 109.5mm in an hour in Linkou Dist. This maximum hourly precipitation exceeds the extreme rainfall in 50-year recurrence interval.

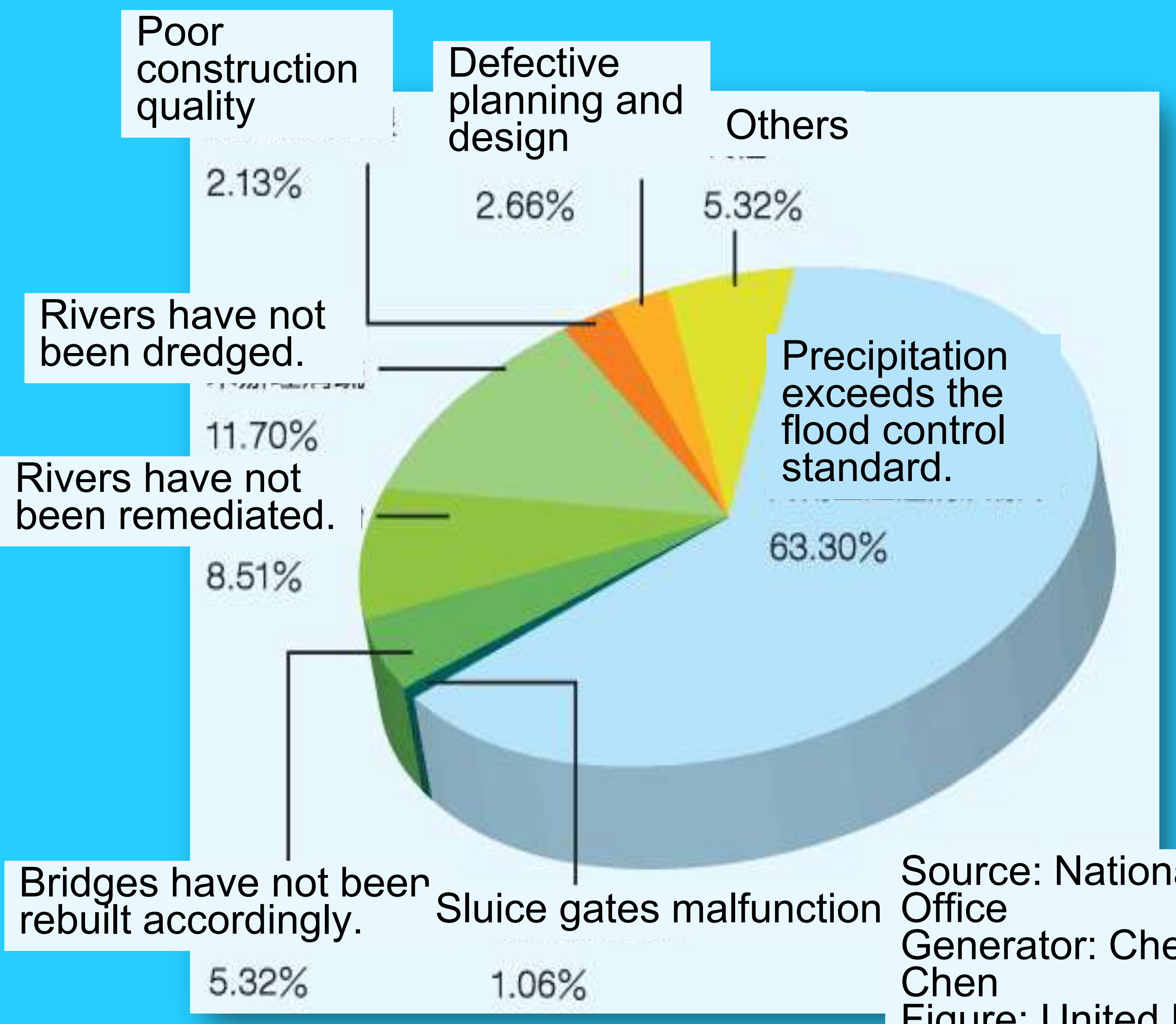

Source: National Audit Office
Generator: Cheng-Yen, Chen
Figure: United Evening News

AI can help?

- To judge when the flooding events will occur through below AI technologies:

- AI forecast
- Rainfall forecast
- Speed of water level rising

Solutions

Properly manage diversified water information including internal and external water.

Floods Detection Dashboard

Timeline of flooding history

Report of flooding event

Location map of sensors

Flooding sensor

Hyetograph

Sewer water level

Floods prediction

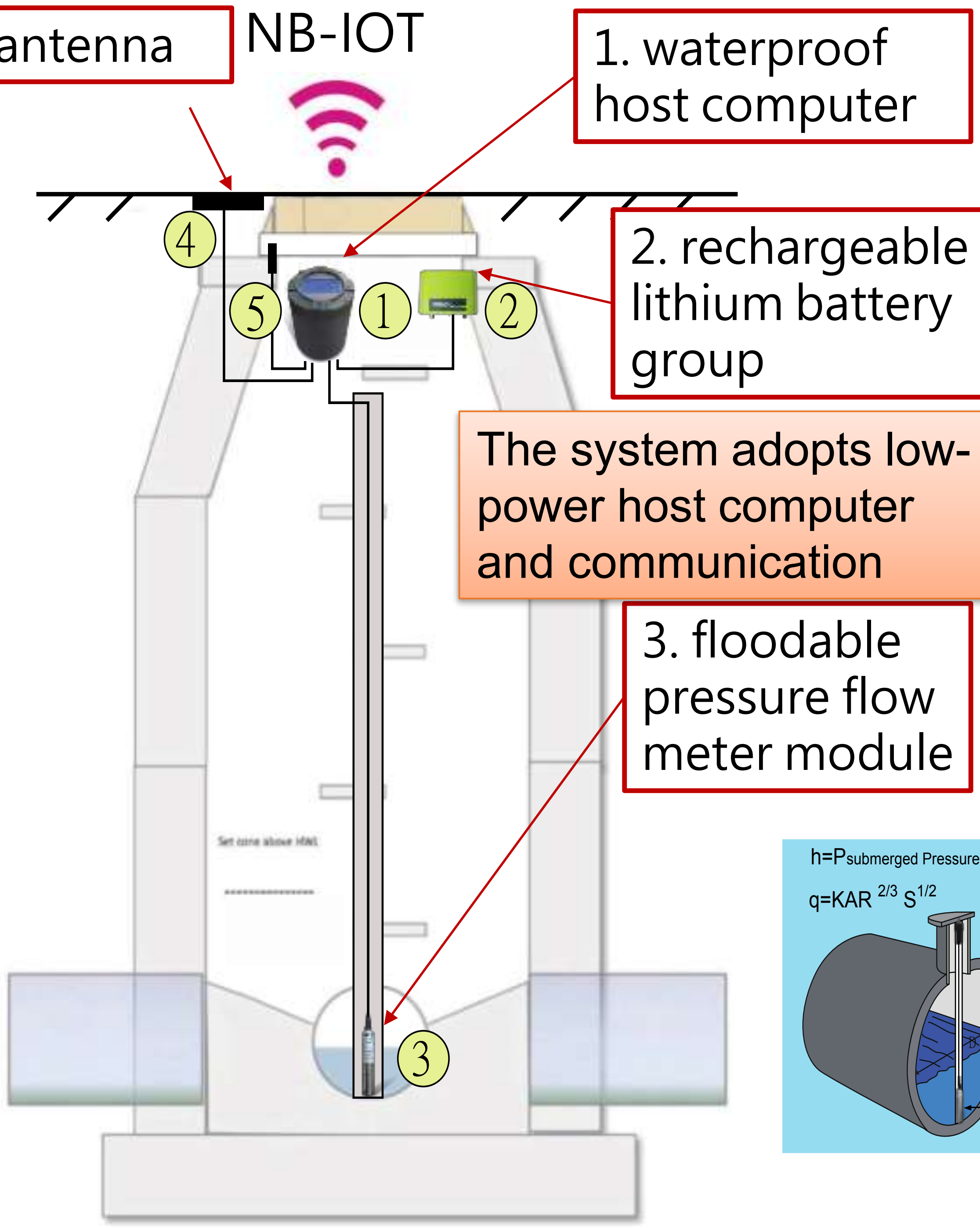

flooding images recognition

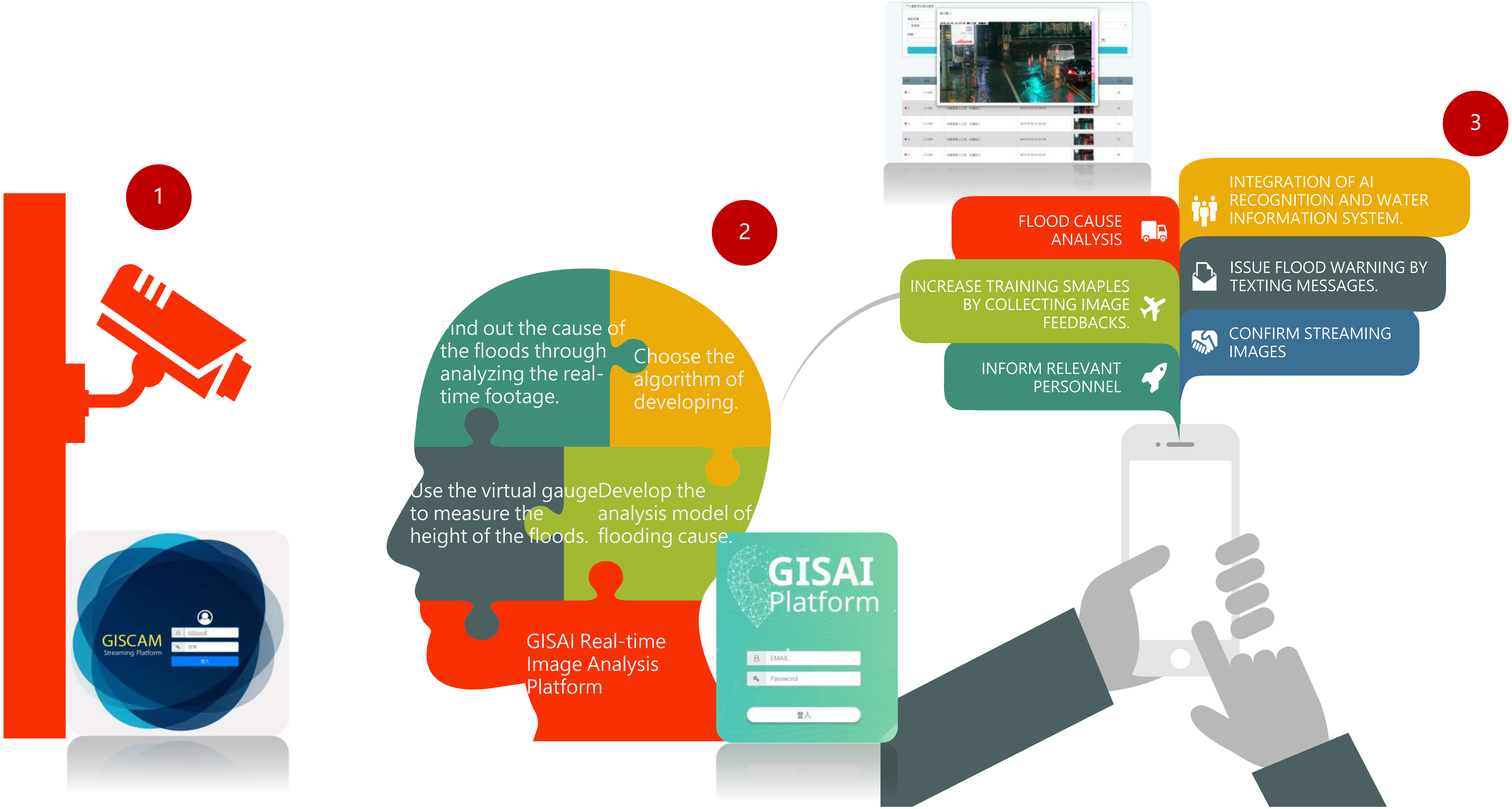

flooding images recognition

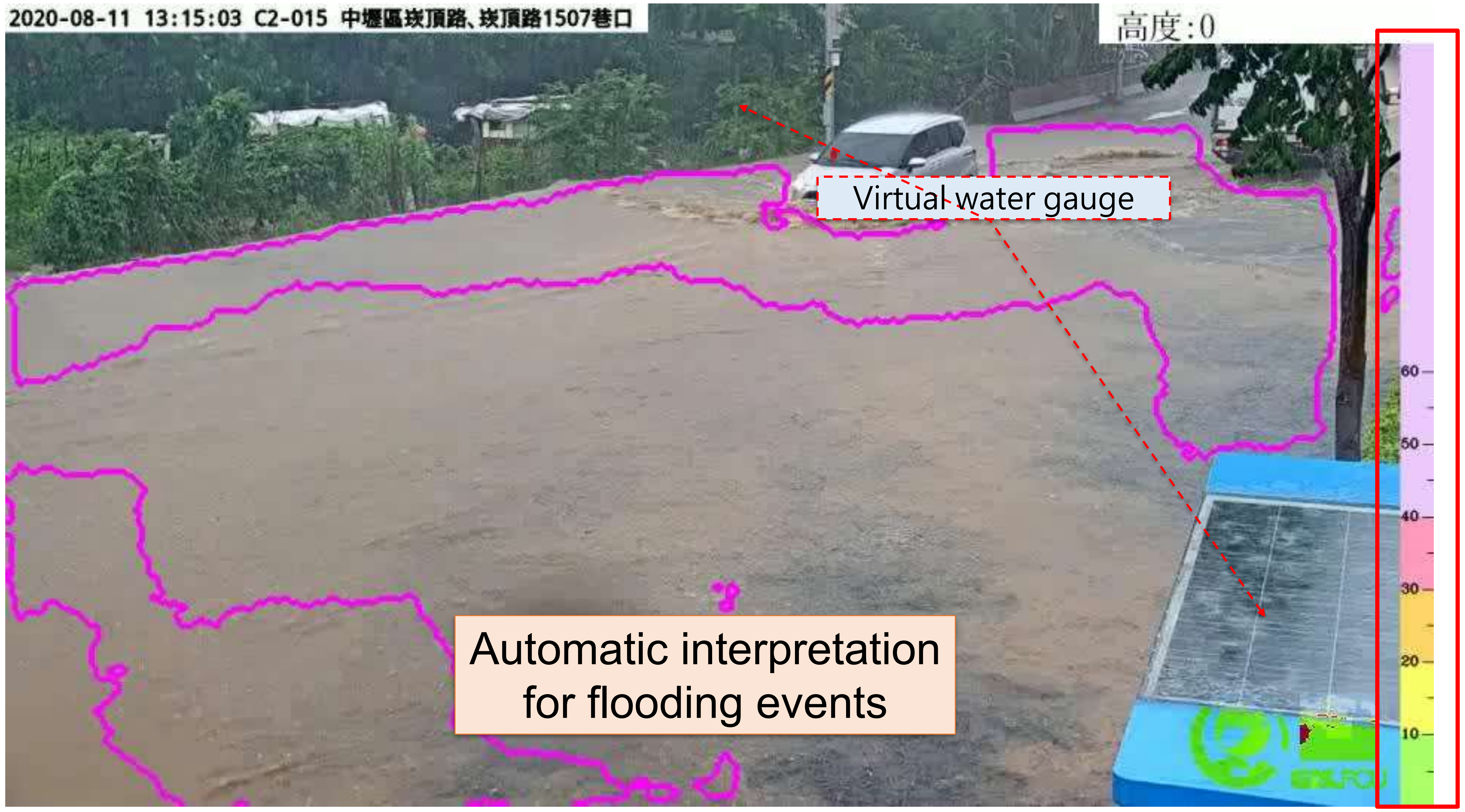

real-time image recognition system by deep learning

AI Flooding Recognition

- Virtual water gauge
- Flooding area
- Group-based image recognition system

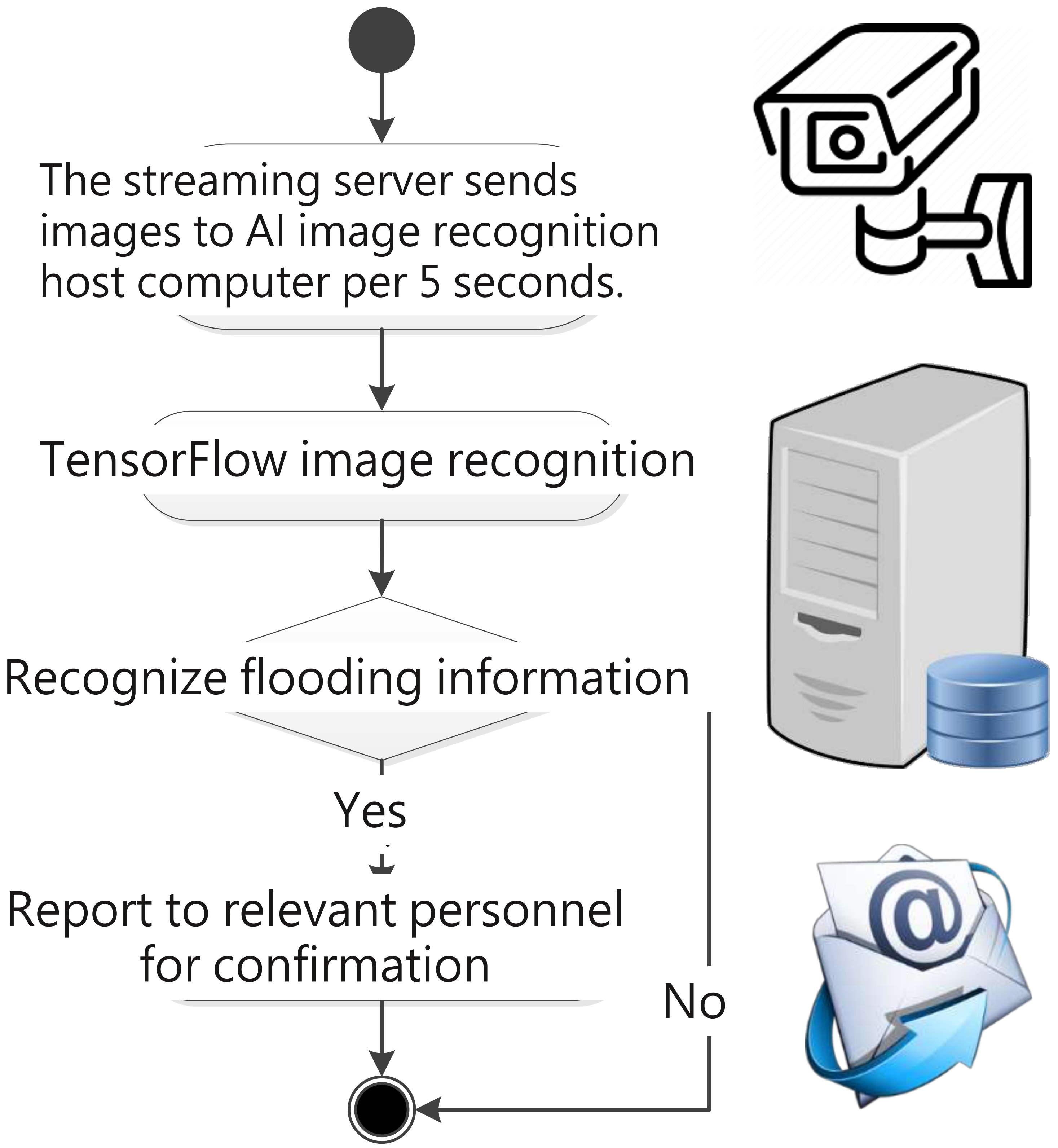

By playing images through the group-based real-time recognition system, relevant personnel can instantly know the AI recognition image of each surveillance camera. Click on any AI real-time recognition screen, and you can open another window to independently display the AI recognition screen of the station.

Surface velocity estimated using GLCM and SVR

Ground truth

1. Water velocity meter is installed in Shenmu station.
2. A camera is installed for obtaining the images that cover the measured surface velocity area.

1. Gray-Level Co-occurrence Matrix (GLCM) is applied for analyzing the spatial distribution of gray-level values in the image.

2. The features derived from GLCM is used for estimating the surface velocity.


Object detector 2019 5 25 上午 12 12 19 - YouTube - Google Chrome 2019_5_25 上午 01_59_58.mp4
加油
SELF SERVICE
24H全天服務
98
95
92
一年車鮮果
Tire2-0~10: 94%
Tire2-0~10: 99%
60
50
40
30
20
10
6:11 / 7:01

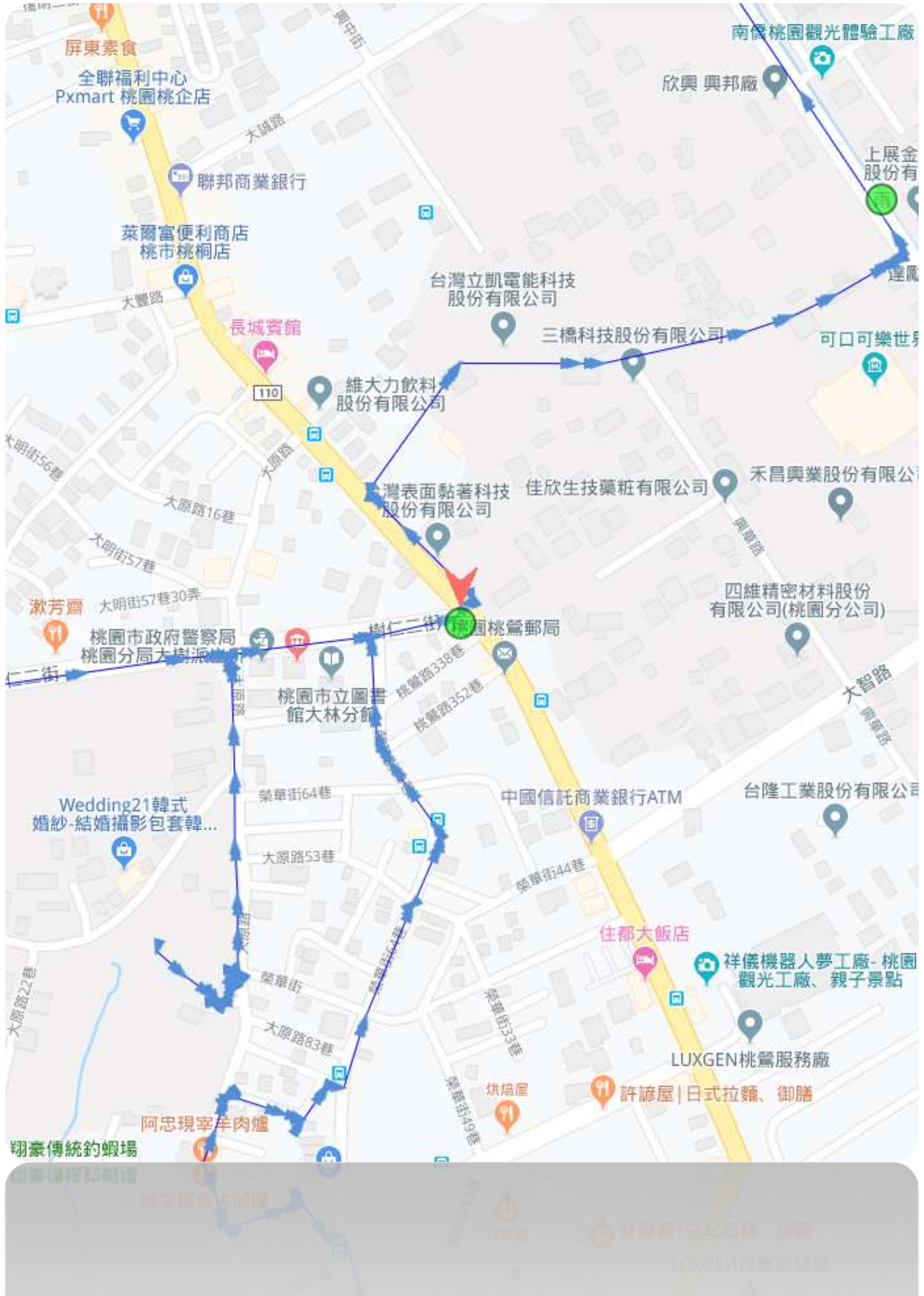
屏東素食
全聯福利中心
Pxmart 桃園桃企店
聯邦商業銀行
萊爾富便利商店
桃市桃桐店
長城賓館
台灣立凱電能科技
股份有限公司
三橋科技股份有限公司
維大力飲料
股份有限公司
佳欣生技藥粧有限公司
禾昌興業股份有限公司
四維精密材料股份
有限公司(桃園分公司)
桃園市政府警察局
桃園分局大樹派出所
桃園市立圖書
館大林分館
桃鶯郵局
中國信託商業銀行ATM
台隆工業股份有限公司
Wedding21韓式
婚紗-結婚攝影包套韓...
佳都大飯店
祥儀機器人夢工廠- 桃園
觀光工廠、親子景點
LUXGEN桃鶯服務廠
許諺屋 | 日式拉麵、御膳
阿忠現宰羊肉爐
翊豪傳統釣蝦場
南僑桃園觀光體驗工廠
欣興 興邦廠
可口可樂世界
大智路

We can detect the water level in real time, which is faster and more accurate than the traditional water level gauge, returned every ten minutes. Currently, it has been applied in a lot of case.

3D Disaster Reduction Smart Cloud System

Subject

- 2D water information display is not intuitive enough

Plan

- Import 3D simulation technology to create Taoyuan digital clone

Efficiency

- Immersive experience of water information
- Easy to interpret on-site conditions

3D Building Flood Simulation

3D pipeline spatial location

The simulation of water level in flooded detention pond

3D water channel level change

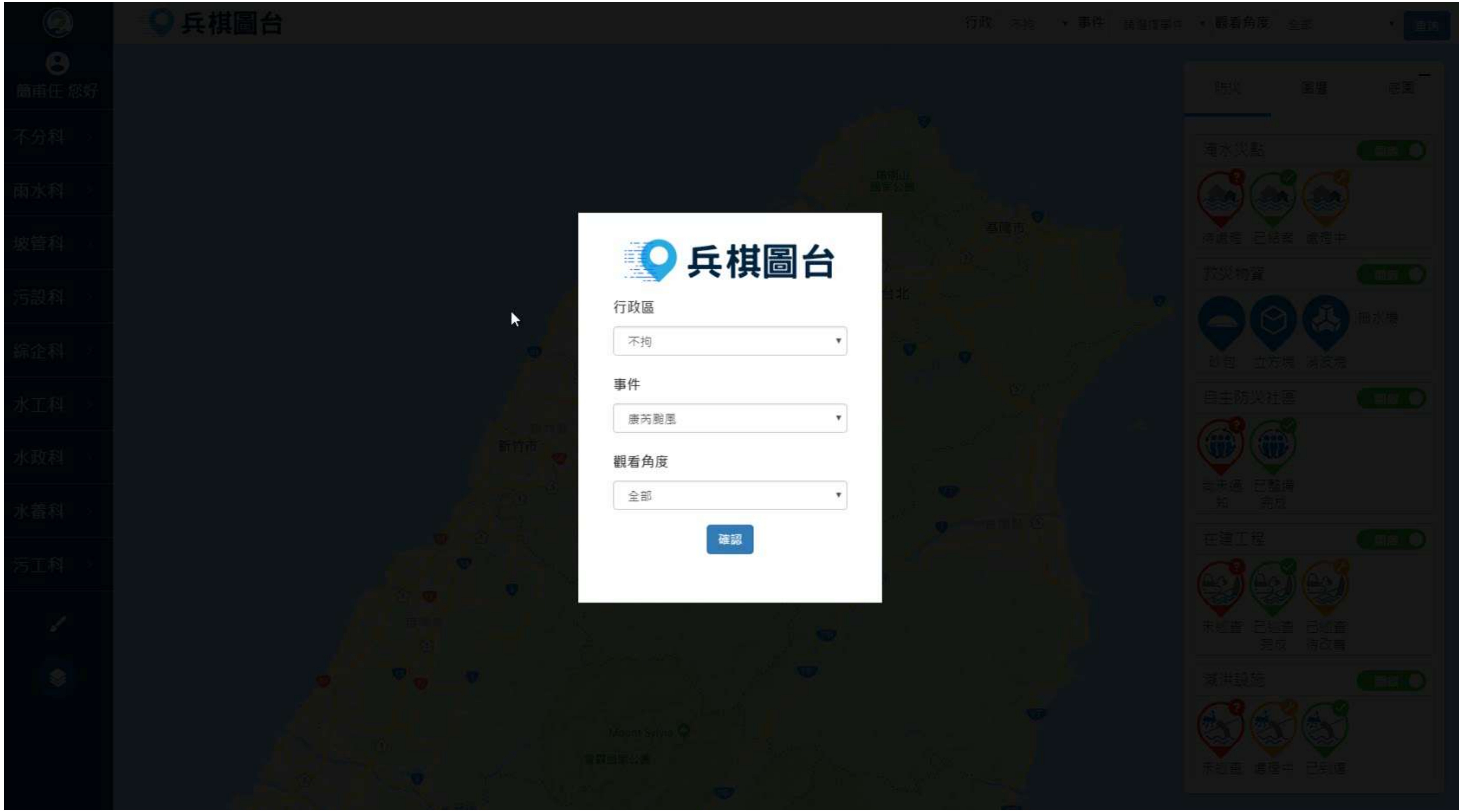
兵棋圖台
行政區
不拘
事件
康芮颱風
觀看角度
全部
確認

Intelligent Governance Systems

Dashboard

- Analyzing **big data** to explore people needs and solve problems. Adjust the municipal planning and policies based on data analyses.
- Meet people needs and drive the innovation to raise the public satisfaction.

Intelligent Operation Center

Intelligent 3D Map Platform & AR

3D construction flooding simulation

3D geospatial location of pipelines

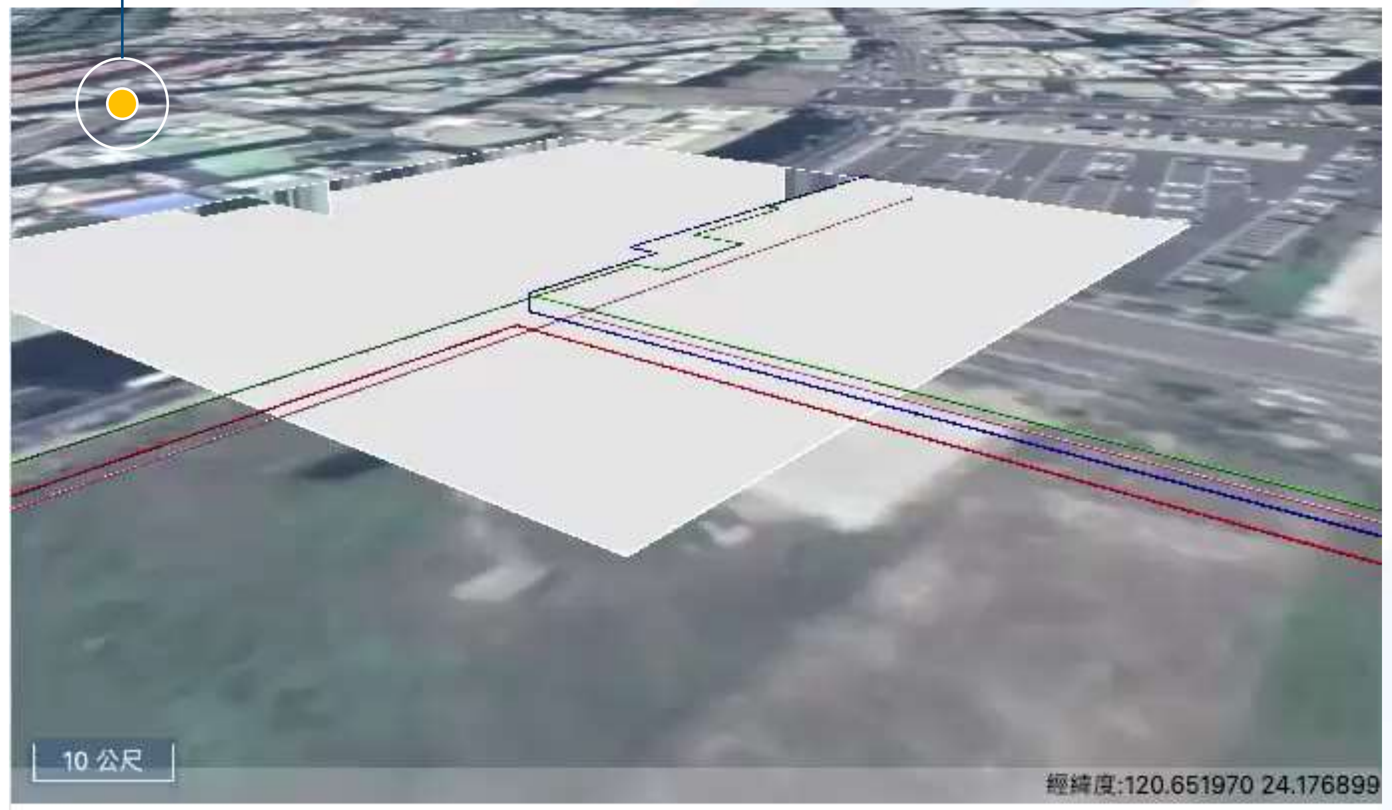

3D AR pipeline

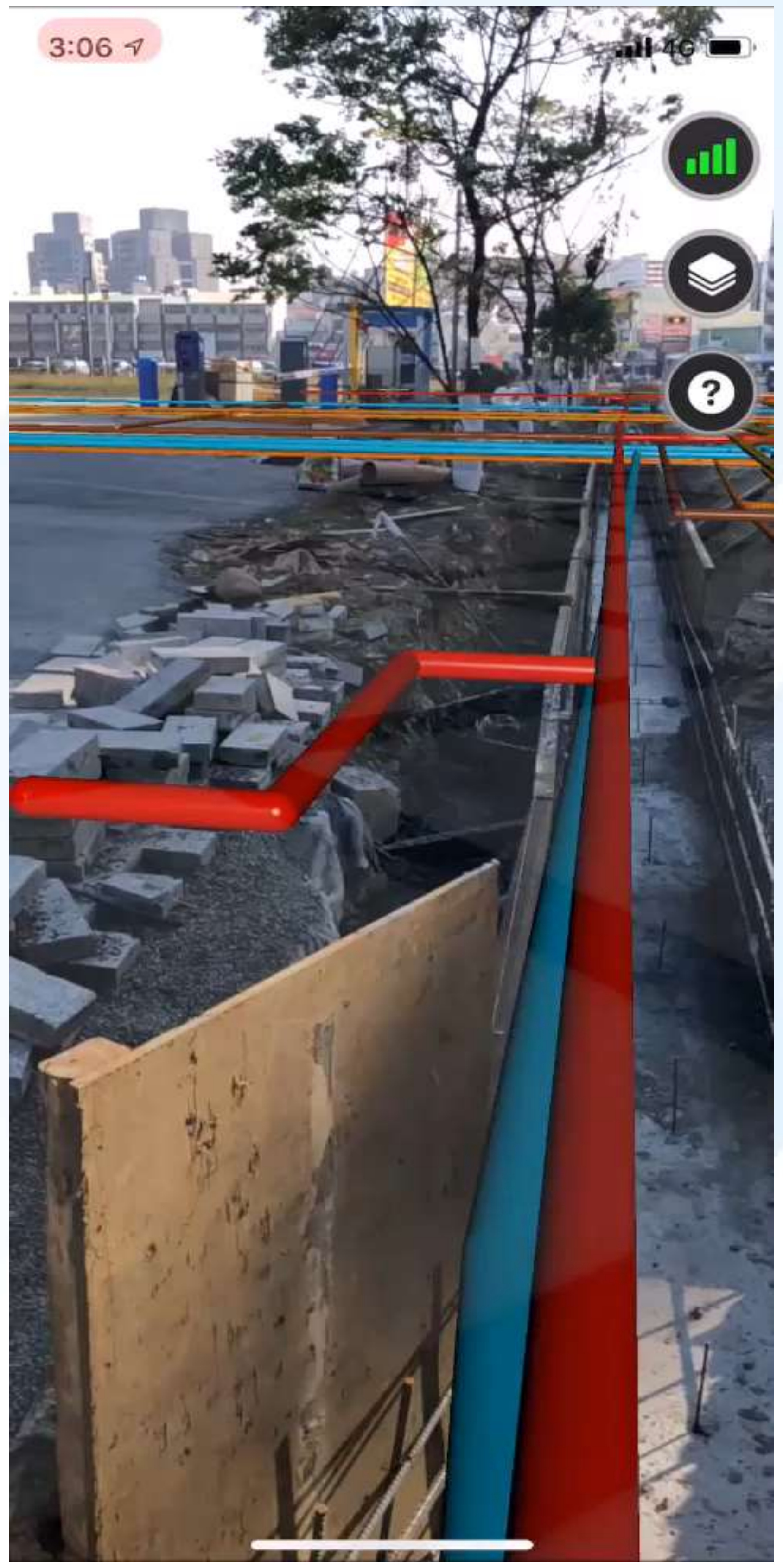

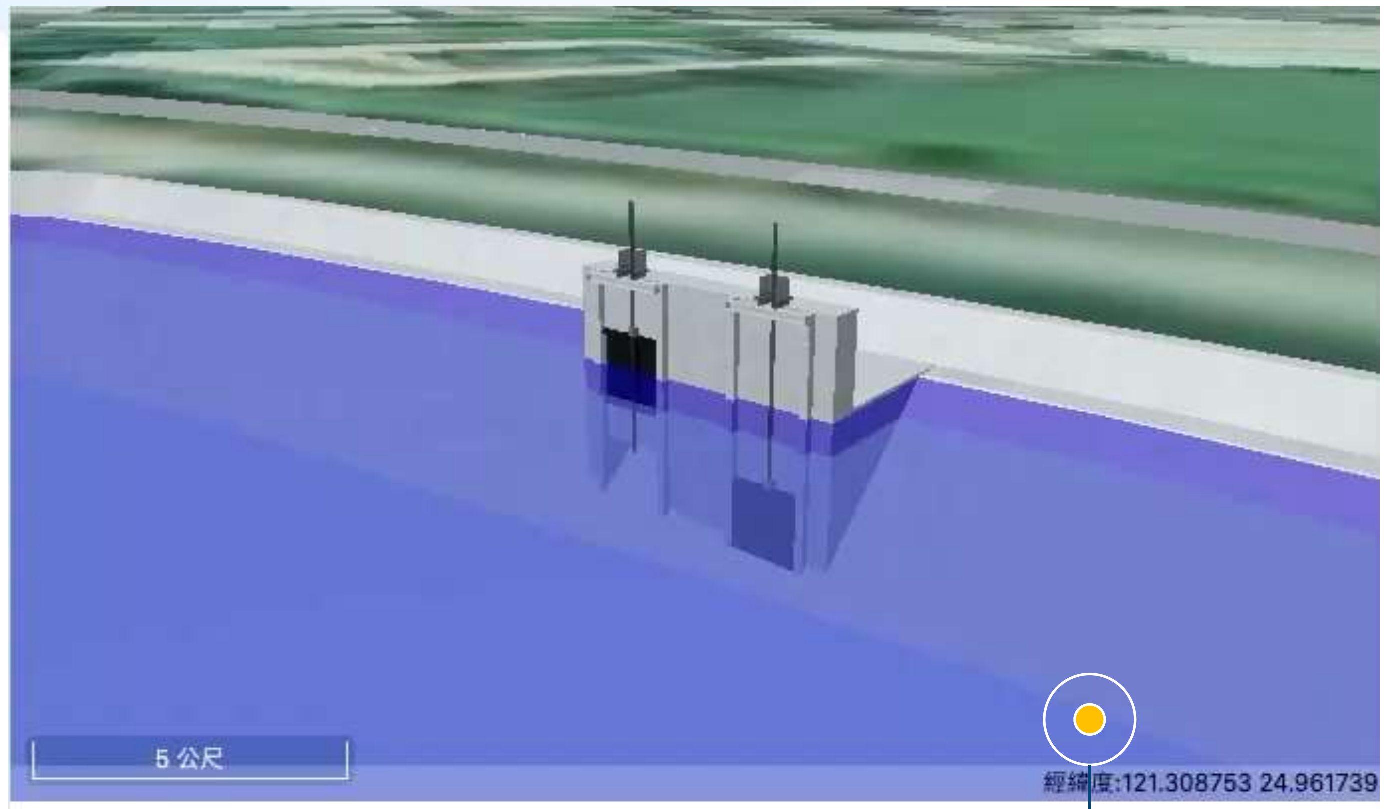

Water level simulation of flood detention pond

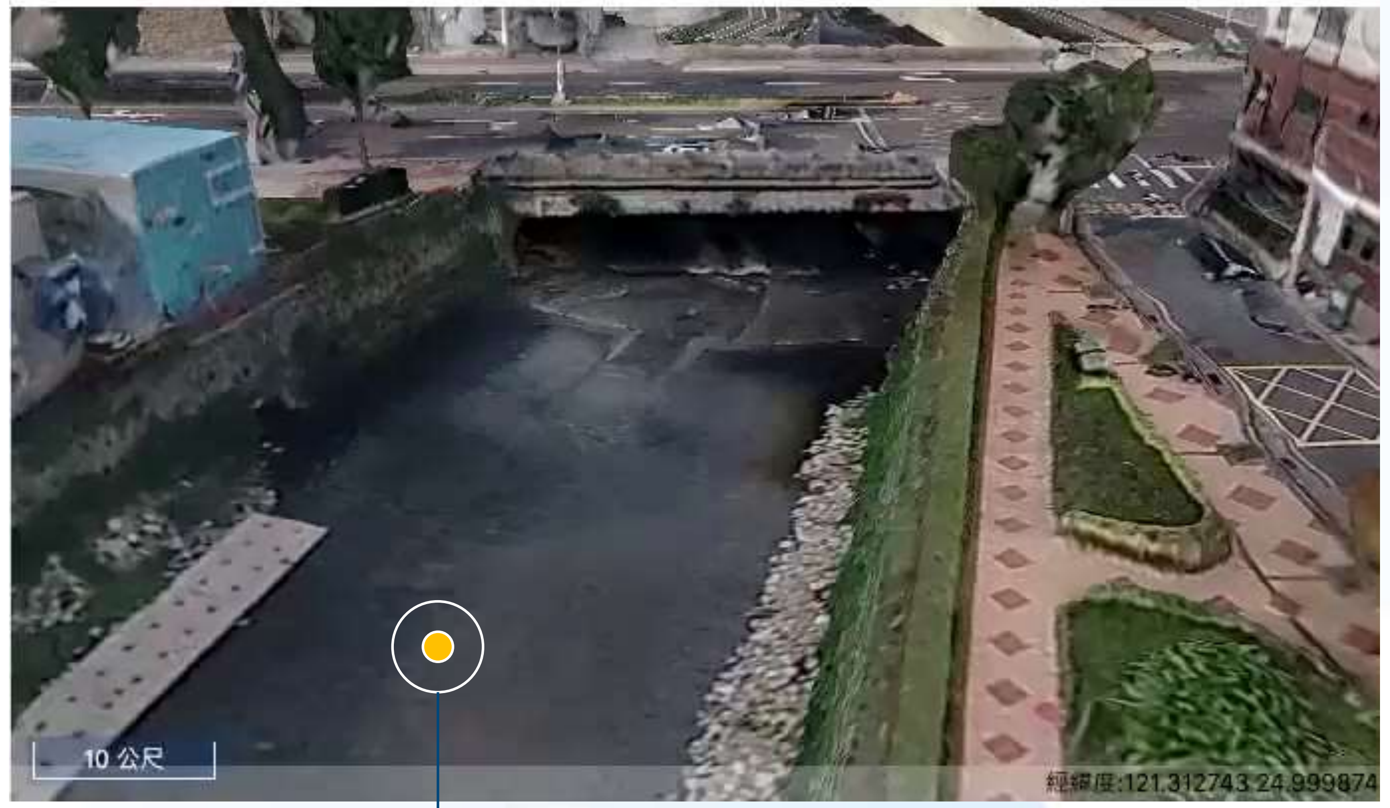

3D water level variety simulation

Smart AIoT

GISAI – Comprehensive Disaster Monitoring

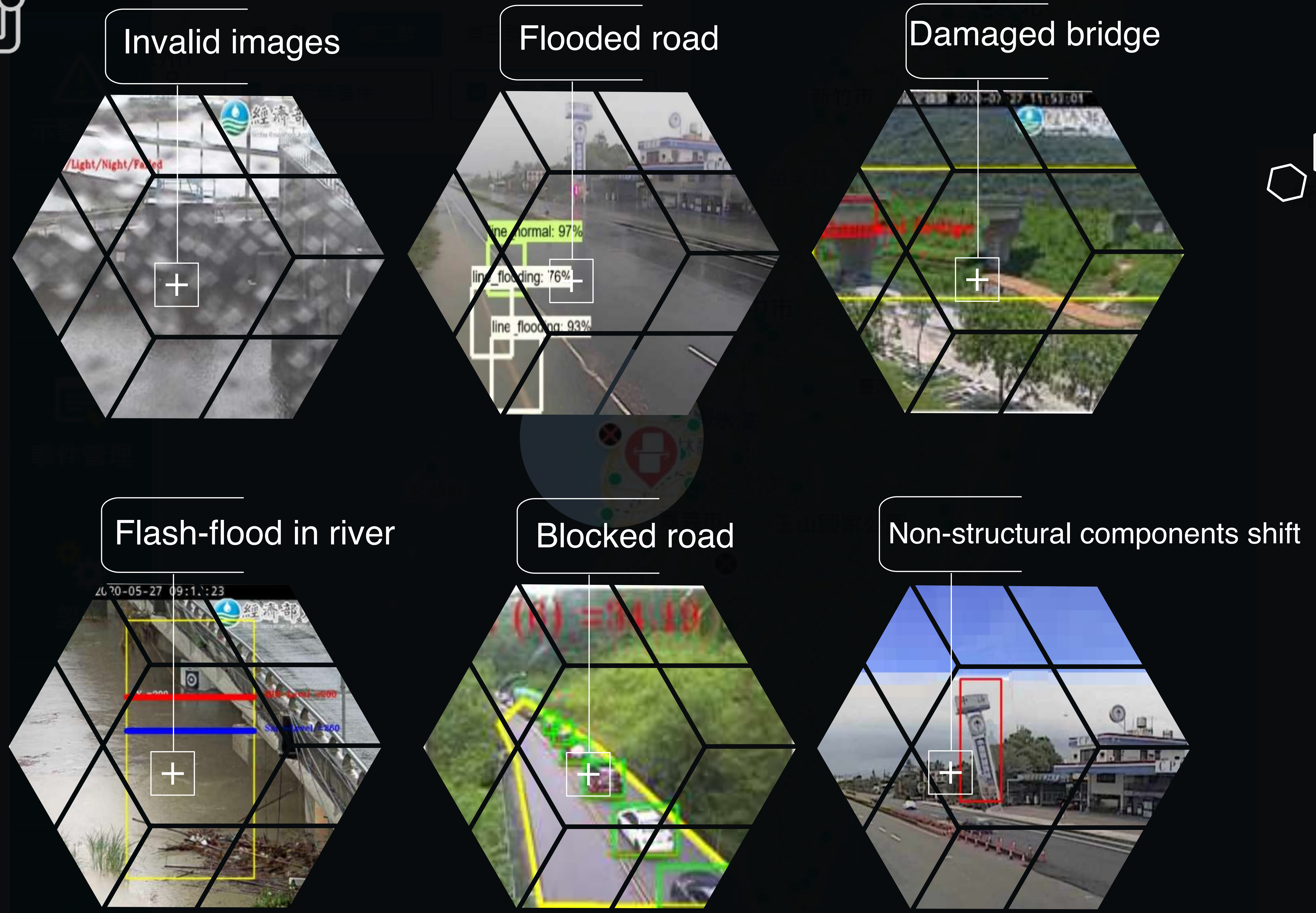

Cross-agency CCTV footages
AI image recognition technology
Comprehensive Disaster Monitoring

SWCB
THB
BOCH
WRA
Local government

Standard

GEO-AI+IoT+3D/AR+DataCube

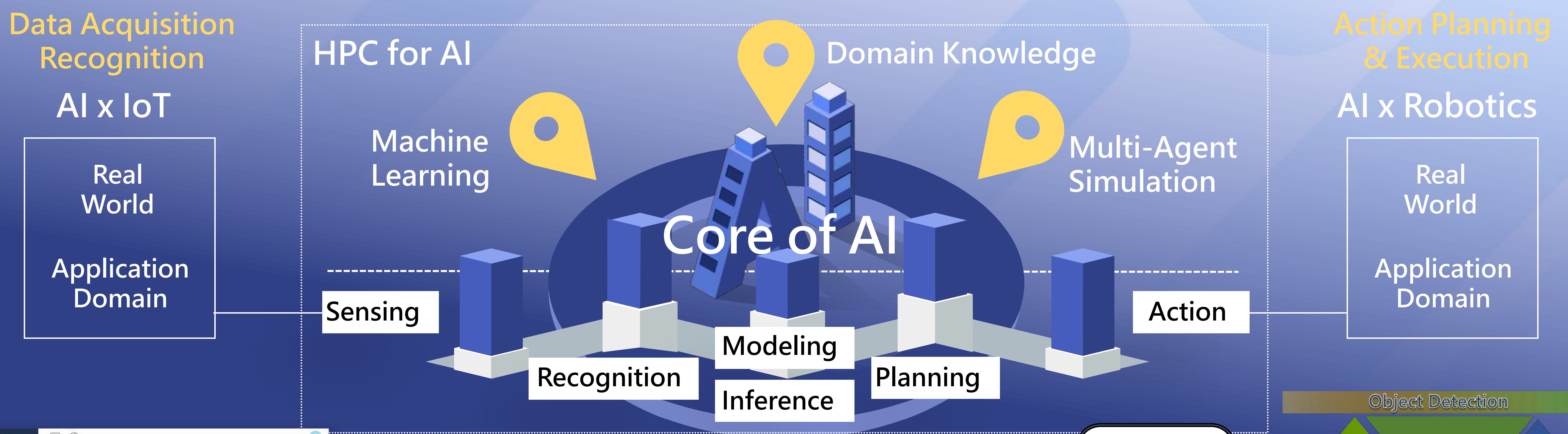

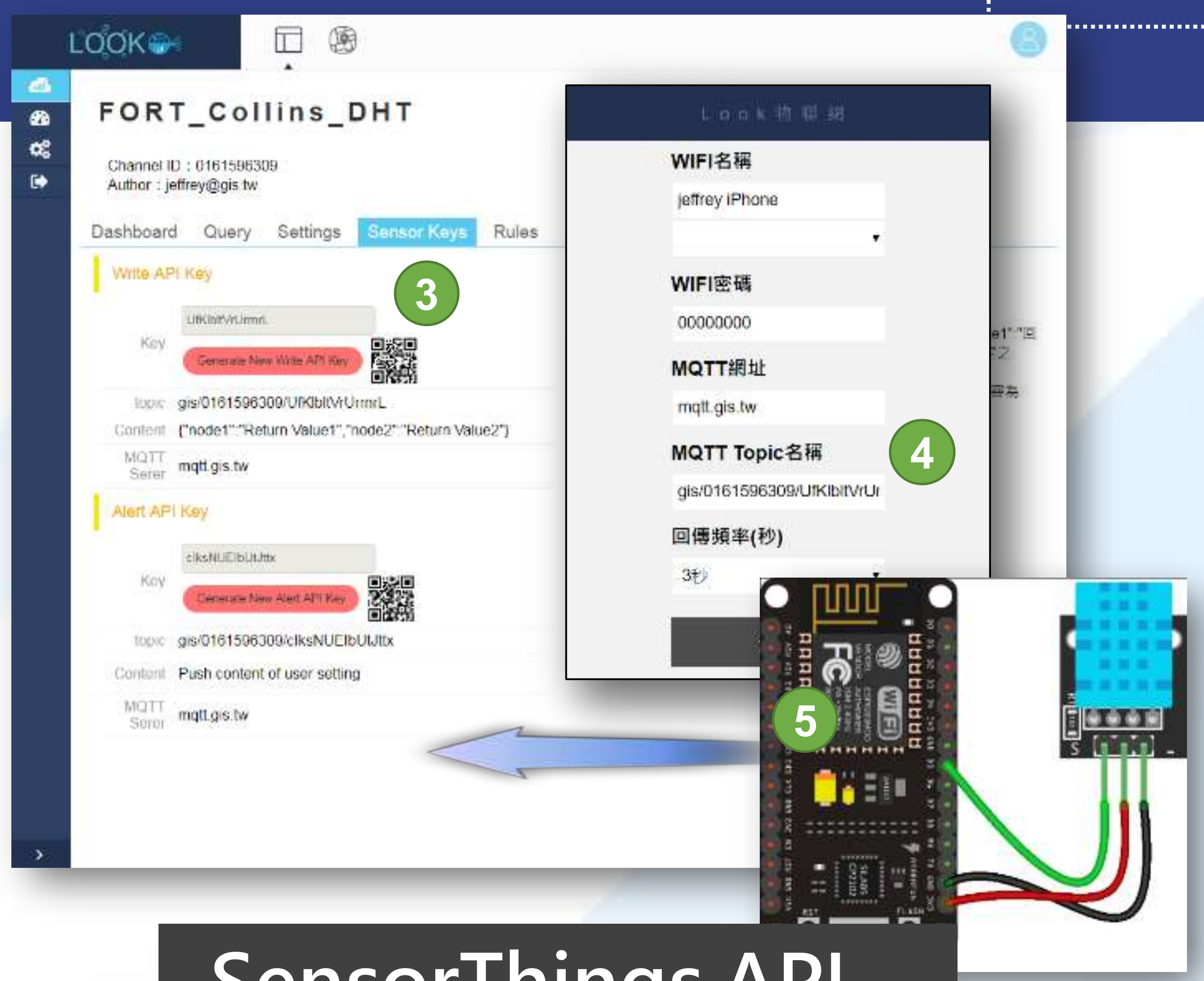

SensorThings API

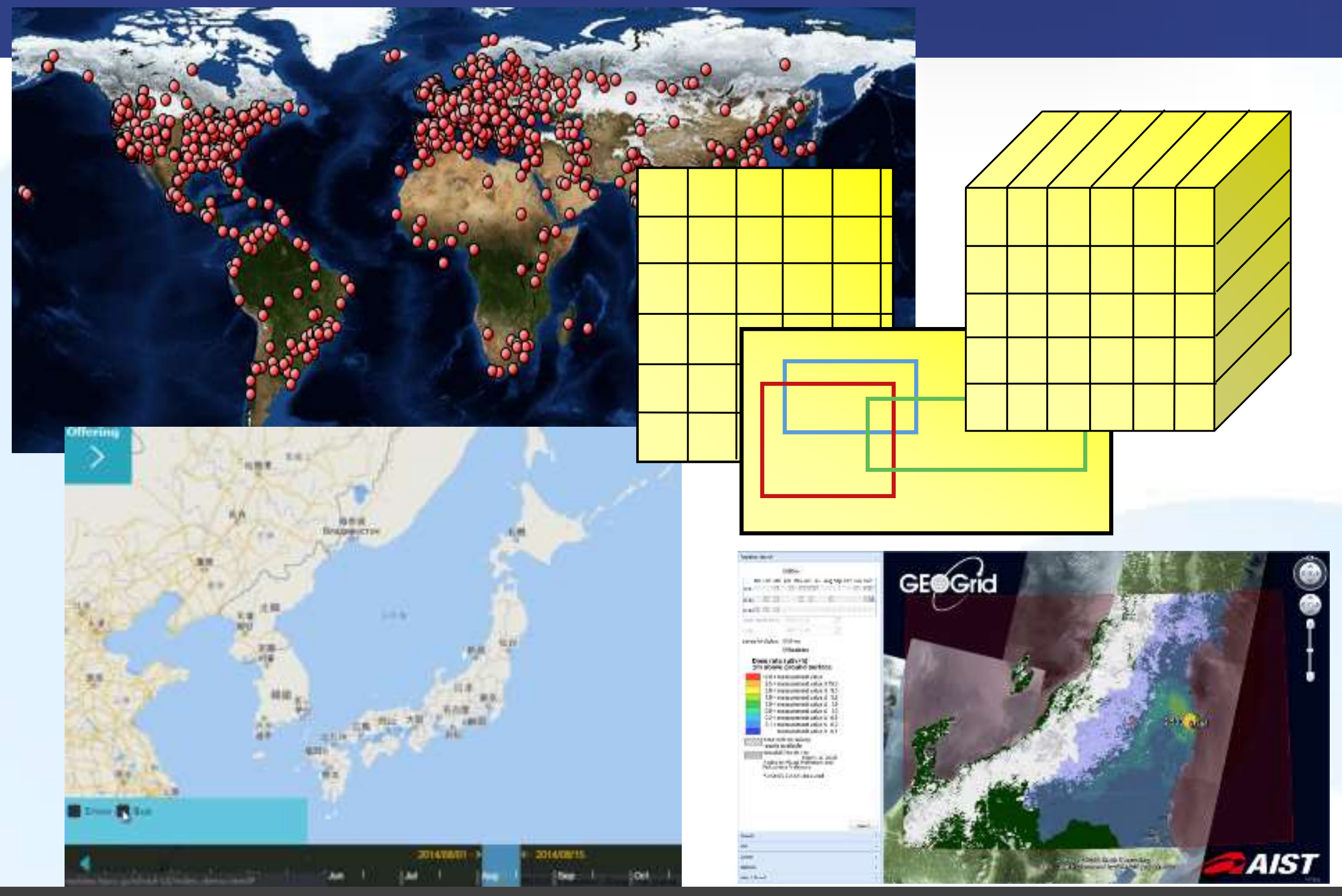

DataCube for Global Observation

CityGML+AR for Pipeline

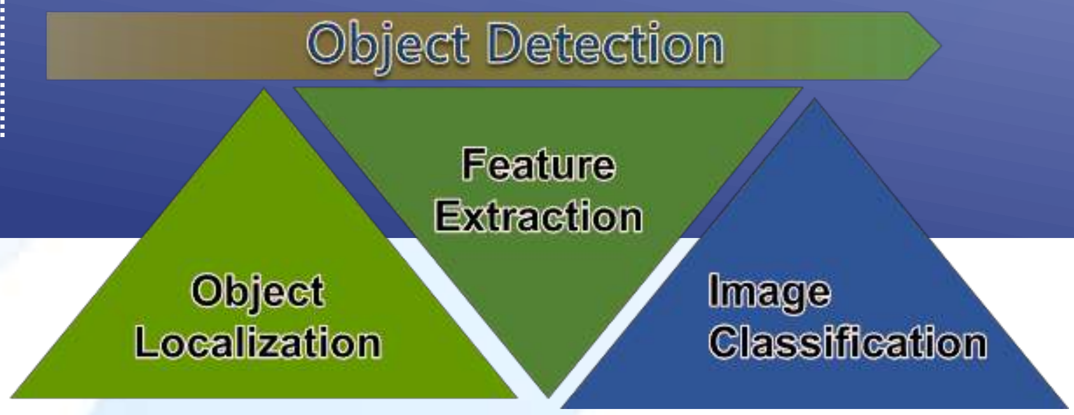

Deep Learning for
Image Recognition

Open, Sharing, Communication
Cooperation across Industry, Academy, and Government

Smiling curve

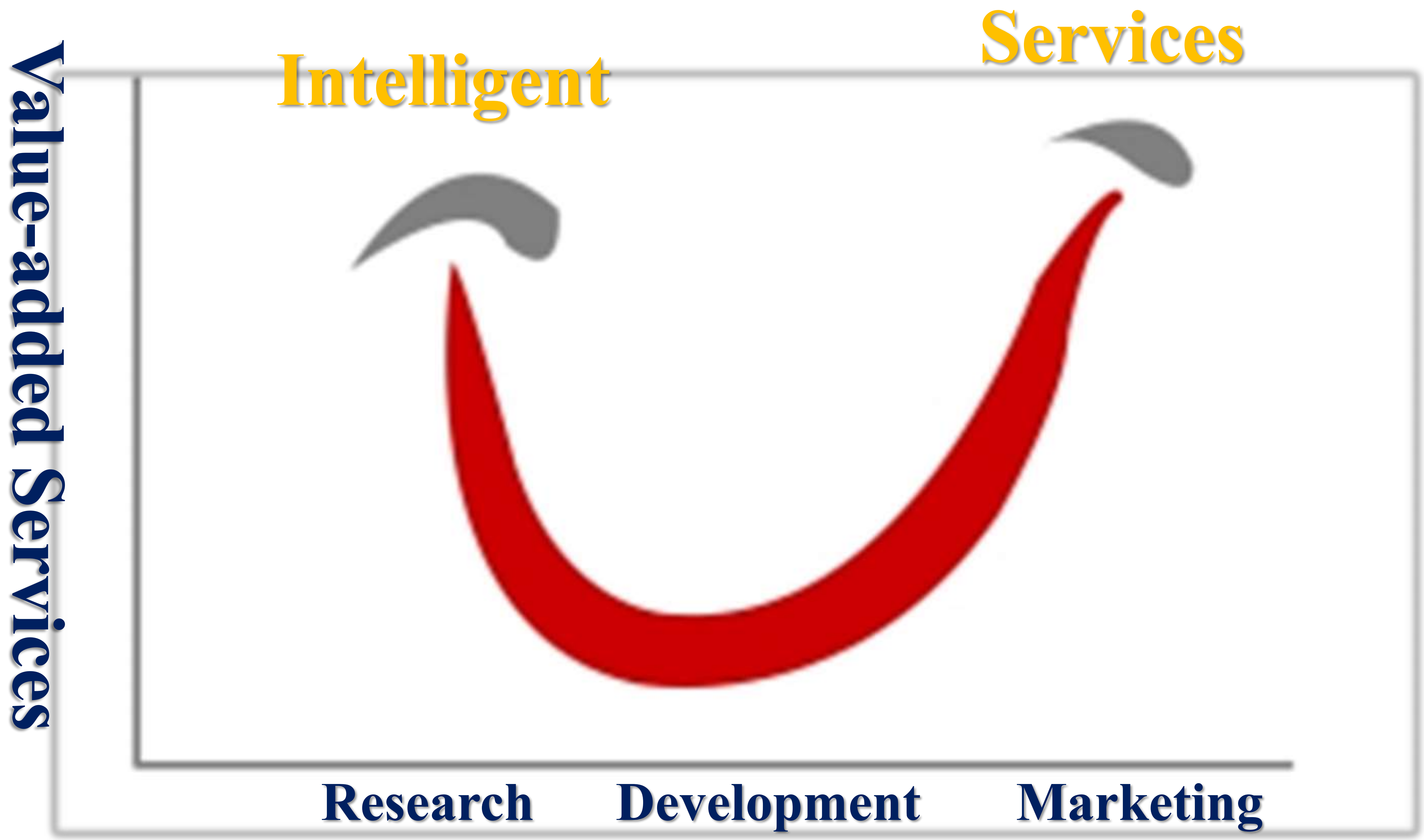

Sensing spatiotemporal change for water resource management

Hone-Jay Chu
Department of Geomatics,
National Cheng Kung University

Innovative Strategies for Water Sustainability
International Forum 2022

Outline

- Introduction
- Sensing the changes
  - Water changes (area, level and storage)
  - Meteorological and vegetation change for drought detection
- Data integration technology
  - Downscaling
  - High-spatio-temporal-resolution Sensing (Data fusion)

Introduction (Motivation)

The earth is facing incredibly serious challenges: Climate change, water depletion, deforestation, air and water pollution.

yahoo!news

Western U.S. faces water and power shortages due to climate change, U.N. warns

Ben Adler · **Senior Editor**
Wed, August 3, 2022 at 5:12 AM · 3 min read

Anglian Water says 'we must be more robust towards drought'

21 hours ago

Laura Tuplin said some of the company's biggest challenges were "using less water and coping with growth"

Introduction (Sensing water changes)

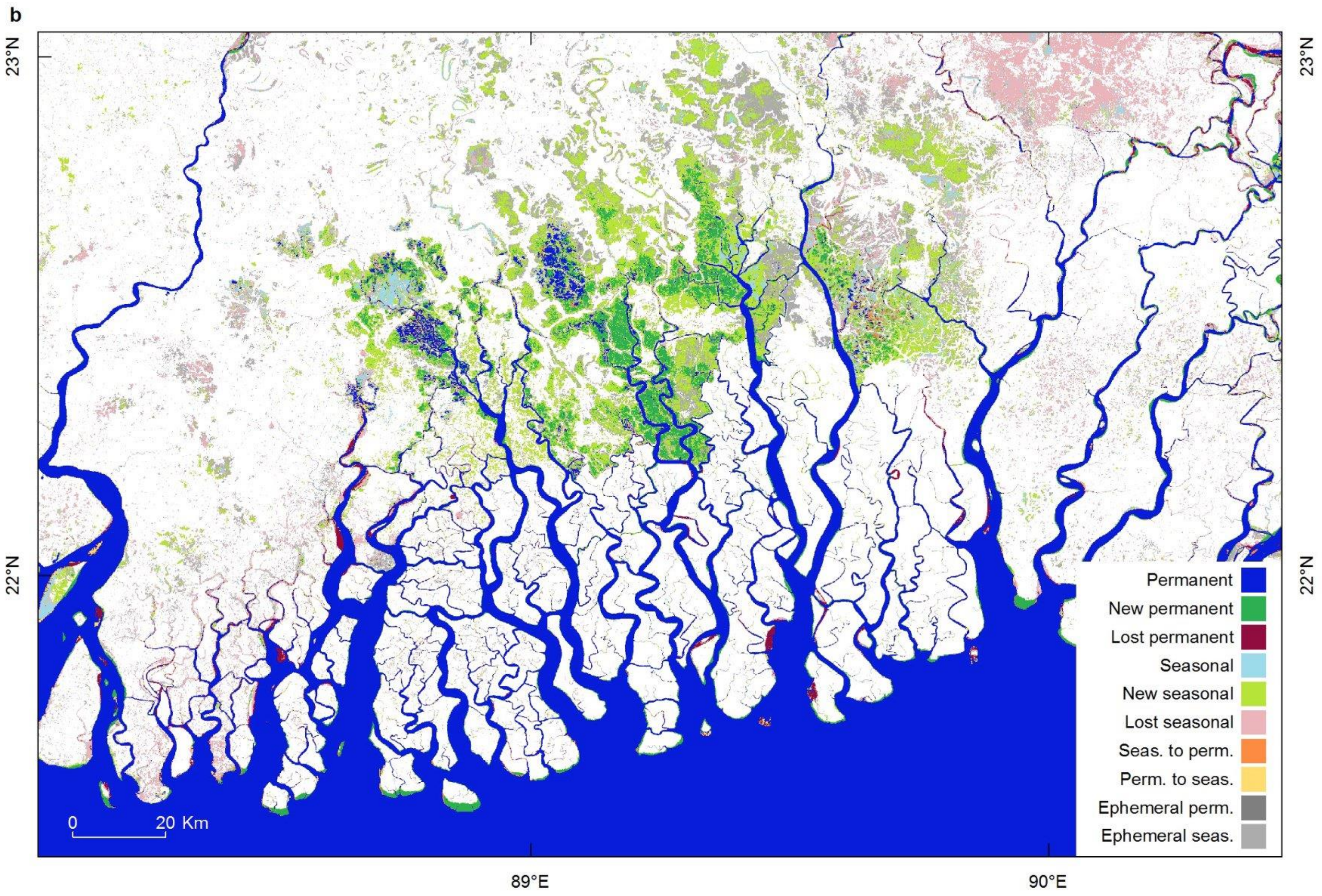

Pekel et al., (2016)

Using three million Landsat satellite images, we quantify changes in global surface water over the past 32 years at 30-metre resolution. We record the months and years when water was present, where occurrence changed and what form changes took in terms of seasonality and persistence.

Introduction (Sensing water changes)

- Over 70 percent of global net permanent water loss occurred in the Middle East and Central Asia. Moreover, losses in Australia and the USA linked to long-term droughts are also evident.
- Supply decreases => Shortage

Trends in annual permanent water surface area

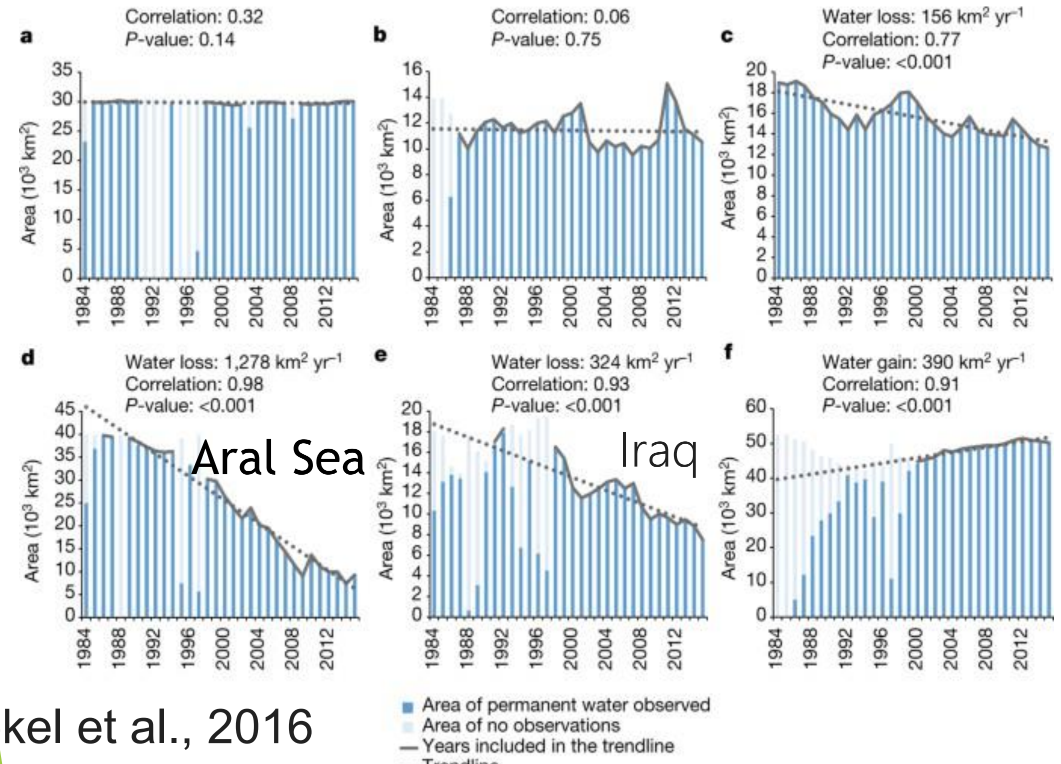

Pekel et al., 2016

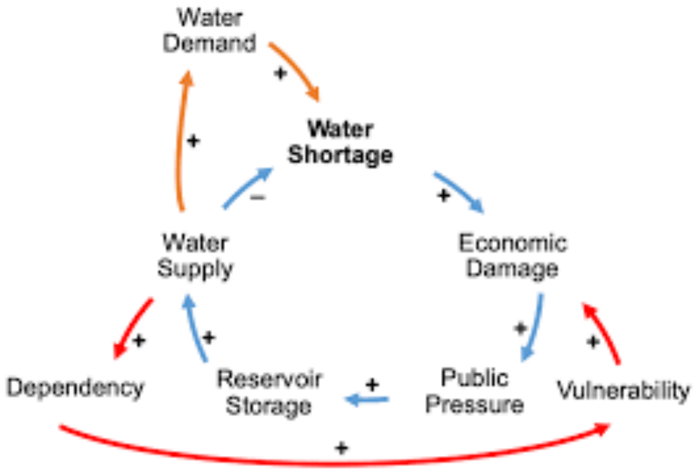

Supply and demand for water resource management

Introduction (Sensing global lake and reservoir storage)

- Seasonal variability: tracking of lake and reservoir storage variability

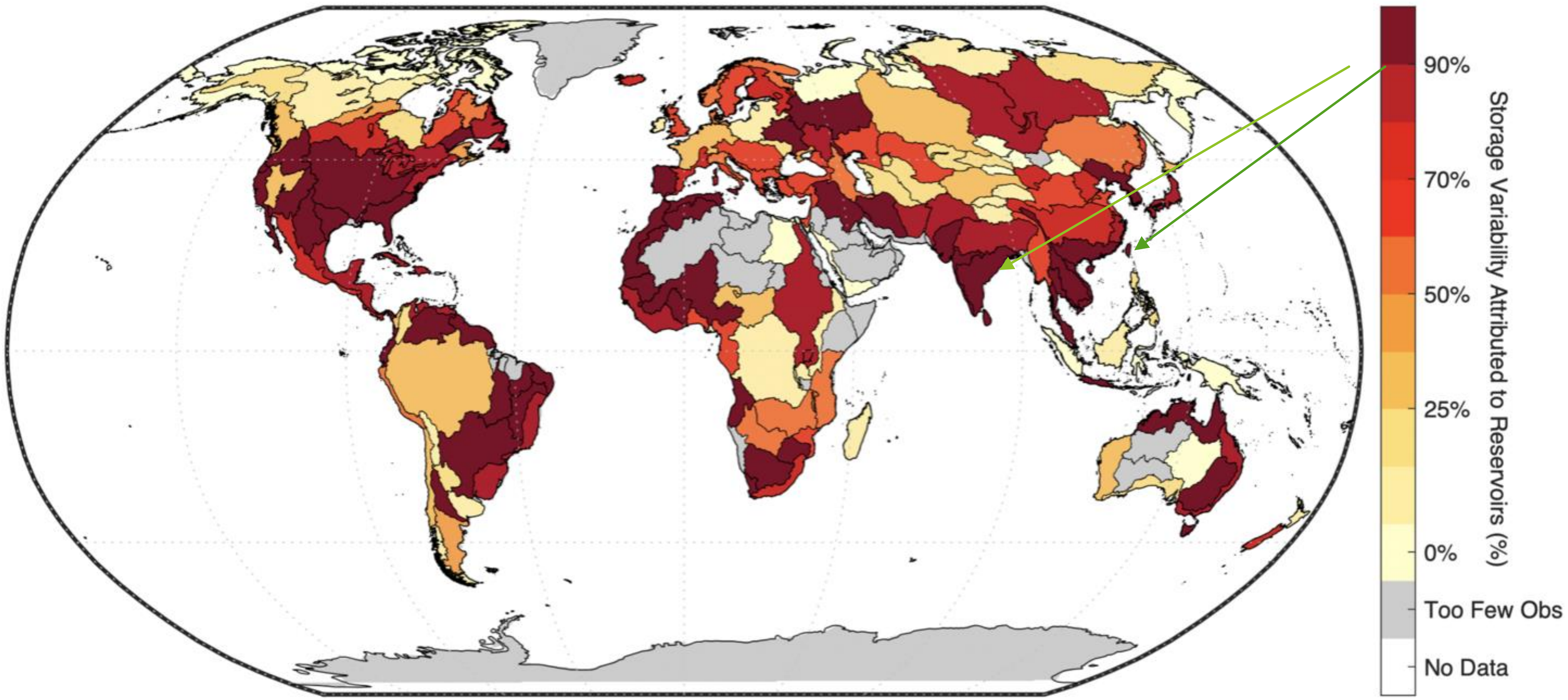

Cooley et al., 2021

Antecedent Precipitation Index	1954	Precipitation; a reverse drought index used for flood forecasting
Moisture Adequacy Index	1957	Precipitation and soil moisture; agricultural drought
Palmer's Index (PDSI and PHDI)	1965	Precipitation and temperature analyzed in a water balance model; comparison of meteorological and hydrological drought across space and time
Crop Moisture Index	1968	Precipitation and temperature analyzed in a water balance model; agricultural drought
Keetch–Byram Drought Index	1968	Precipitation and soil moisture analyzed in a water budget model; used by fire control managers
Surface Water Supply Index	1981	Snowpack, reservoir storage, streamflow, and precipitation; computed primarily for western river basins; statistical properties not well analyzed or understood
Standardized Precipitation Index	1993	Precipitation; allows measurement of droughts and wet spells in terms of precipitation deficit, percent of "normal," probability of nonexceedance, and SPI at multiple simultaneous timescales with potentially different behavior at all of them
Vegetation Condition Index	1995	Satellite AVHRR radiance (visible and near-IR); measures "health" of vegetation
Drought Monitor	1999	Integrates several drought indices and ancillary indicators into a weekly operational drought-monitoring map product; multipurpose

A Review of Twentieth-Century Drought Indices Used in the United States

BY RICHARD R. HEIM JR.

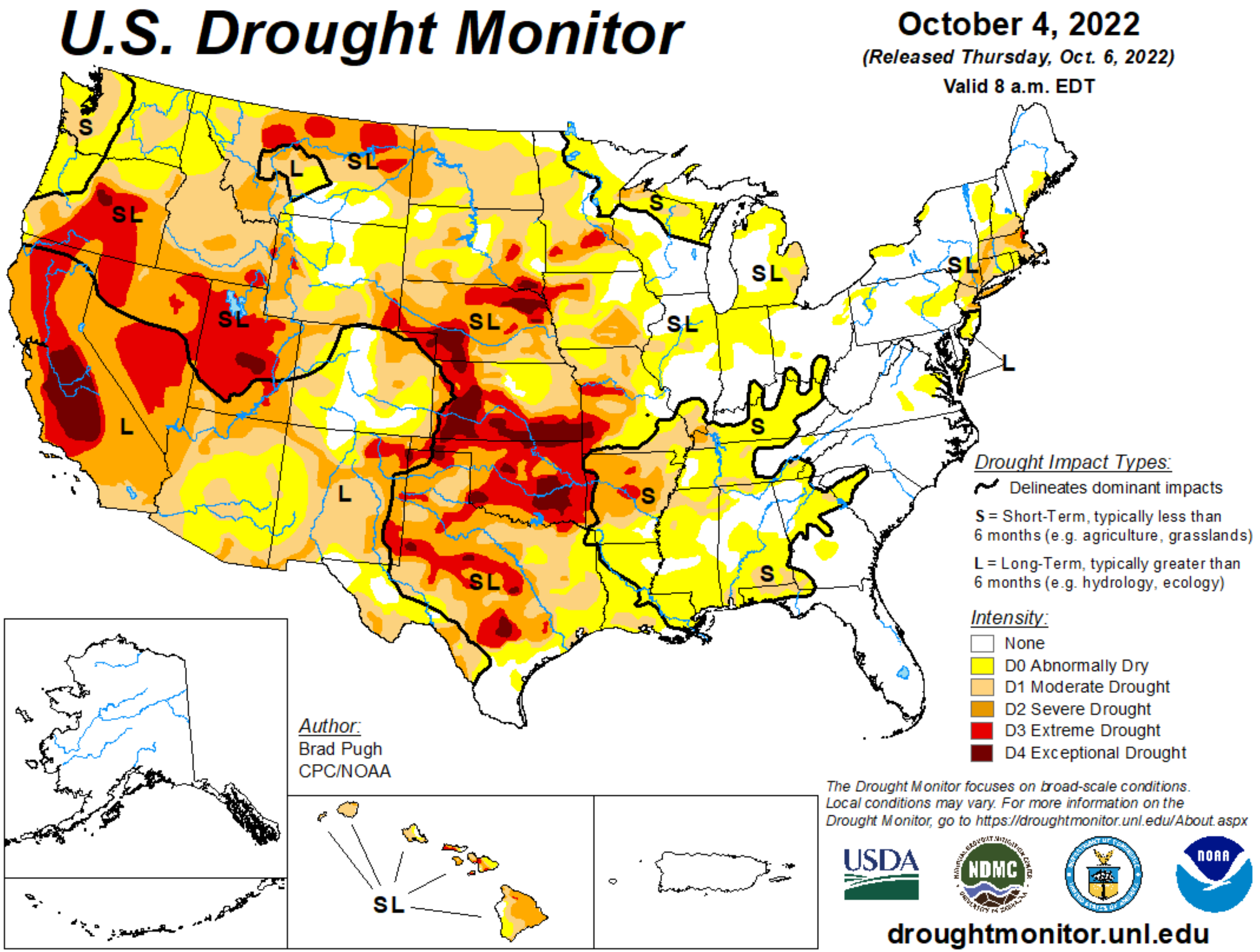
U.S. Drought Monitor
October 4, 2022
(Released Thursday, Oct. 6, 2022)
Valid 8 a.m. EDT
Drought Impact Types:
Delineates dominant impacts
S = Short-Term, typically less than 6 months (e.g. agriculture, grasslands)
L = Long-Term, typically greater than 6 months (e.g. hydrology, ecology)
Intensity:
None
D0 Abnormally Dry
D1 Moderate Drought
D2 Severe Drought
D3 Extreme Drought
D4 Exceptional Drought
Author:
Brad Pugh
CPC/NOAA
The Drought Monitor focuses on broad-scale conditions. Local conditions may vary. For more information on the Drought Monitor, go to https://droughtmonitor.unl.edu/About.aspx
USDA
NDMC
NOAA
droughtmonitor.unl.edu

Part I: Sensing the changes

- Water changes (surface water area, water level and groundwater storage)
- Meteorological, soil moisture and vegetation change for drought detection

1. Sensing water changes in Taiwan

- Many reservoirs in Taiwan are at less than 20% capacity, with water levels at some falling below 10% in 2021.

Remote Sensing Drought Observatory

- [Global Drought Conditions] This map shows the 3-month Standardized Precipitation Index (SPI)
- [EDO - European Drought Observatory] derived from different data sources

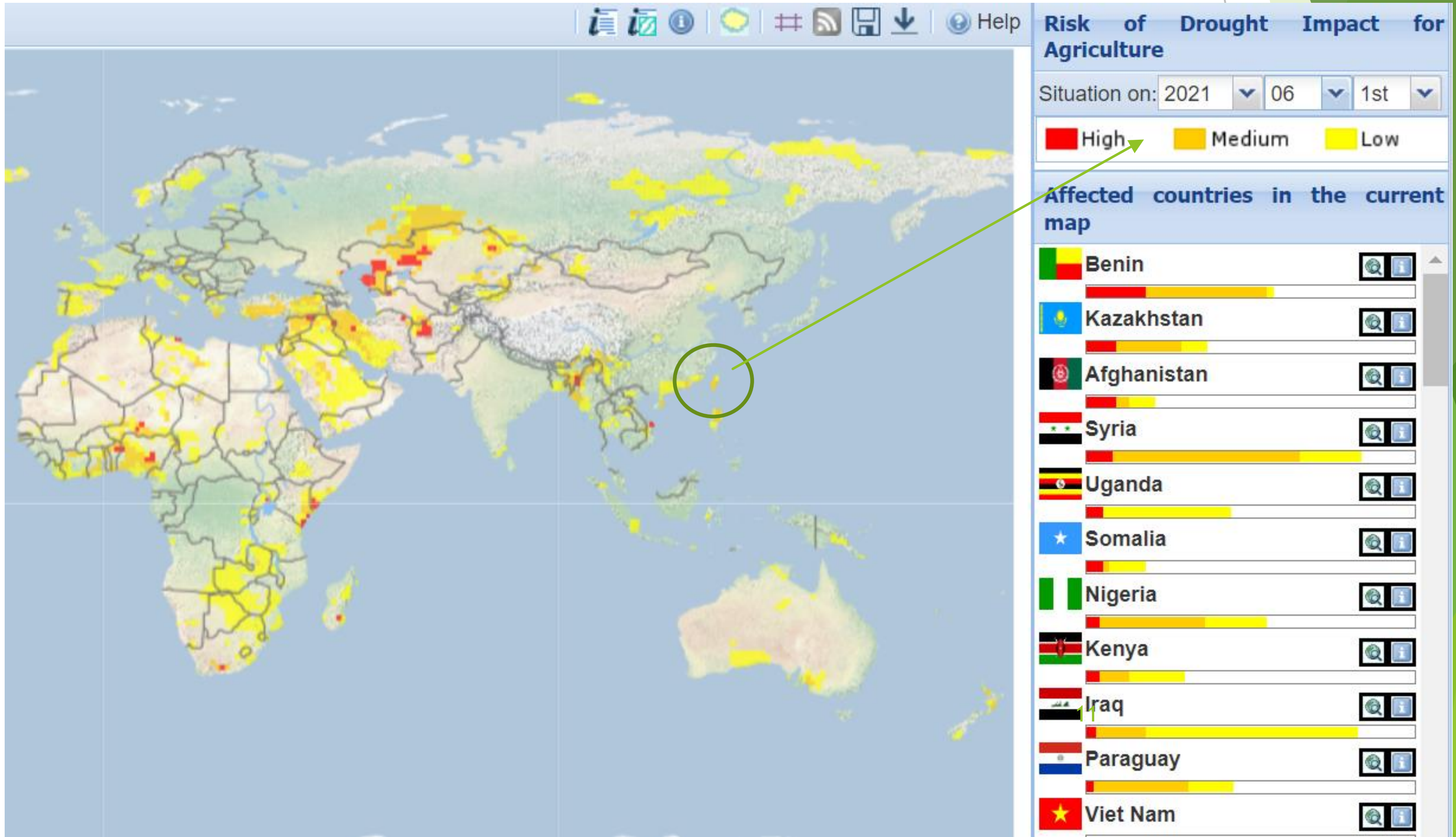

Sensing case in Taiwan

Data

- Reservoir water area change: Sentinel 2 image
- Reservoir water level change: ICESat-2 data

Sensing water changes in Taiwan

Monitoring water area change of Tsengwen Reservoir

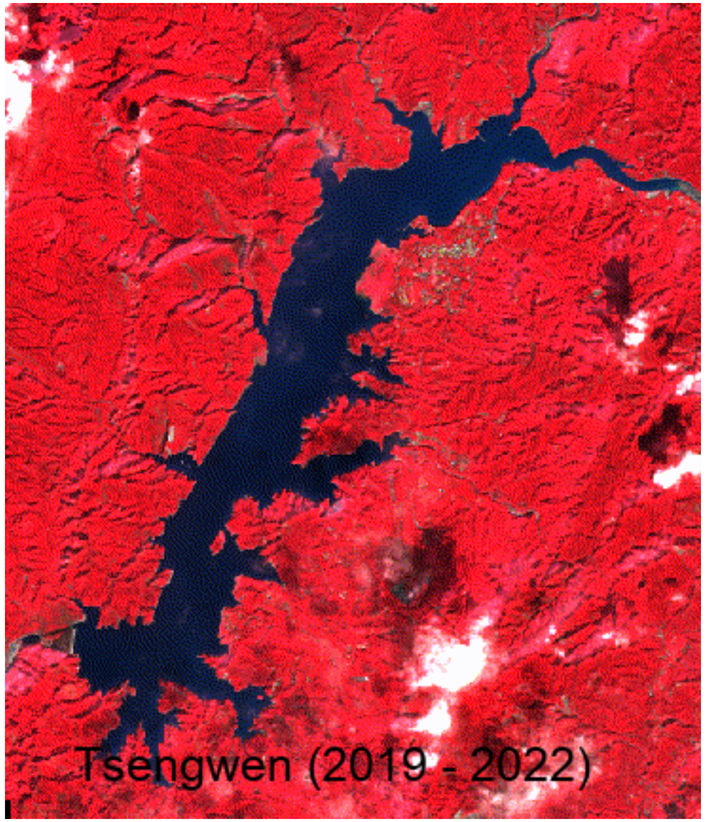

Sensing water changes in Taiwan

- Monitoring water level change from ICESat-2 data

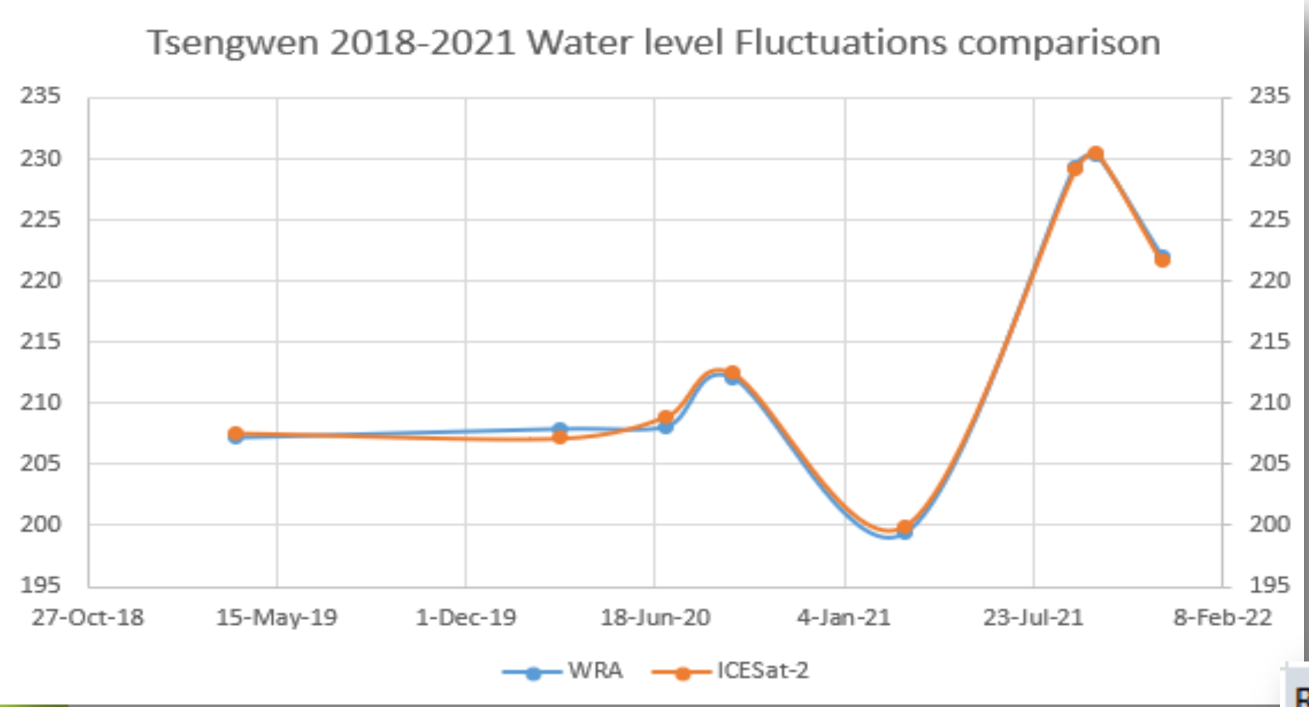

m

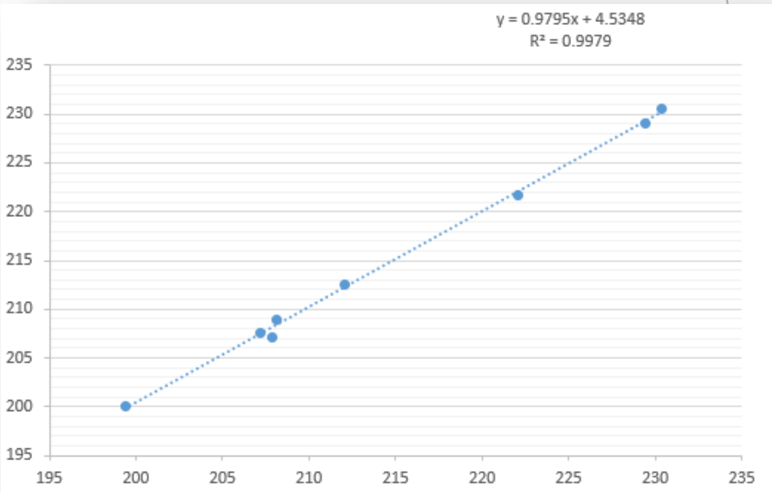

at Tsengwen

R^2	0.997
RMSE	0.538
MAE	0.496

m

2. Drought detection

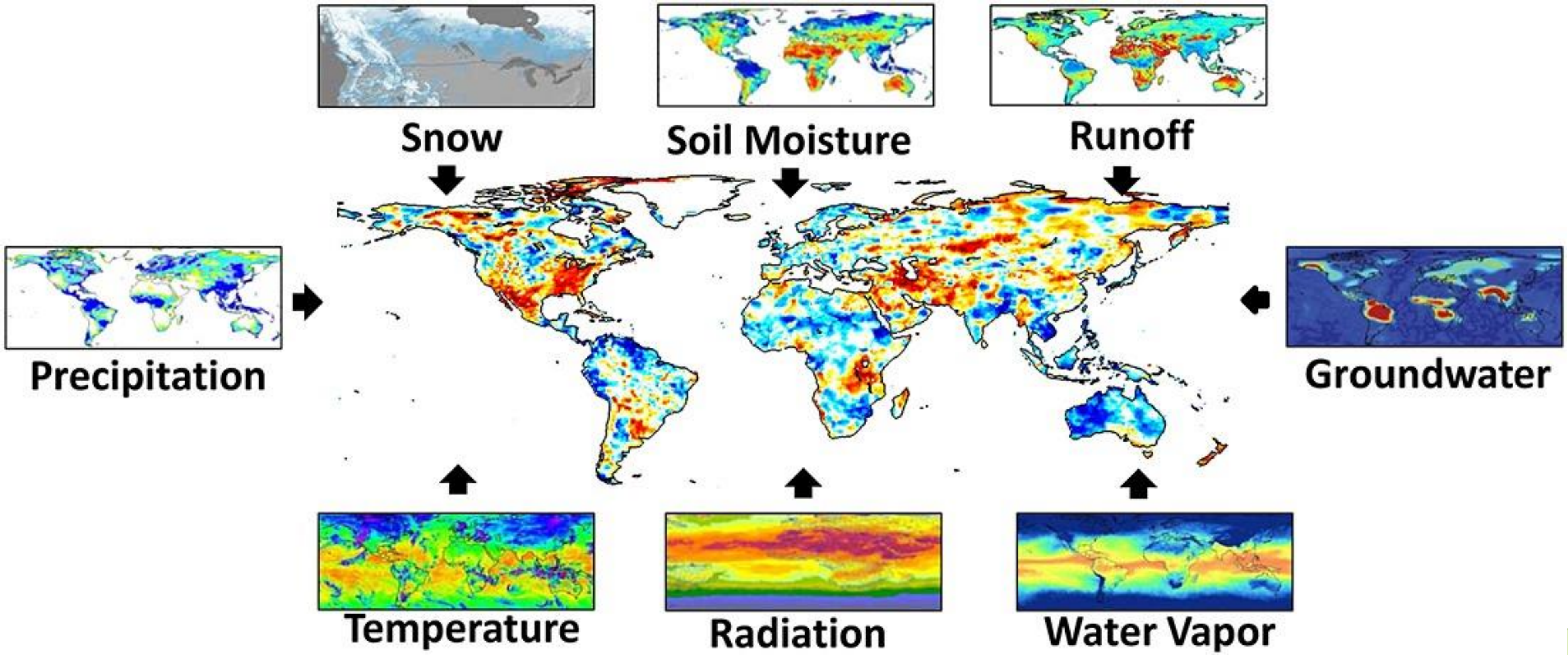

Sensing case in India

Data

- Precipitation: gridded precipitation
- Soil moisture: ESA CCI-SM
- Surface temperature: MOD11C3-006
- NDVI: MOD13C2 VI CMG L3 product

- Groundwater change: GRACE data

Annual rainfall amounts to 1,100 mm
75% of India's annual rainfall in monsoon season

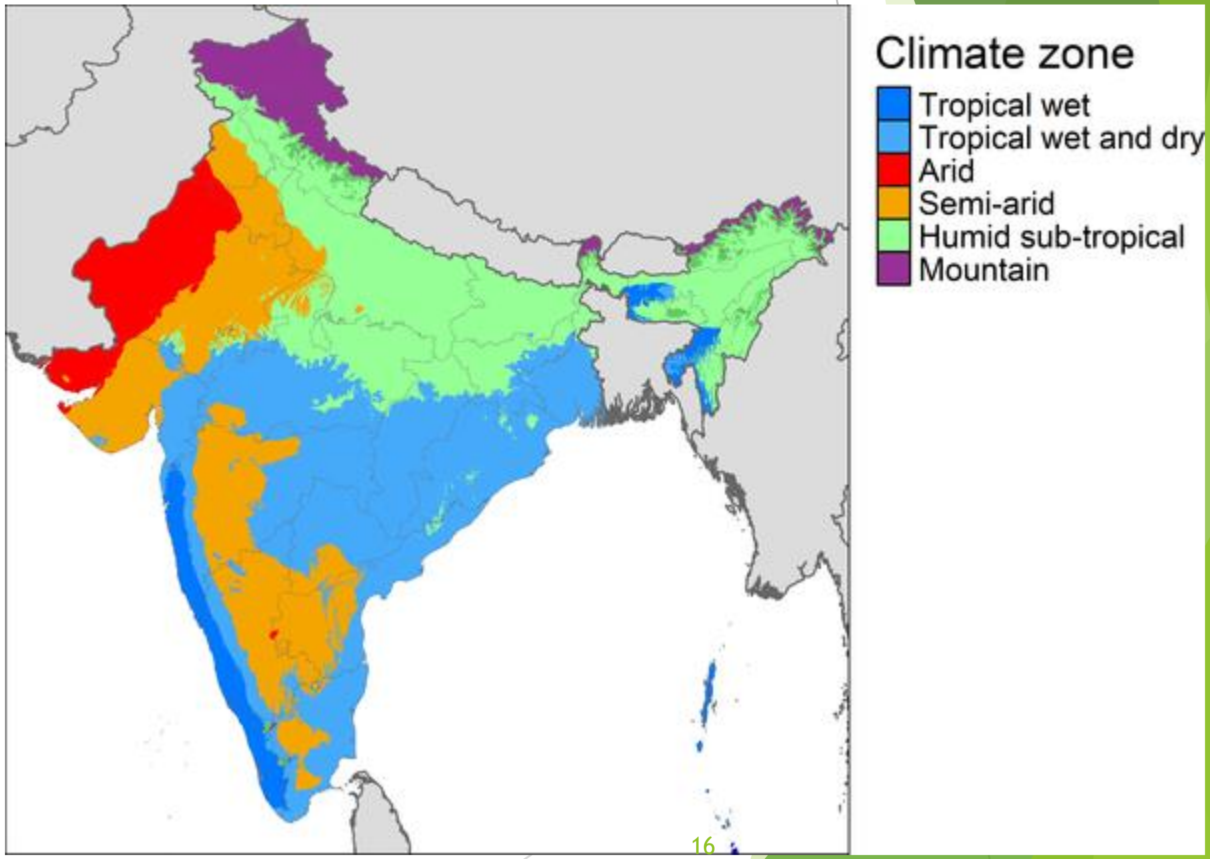

Multi senor data for drought detection

- The standardized drought analysis approach was utilized to compute multi sensor drought indexes. φ denotes the standard normal distribution function.

$$Y = \varphi^{-1}(p(x))$$

- Empirical probability from data distribution (Aghakouchak et al., 2015)
- Using empirical function.

$$p(x_i) = \frac{i - 0.44}{n + 0.12}$$

Category	SPI, SSI, SVCI and SVHI
Extremely wet	≥ 2.00
Severely wet	1.50 to 1.99
Moderately wet	1.00 to 1.49
Mild wet	0.00 to 0.99
Mild drought	−0.99 to 0.00
Moderate drought	−1.49 to −1.00
Severe drought	−1.99 to −1.50
Extreme drought	≤ −2.00

Multi senor data for drought detection

Vegetation condition index (VCI)

$$VCI = \frac{NDVI_i - NDVI_{min}}{NDVI_{max} - NDVI_{min}},$$

Temperature condition index (TCI)

$$TCI = \frac{LST_{max} - LST_i}{LST_{max} - LST_{min}},$$

LST: land surface temperature

Vegetation health index (VHI)

$$VHI = \alpha\, VCI + (1 - \alpha) TCI,$$

Multi senor data for drought detection in India

2009

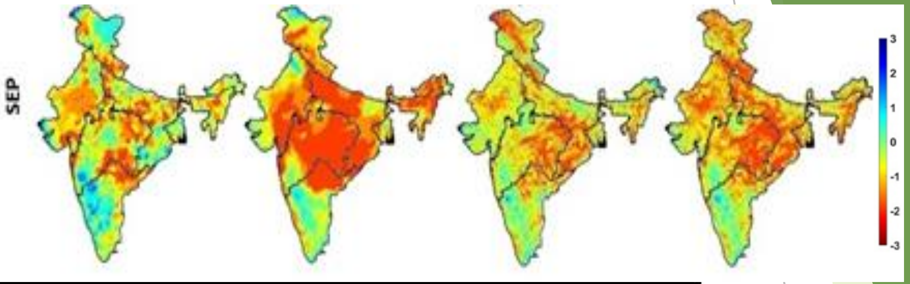

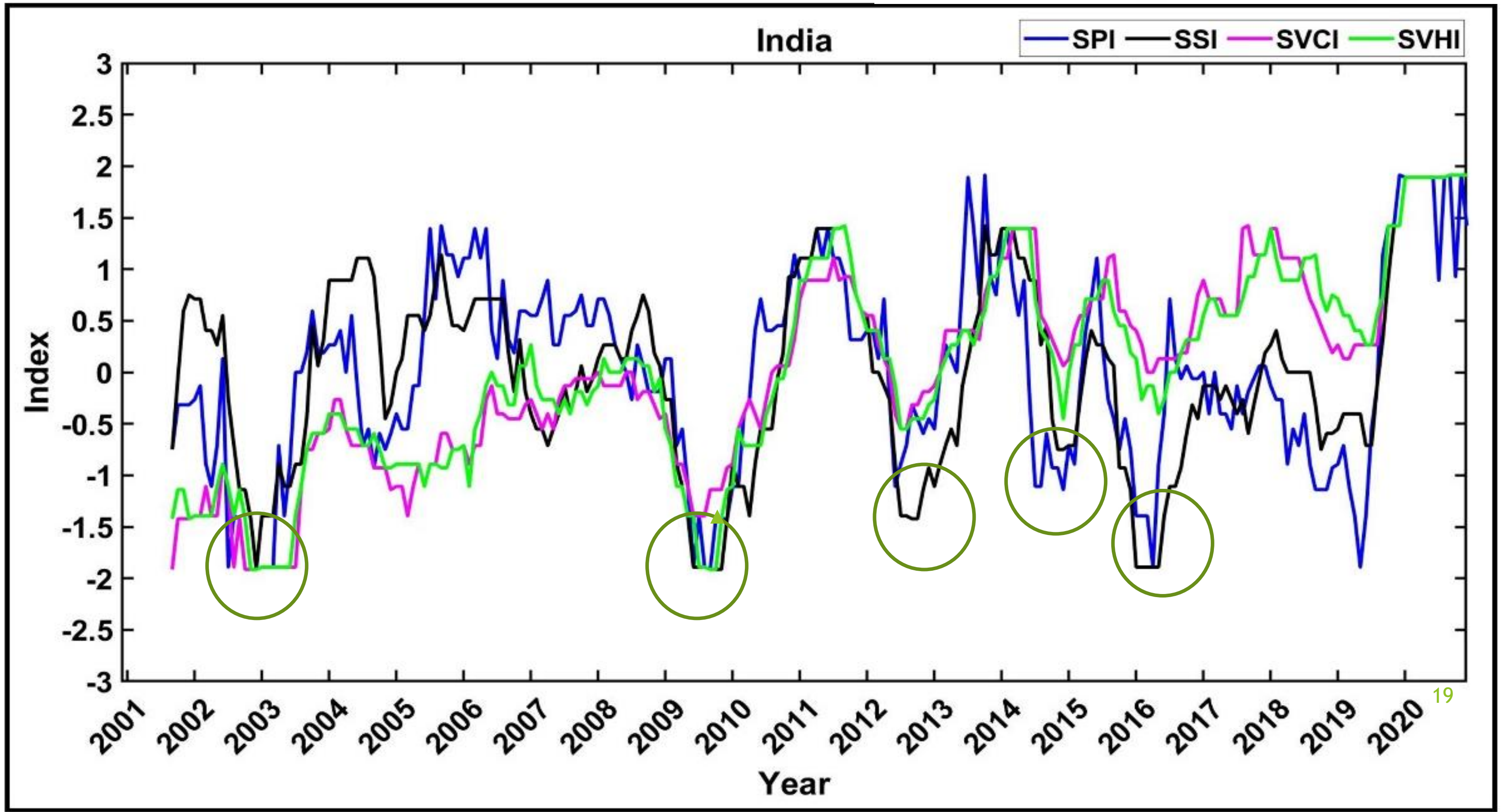

Groundwater Storage Depletion Detection using GRACE Measurement

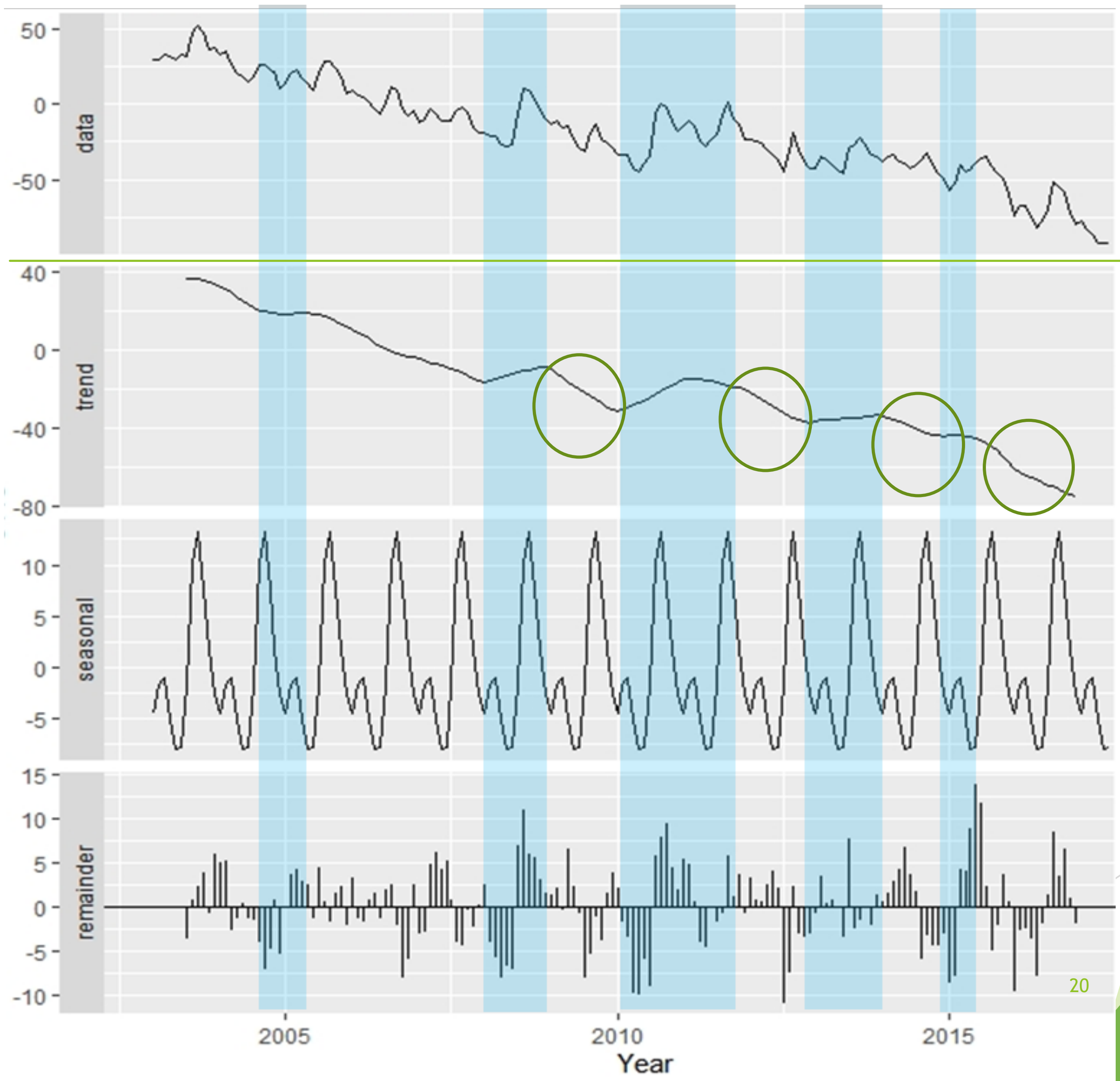

= Trend + Seasonality + Random

Spatial resolution:
27.75 km

Comparison

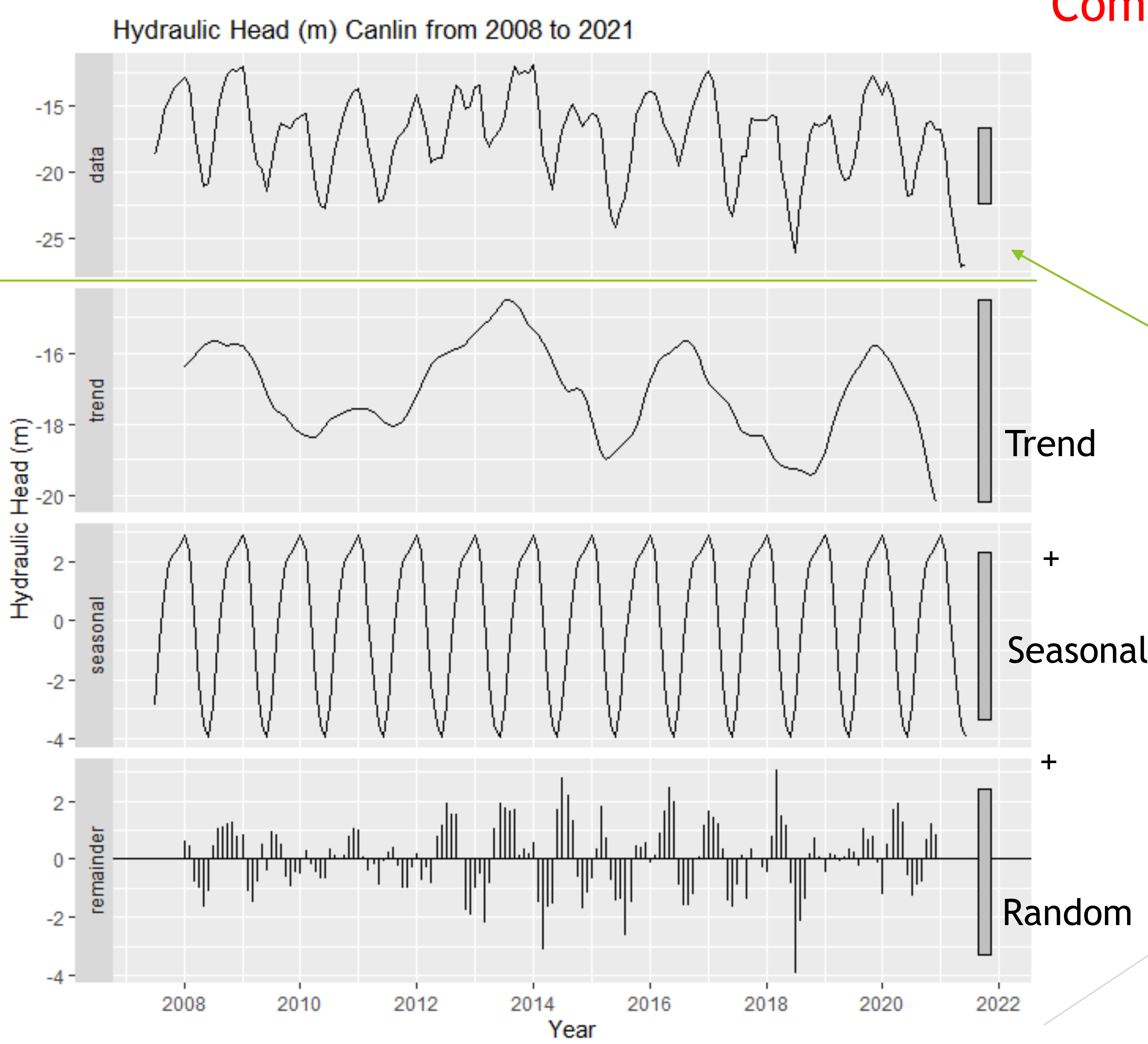
Hydraulic Head (m) Canlin from 2008 to 2021
data
trend
seasonal
remainder
Hydraulic Head (m)
Year
Trend
+
Seasonality
+
Random

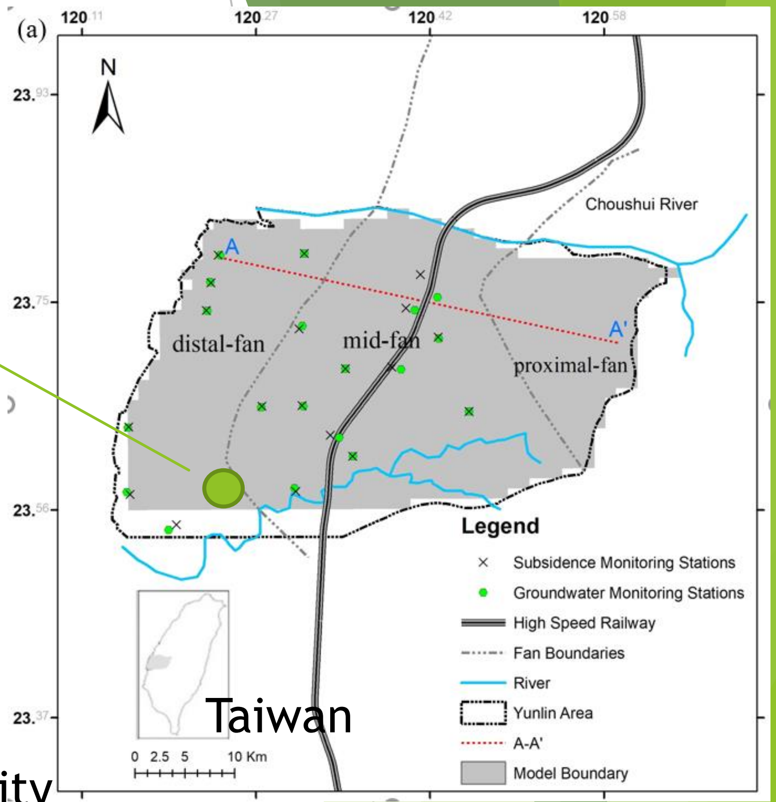
(a)
Choushui River
distal-fan
mid-fan
proximal-fan
A
A'
Taiwan
0 2.5 5 10 Km
Legend
Subsidence Monitoring Stations
Groundwater Monitoring Stations
High Speed Railway
Fan Boundaries
River
Yunlin Area
A-A'
Model Boundary

Drought detection in central Taiwan

Groundwater change in Taiwan Using 81 observed wells with 2001~2021/6

- Severe drought happened at 2004 and 2021 from SGI

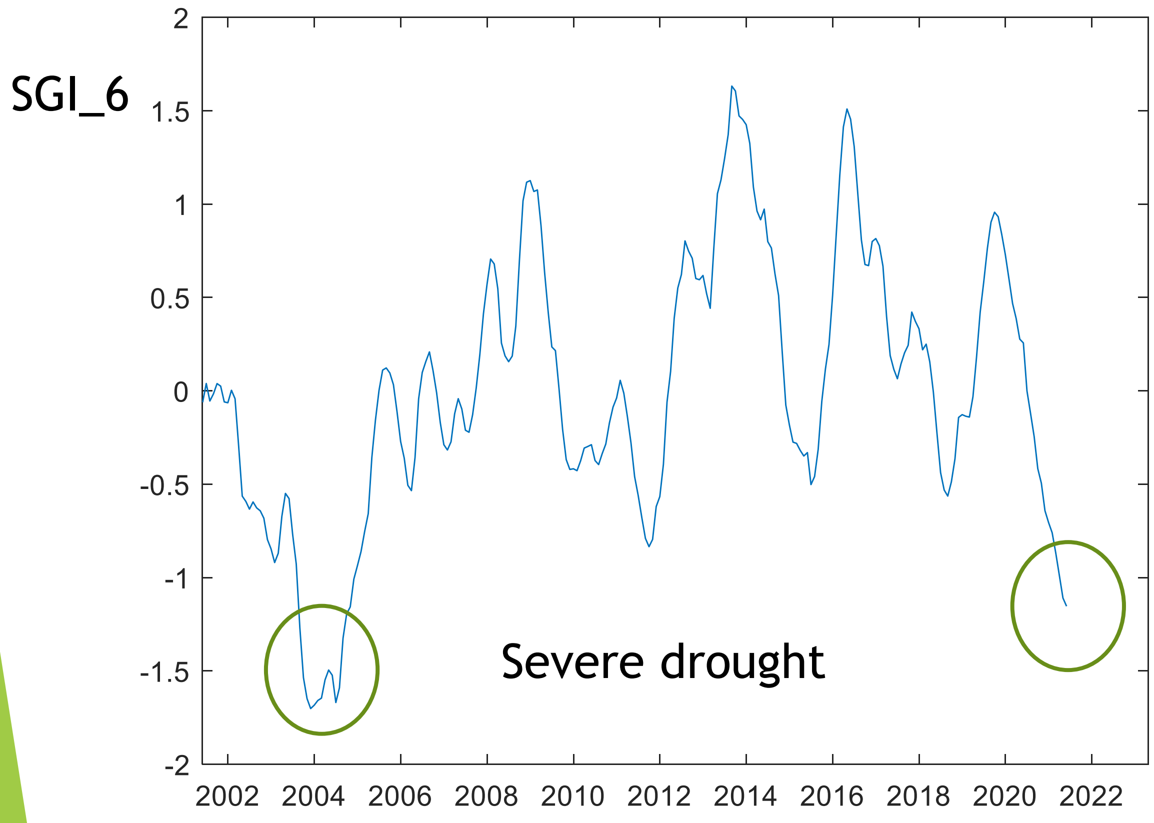

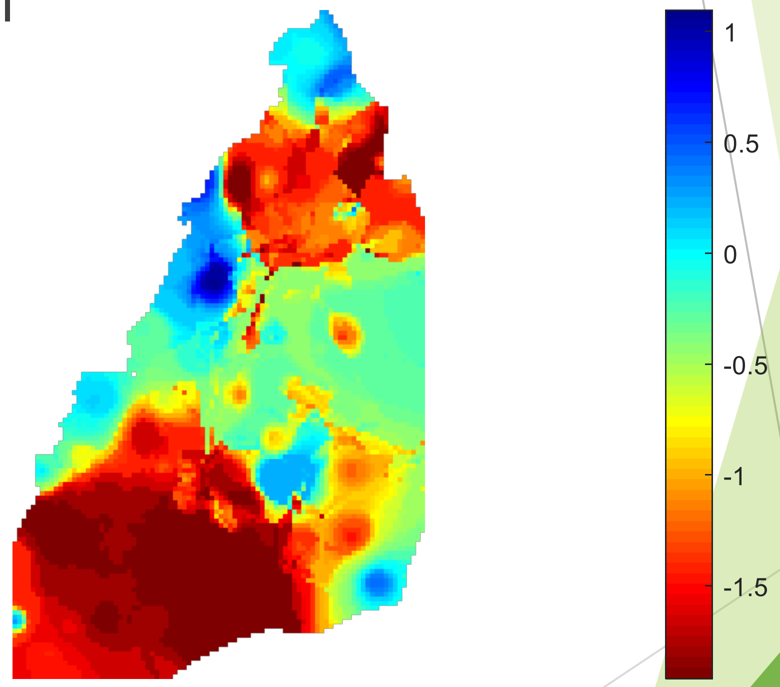

Spatial patterns in 2021

Part II:

- Data integration technology
  - High-spatial-resolution Sensing (Downscaling)
  - High-spatio-temporal-resolution Sensing (Data fusion)

3. Data integration for downscaling

- TRMM rainfall data: spatial resolution of 0.25°

- The ability of a remote sensing sensor to detect details is referred to as spatial resolution: Downscaling

- Sentinel 3 SLSTR: NDVI and LST

  spatial resolution of 1 km

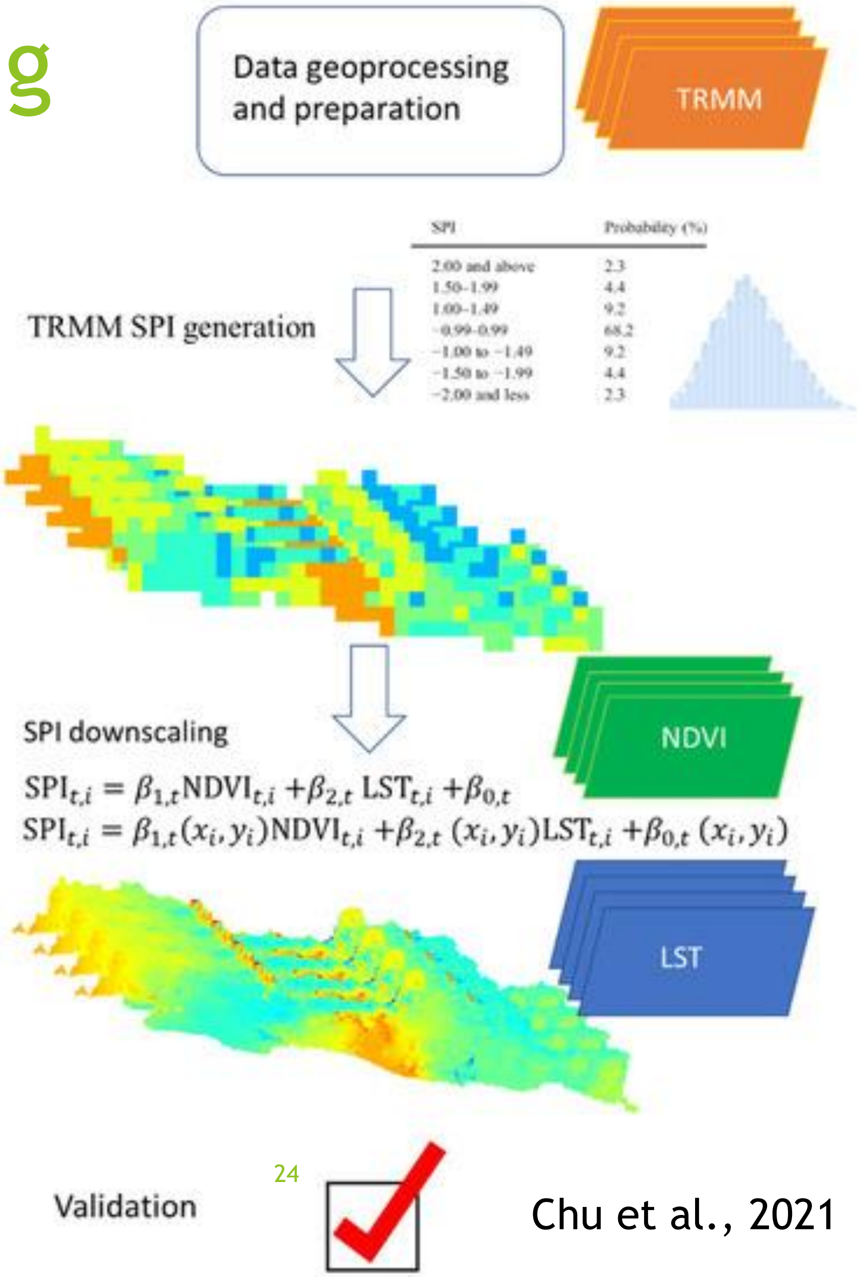

Chu et al., 2021

Data integration for downscaling

- Drought index (SPI)

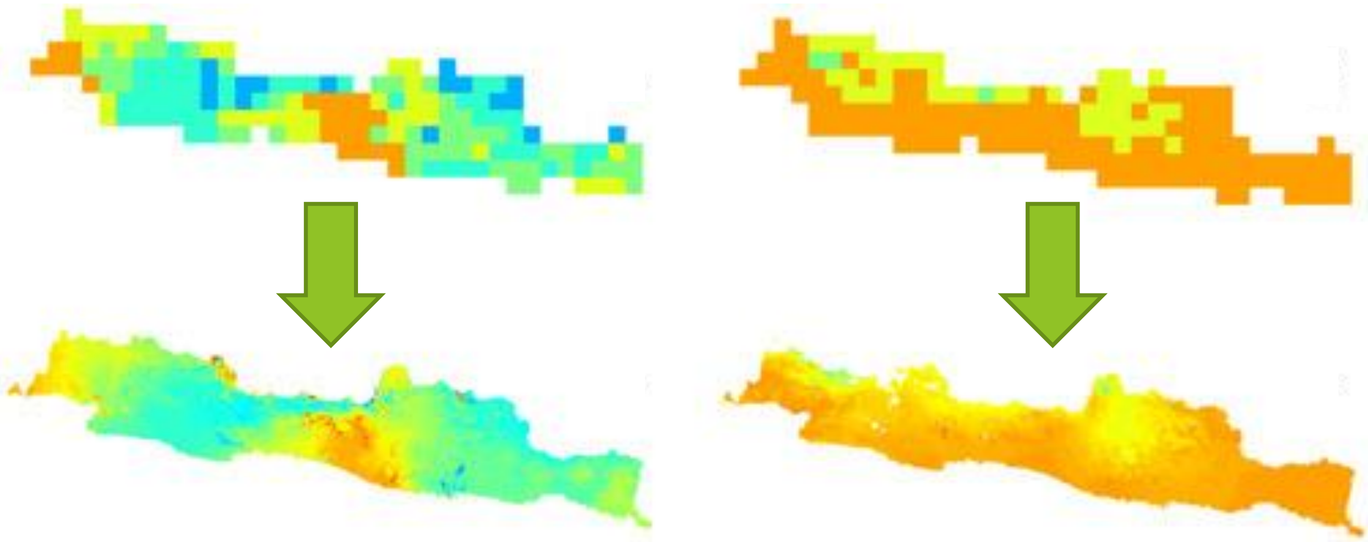

27.75 km

1 km

June in 2019

December in 2019

Data integration: High-spatio-temporal-resolution Sensing

- Data fusion

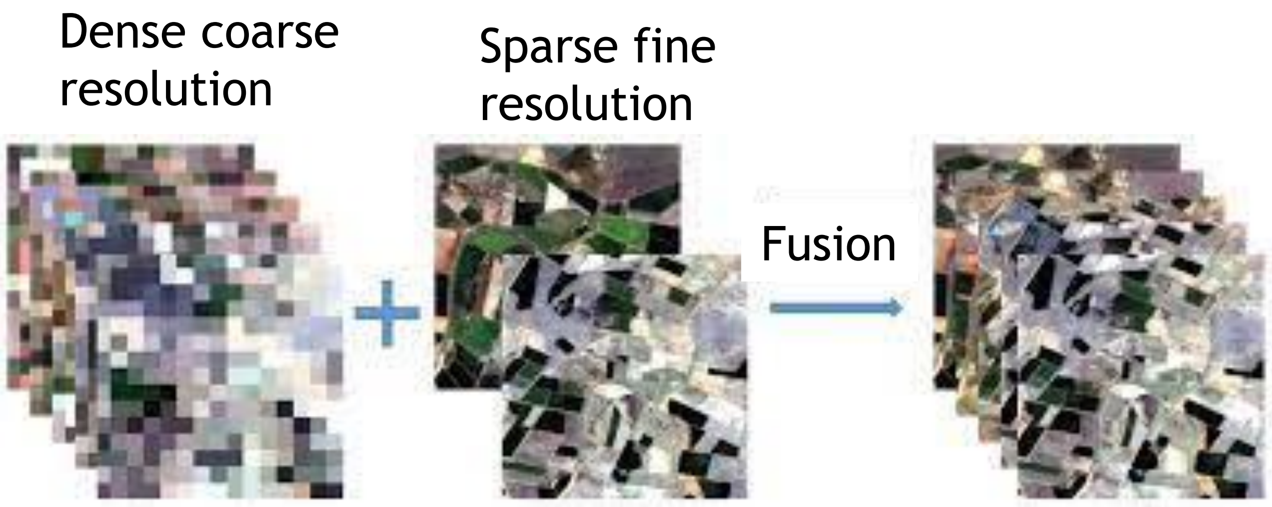

Sentinel 3	Sentinel 2	
2 days	5 days	Temporal resolution
300 m	10 m	Spatial resolution

Data integration: High-spatio-temporal-resolution Sensing

- Fusion using machine learning for water quality mapping

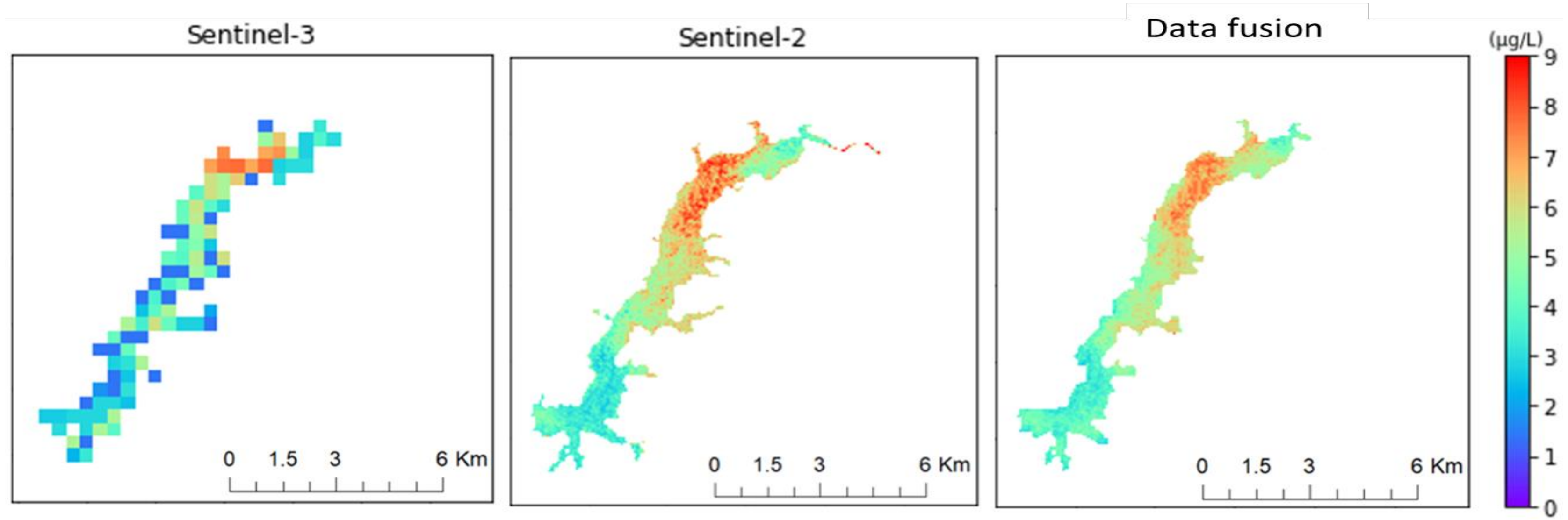

Chusnah (2021)

Data integration: High-spatio-temporal-resolution Sensing

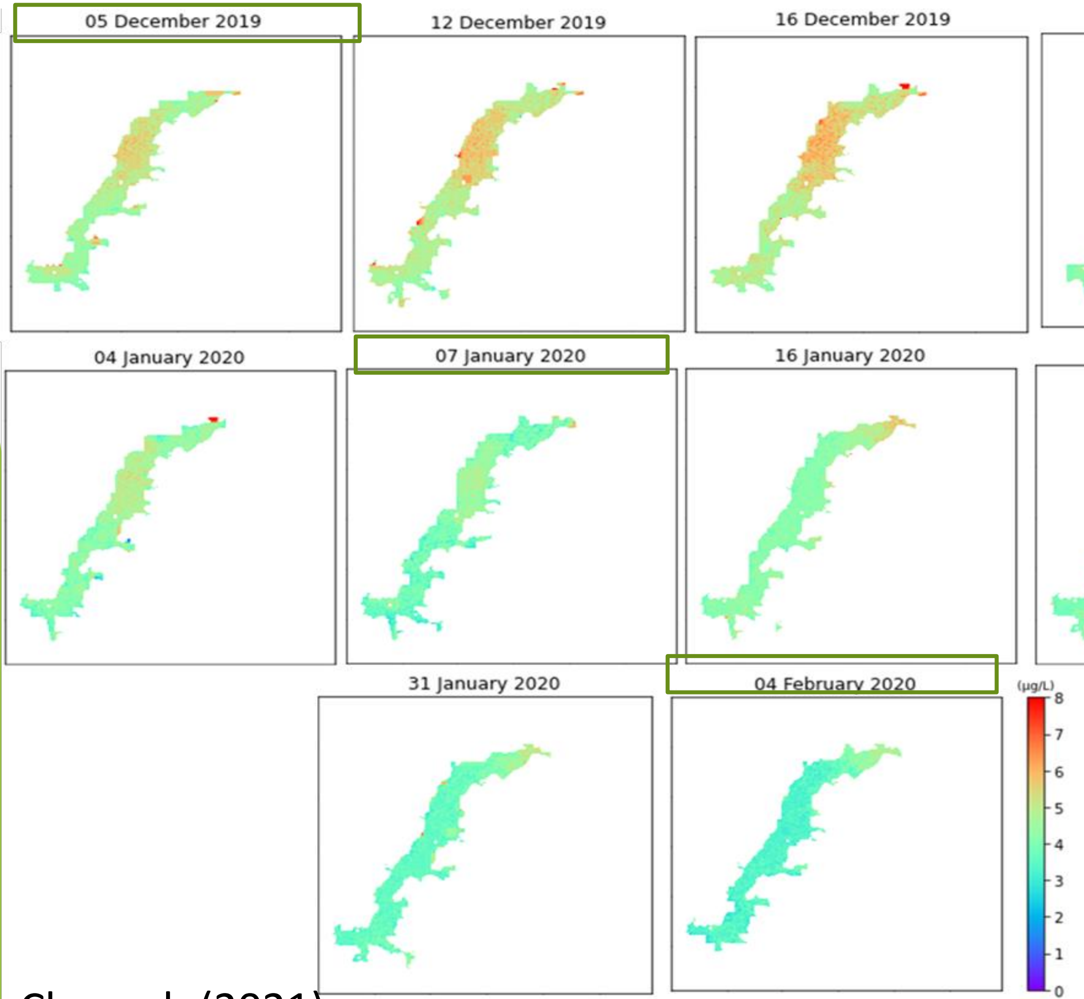

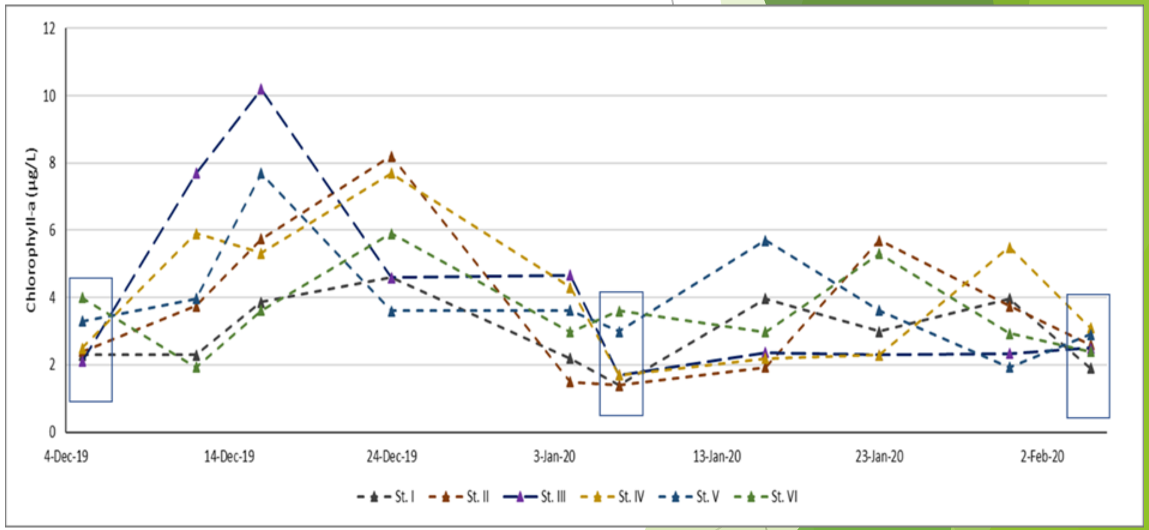

EPA Observation

Chusnah (2021)

Conclusion I

- This study examined variation in many components with changes. Many existing changes are stressed in water scarcity and flood risk.
- Sensing data sets captured the inter- and intra-annual variability of surface water occurrences, such as reservoir changes, and groundwater storages changes.
- Drought detection helped us to assess severe impacts for management over space and time.
- When compared to the case in India, groundwater storage in Taiwan is more stable without depletion.

Conclusion II

- Leverage a combination of sensors and techniques across a range of spatiotemporal scales. Data fusion and visualization are the tools to understand the changes.
- To progress and advance our understanding, characterization and description of water resources will be considered from multi-senor in the future.
- This study will quantify the influence of changes on hydrologic cycles.

Suggestion

- Real-time drought observation
- AI-based drought detection for water management
- Future drought prediction and adaption under climate change

Suggestion

DATA & MAPS

National Current Conditions

September 28, 2022 - October 4, 2022

Drought and Abnormal Dryness (D0) continue to develop and intensify from the Plains through the Mississippi River Basin, and have now extended further into the Midwest and Southeast. Low water levels are impacting barge traffic on the Mississippi River during the harvest, a crucial time. As of October 4, 2022, 44.04% of the U.S. and 52.55% of the lower 48 states are in drought.

44.04%
of the U.S. and 52.55% of the lower 48 states are in drought this week.

up 3.3% since last week
up 19.2% since last month

321.6 Million
acres of crops in U.S. are experiencing drought conditions this week.

same 0.0% since last week
up 33.4% since last month

126.2 Million
people in the U.S. and 125.3 Million in the lower 48 states are affected by drought this week.

up 5.0% since last week
up 10.6% since last month

41
U.S. states are experiencing Moderate Drought (D1) or worse this week.

down 1 state since last week
down 2 states since last month

https://www.drought.gov/current-conditions

References

- Global land use changes are four times greater than previously estimated
- High-resolution mapping of global surface water and its long-term changes
- The impact of global land-cover change on the terrestrial water cycle
- Global Characterization of Inland Water Reservoirs Using ICESat-2 Altimetry and Climate Reanalysis
- Effects of land cover changes induced by large physical disturbances on hydrological responses in Central Taiwan
- Land Use and Cover Change in the Industrial Era: A Spatial Analysis of Alpine River Catchments and Fluvial Corridors
- Multi-sensor remote sensing for drought characterization: current status, opportunities and a roadmap for the future
- **Human alteration of global surface water storage variability**
- Time Varying Spatial Downscaling of Satellite-Based Drought Index

- Email: honejaychu@gmail.com

NATIONAL CHENG KUNG UNIVERSITY 1931

SATU

Satellite Remote Sensing of Blowing Dust and Impact Assessment Around Riverside in Central Taiwan

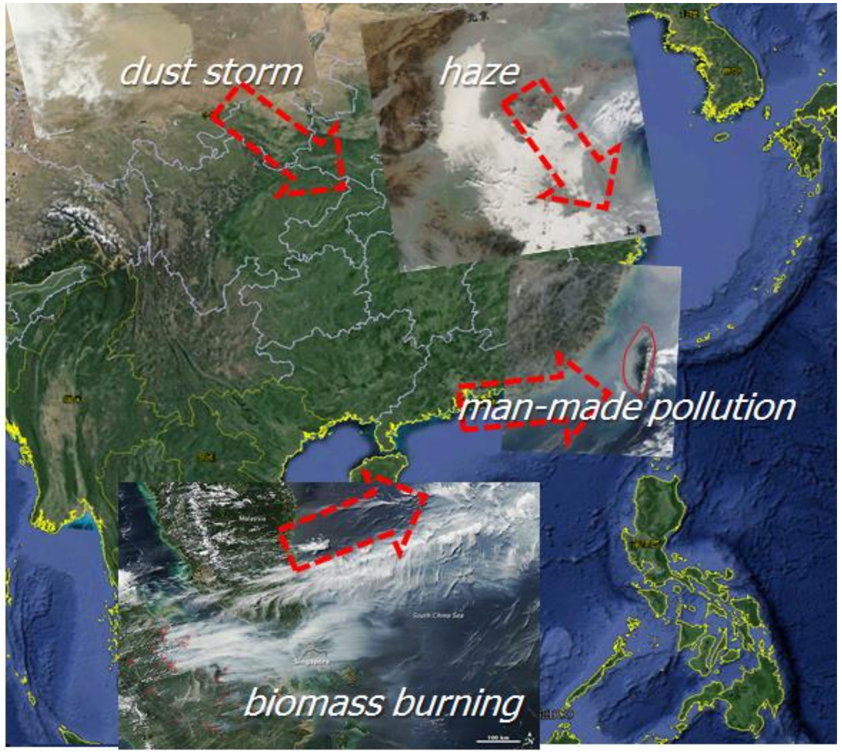

Tang-Huang Lin, Distinguished Prof. & Director
Center for Space and Remote Sensing Research, National Central University
E-mail: thlin@csrsr.ncu.edu.tw

國立中央大學
National Central University

CSRSR

ERSL
Environmental Remote Sensing Laboratory

Outline

- Background
  - ✓ Sources of Atmospheric Aerosols
  - ✓ Satellite Observation
- Advanced Remote Sensing of Aerosols
  - ✓ Aerosol Partitioning
  - ✓ Aerosol Profile Fitting
- Application- Blowing Dust Monitor
- Discussions

◆Background

✓ **Sources of atmospheric aerosols**

➢ **Nature**

➢ **Man-made**

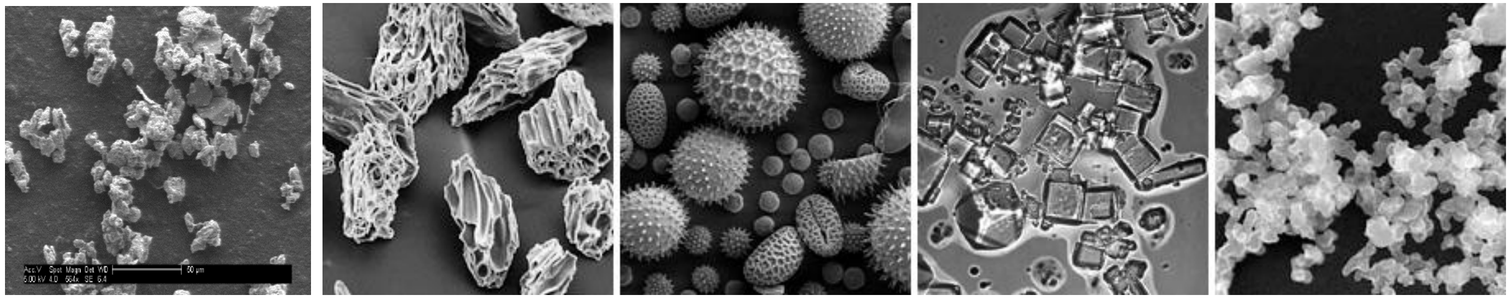

dust **volcanic ash** **pollen** **sea salt** **soot**

Satellite Observations

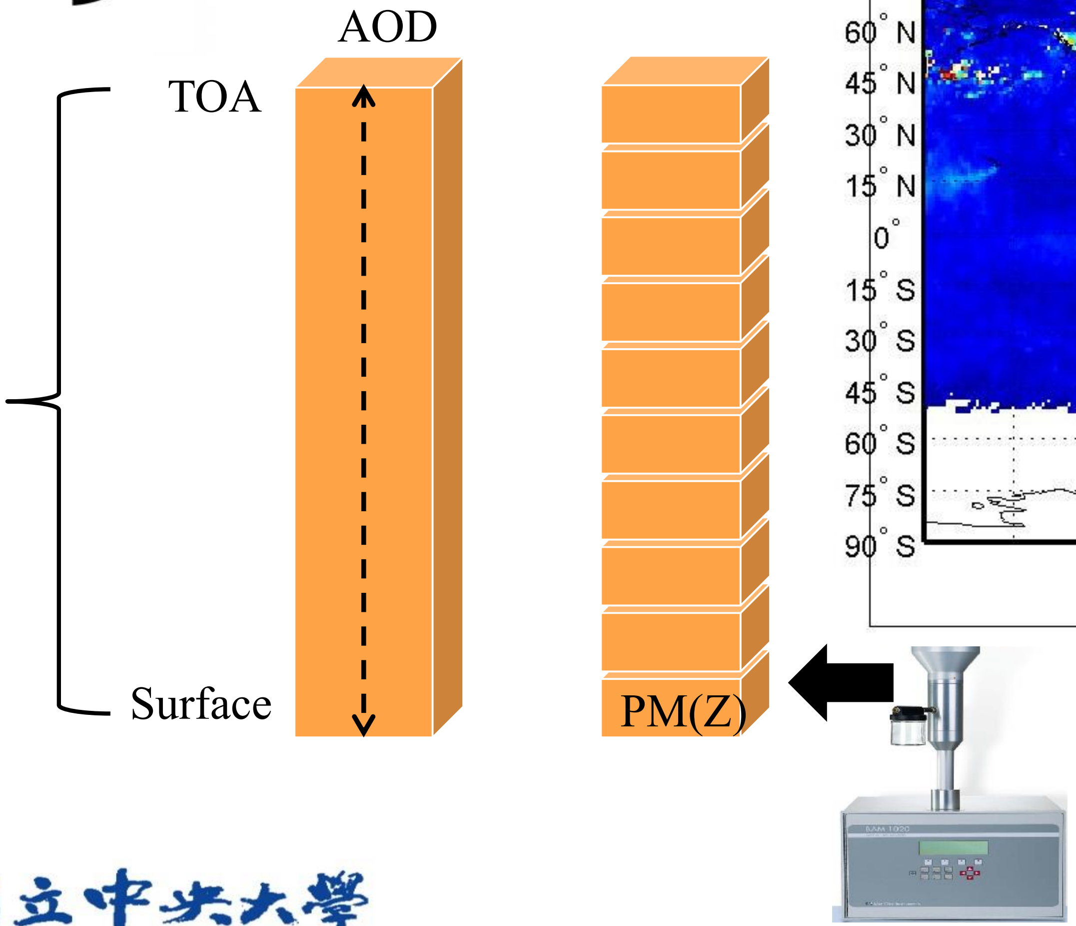

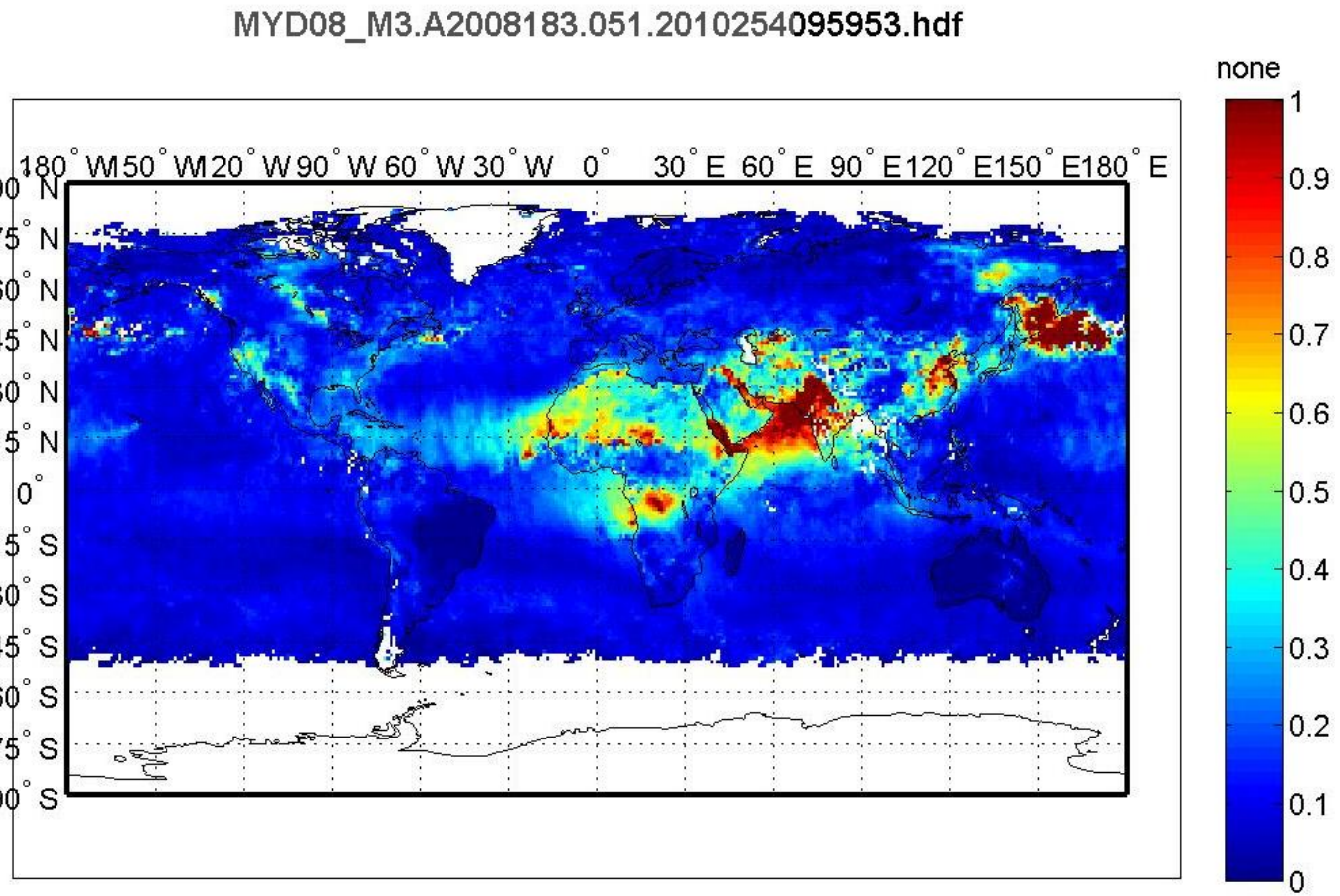

Aerosol Optical Depth (AOD, τ)

AOD

PM

$$\boxed{\tau_{a,0.55\ \mu m}} = \int_0^{TOA} \boxed{\rho(z)}\,\sigma^{ext}_{0.55\ \mu m}$$

Vertical p

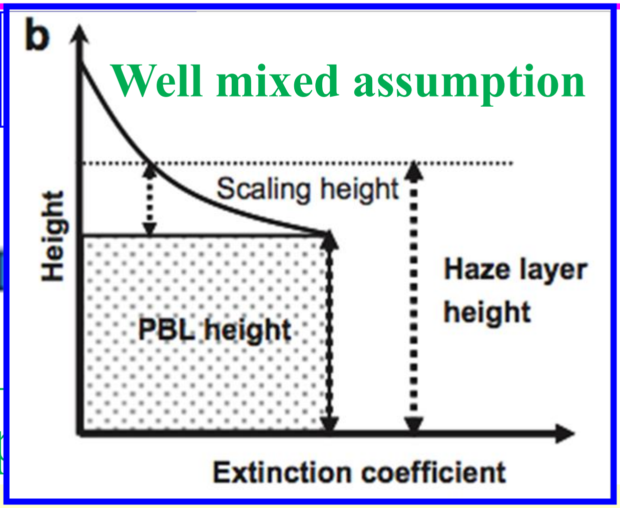

?

Spatial Distribution of Aerosols

(Simulated by NASA & NOAA)

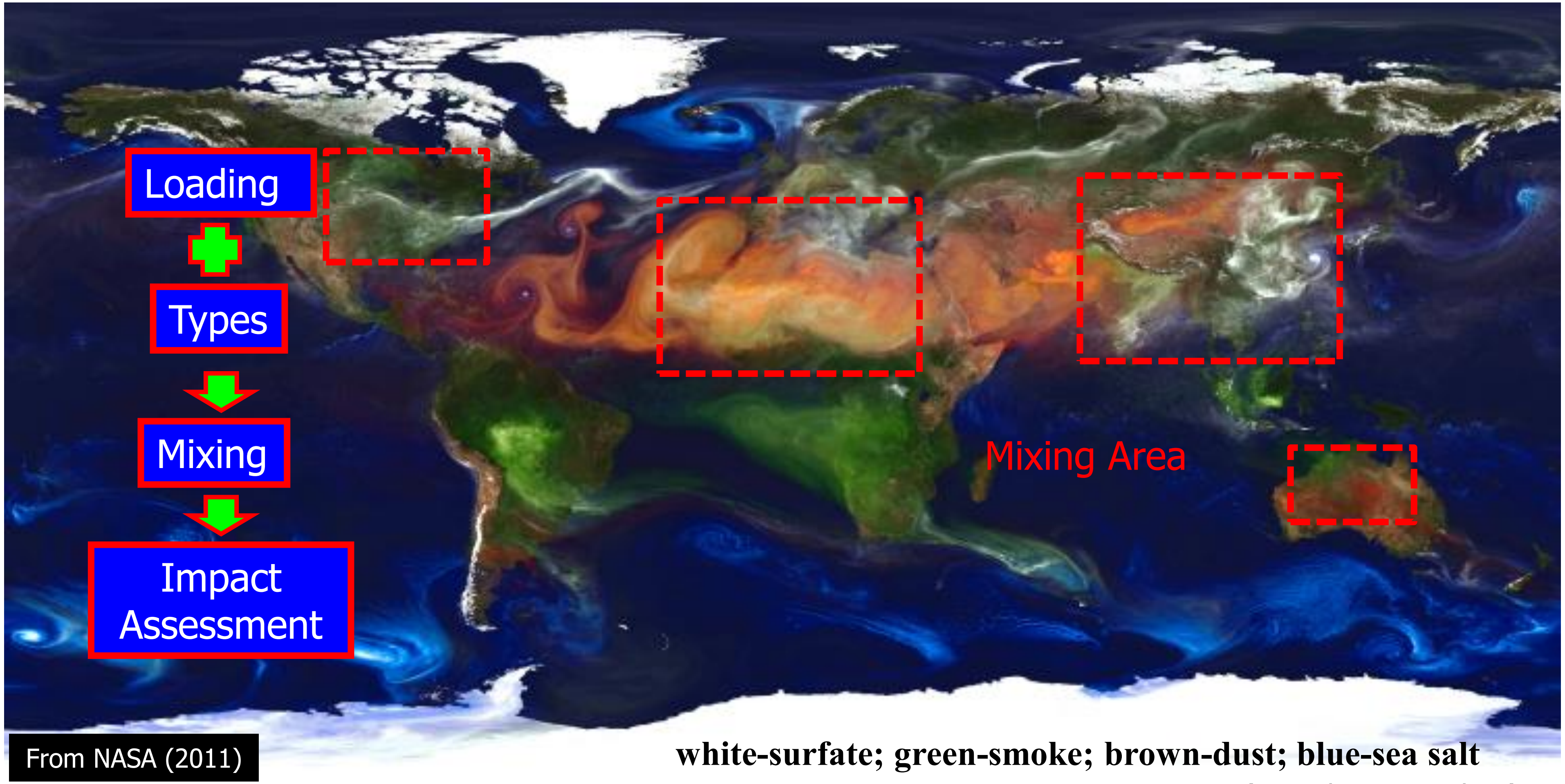

white-surfate; green-smoke; brown-dust; blue-sea salt

(2006/08~2007/04)

http://youtu.be/oRsY_UviBPE

$PM_{2.5}$ Estimation- present

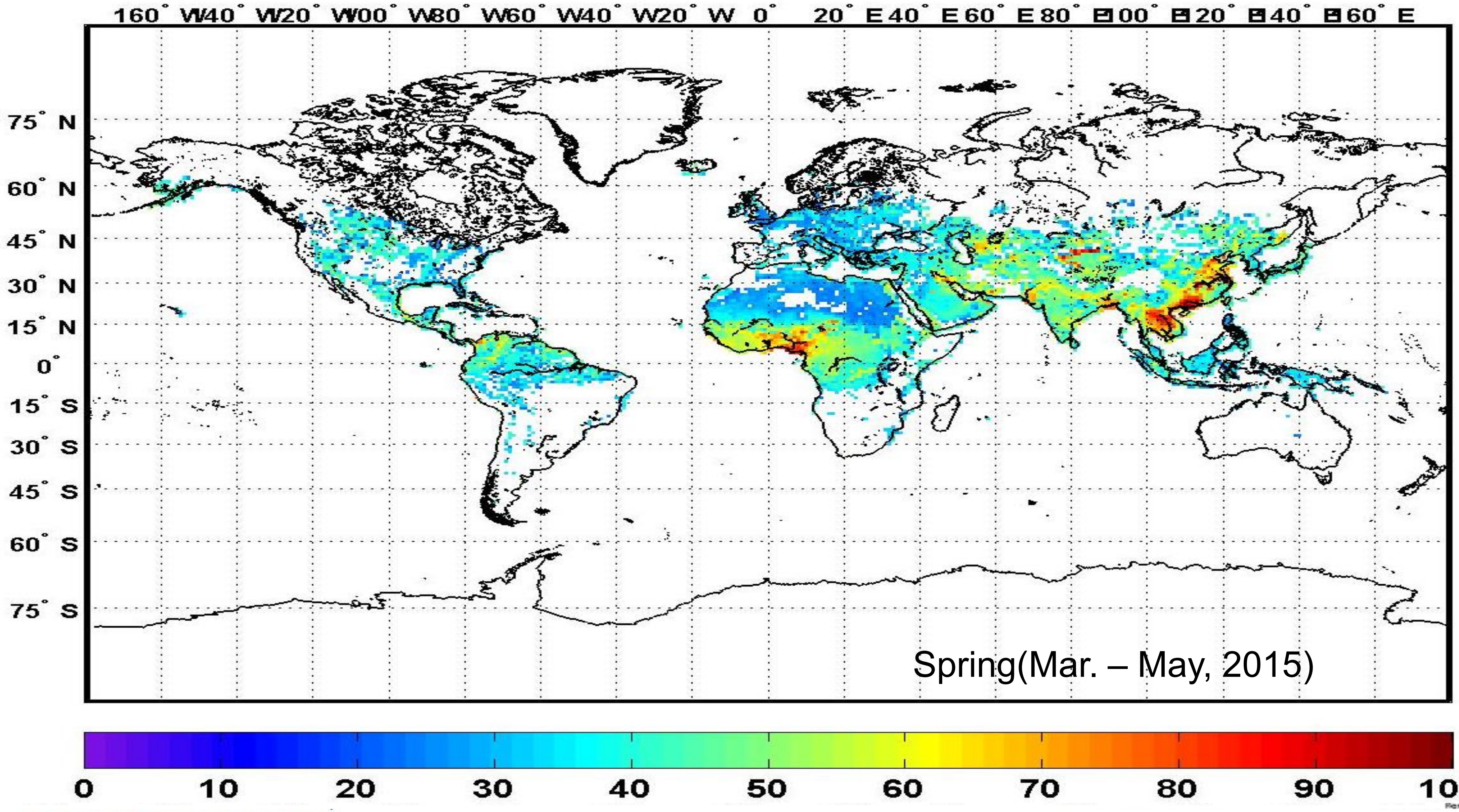

Focal Points- Remote Sensing (The Challenges)

- ✓**Aerosol identification & partition -** *major components* (mineral dust(DS), biomass burning(BB) and anthropogenic pollutant(AP) with *fraction*
- ✓**Vertical distribution -** Mathematical mapping
- ✓**Water effect -** Model simulation
- ✓**Relationship between AOD and $PM_{2.5}$ / PM_{10}**

✓ Aerosol Type Identification & Partition

➢ Data- global AERONET sites

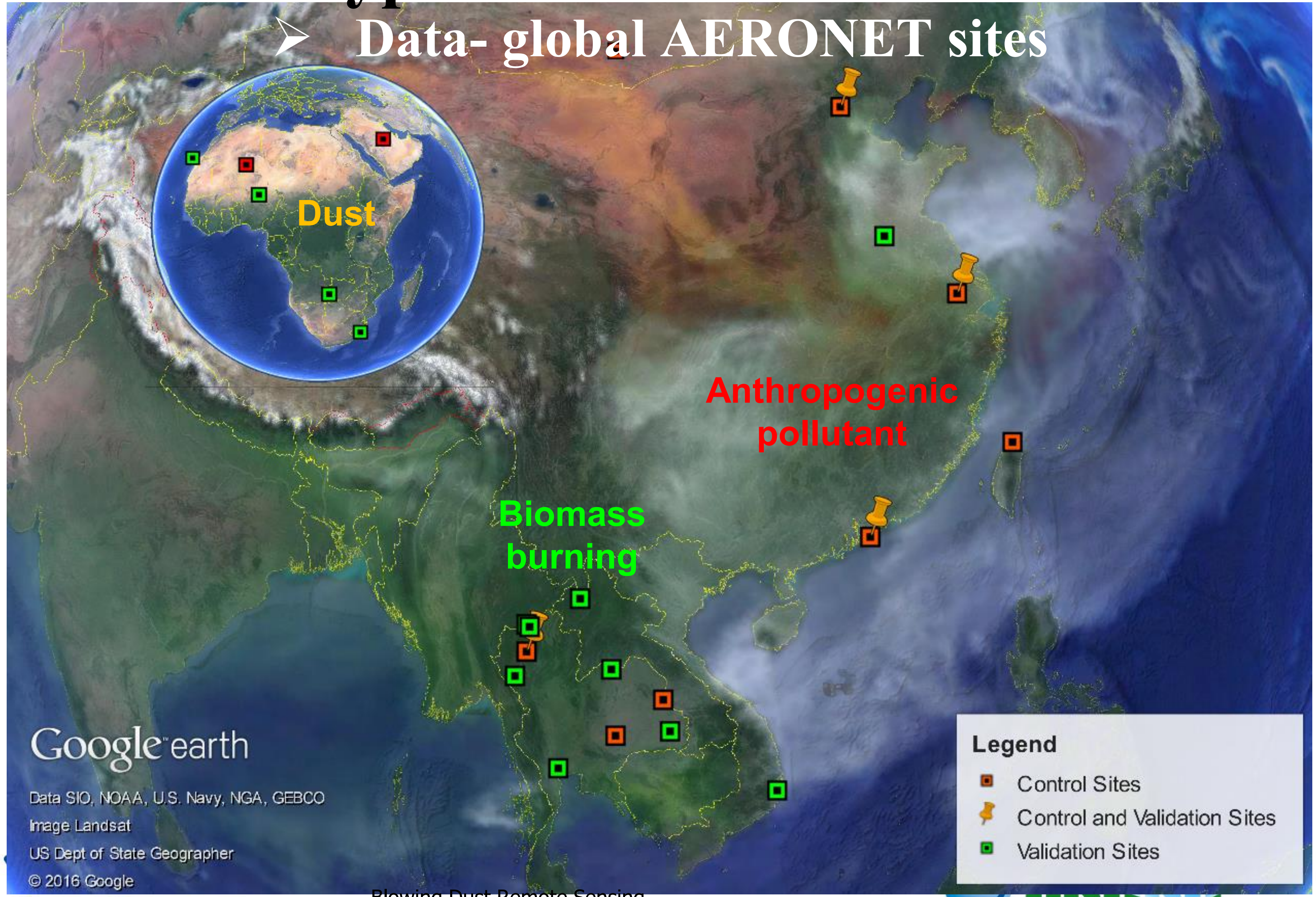

Control Dataset for Particle Size & Scattering/Absorption

AERONET (Surface)	Dusts (DS)	Biomass Burning (BB)	Anthropogenic Pollutants (AP)
Ångström exponent (**AE**) 440_675nm (**Particle Size**)	0.066 ± 0.055 (Coarse)	1.499 ± 0.096 (Fine mode)	1.105± 0.269 (Fine mode)
Single scattering albedo (**SSA**) 675nm (**Absorption; Scattering**)	0.958 ± 0.002	0.903 ± 0.024 (absorptive)	0.940 ± 0.031 (scattered)

MODIS (Satellite)	Dusts (DS)	Biomass Burning (BB)	Anthropogenic Pollutants (AP)
Ångström exponent (**AE**) 440_675nm	0.523±0.1833	1.3395±0.286	1.158±0.492
Single scattering albedo (**SSA**) 675nm	0.9311±0.0286	No information	No information

(with AOD > 0.8)

Physical Model & Normalization

Normalized Derivative Aerosol Index (NDAI) –

Spectral derivatives of optical depth in partitioning aerosol/ $PM_{2.5}$ types

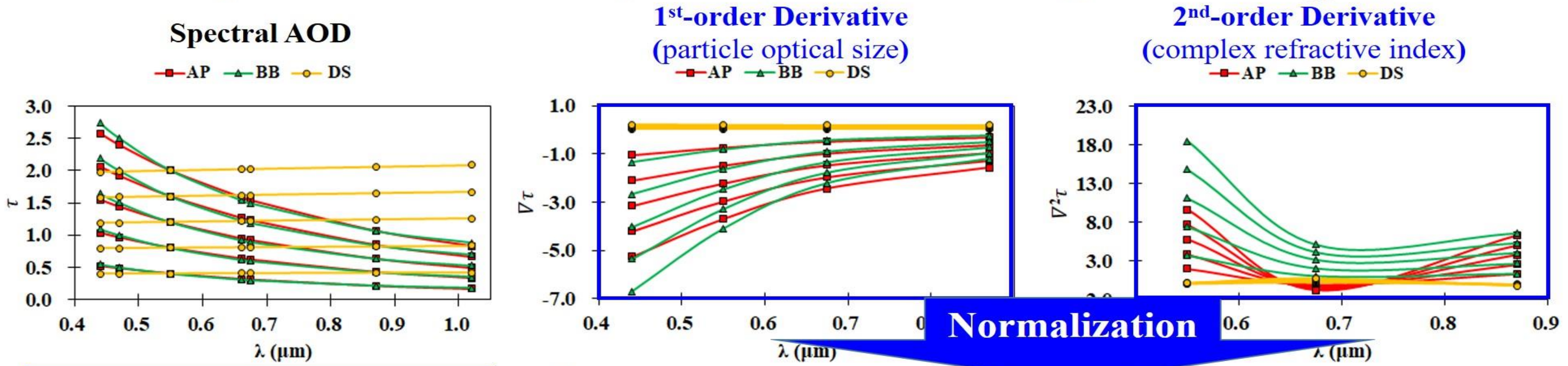

Normalized Intrinsic Parameters:

$$\mathrm{NDAI}_{(\lambda_1,\lambda_2)} \equiv \nabla\tau_{(\lambda_1,\lambda_2)} / \tau_{\lambda_{ref}}$$

$$\frac{\partial^2\tau}{\partial\lambda^2} / \tau_{\lambda_{ref}} \cong \nabla^2\tau_{(\lambda_1,\lambda_2,\lambda_3)} / \tau_{\lambda_{ref}}$$

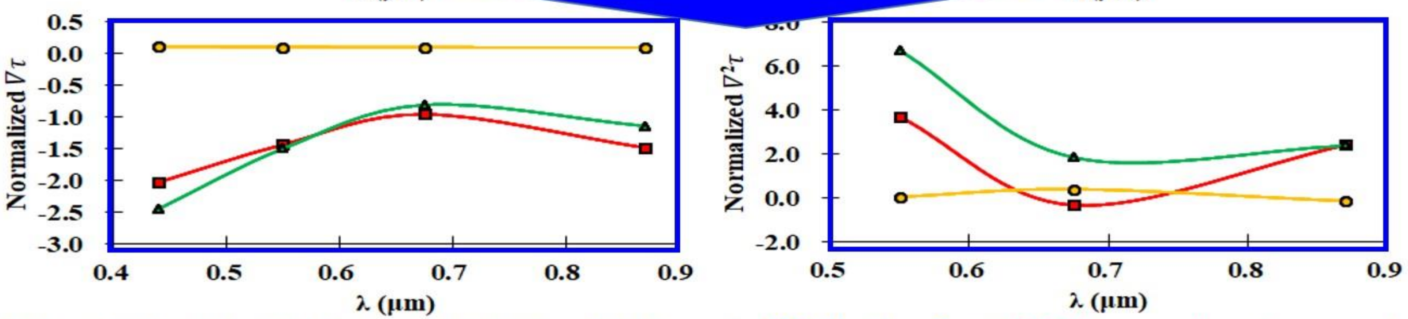

The simulated spectral aerosol optical depths (AODs) at 0.44, 0.47, 0.55, 0.66, 0.675, 0.87 and 1.02 μm for DS (dust, yellow), BB (biomass burning, green) and AP (anthropogenic pollutant, red) aerosols under $AOD_{(0.55\ \mu m)}$ values of 0.4, 0.8, 1.2, 1.6 and 2.0 from the 6S (Second Simulation of a Satellite Signal in the Solar Spectrum) model with the experimental dataset, and the results of spectral derivatives before and after AOD normalization indicating the intrinsic optical parameters.

Dataset Construction & Comparisions

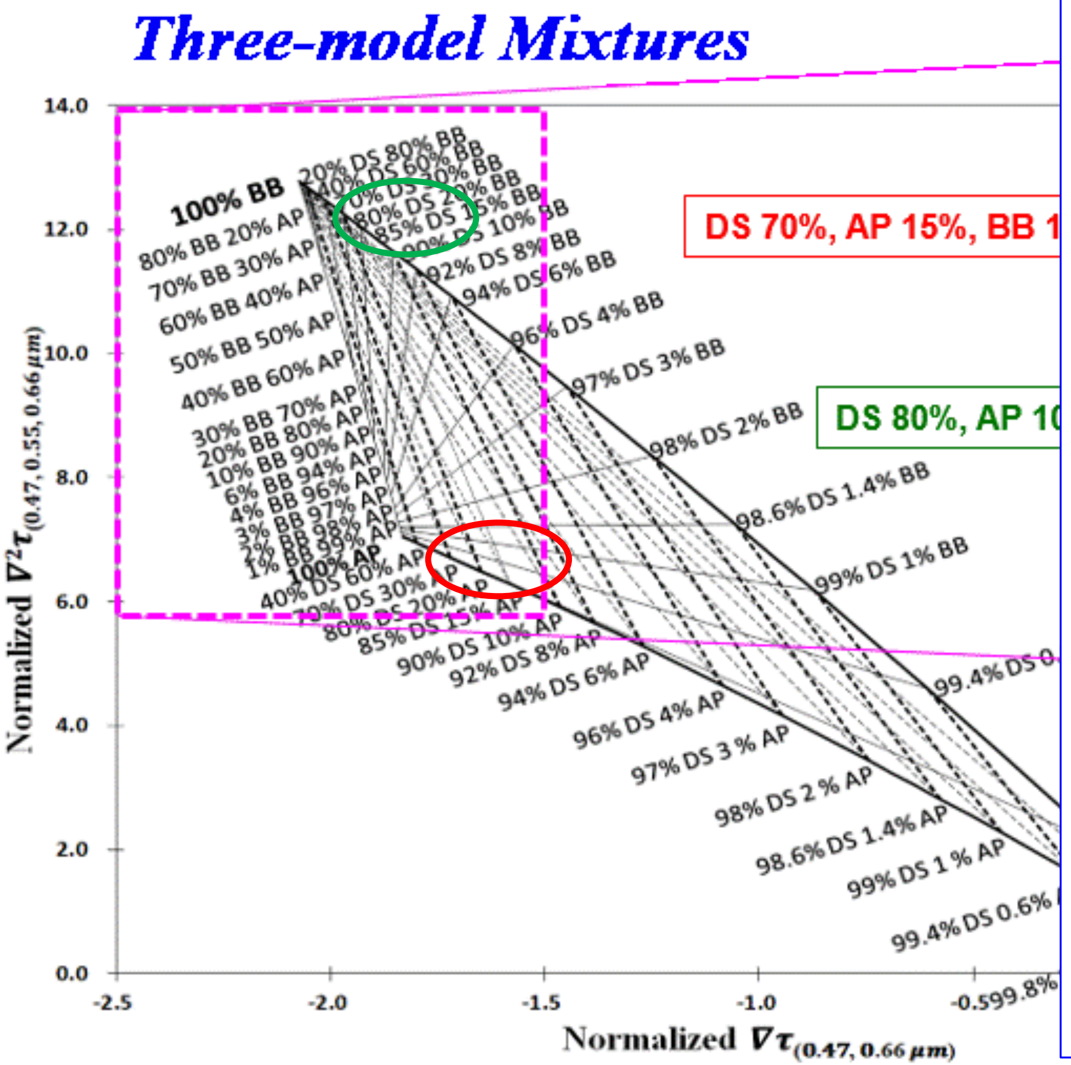

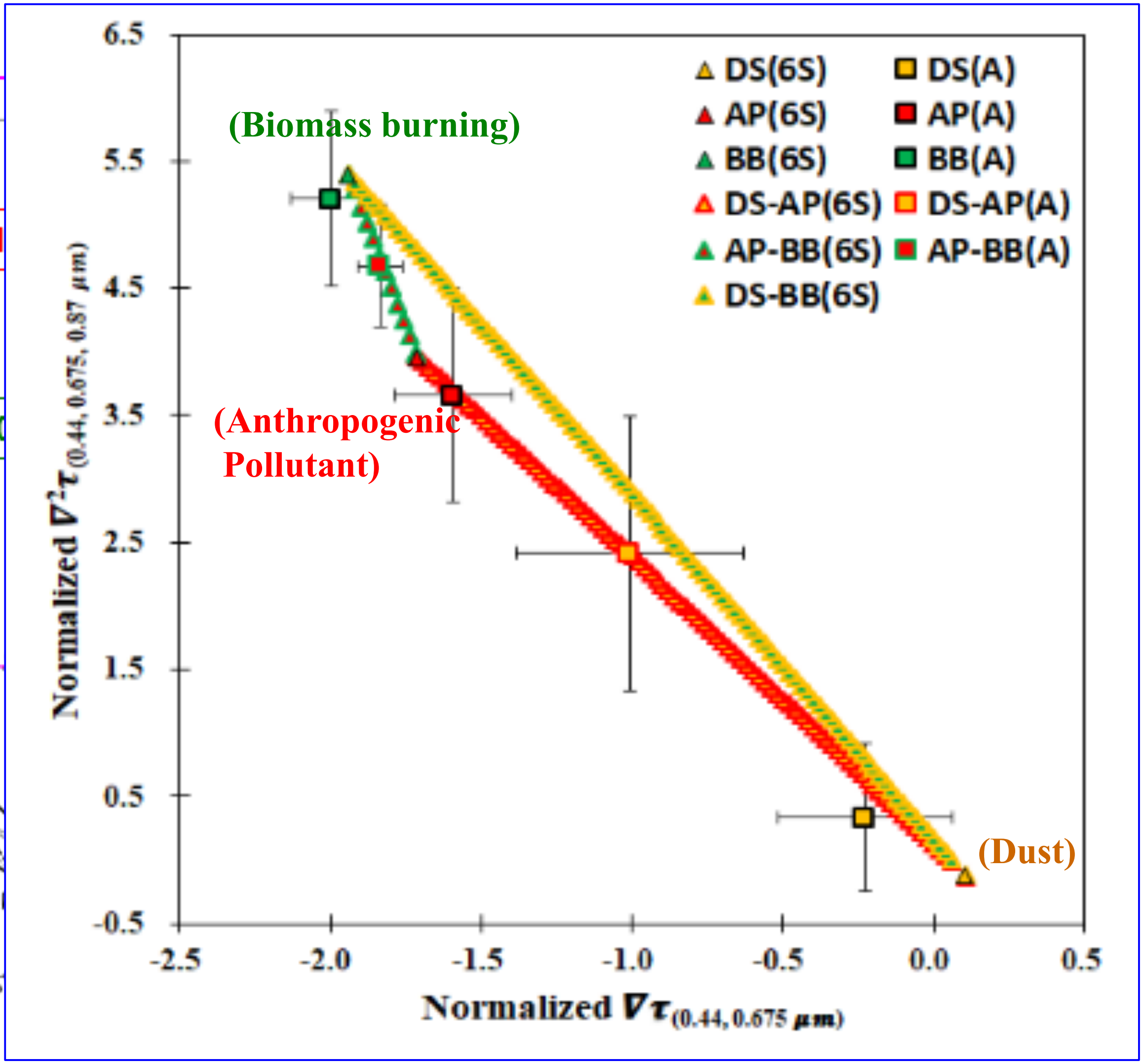

Case study- Aqua MODIS March 14, 2014

(e) Vertical aerosol subtypes

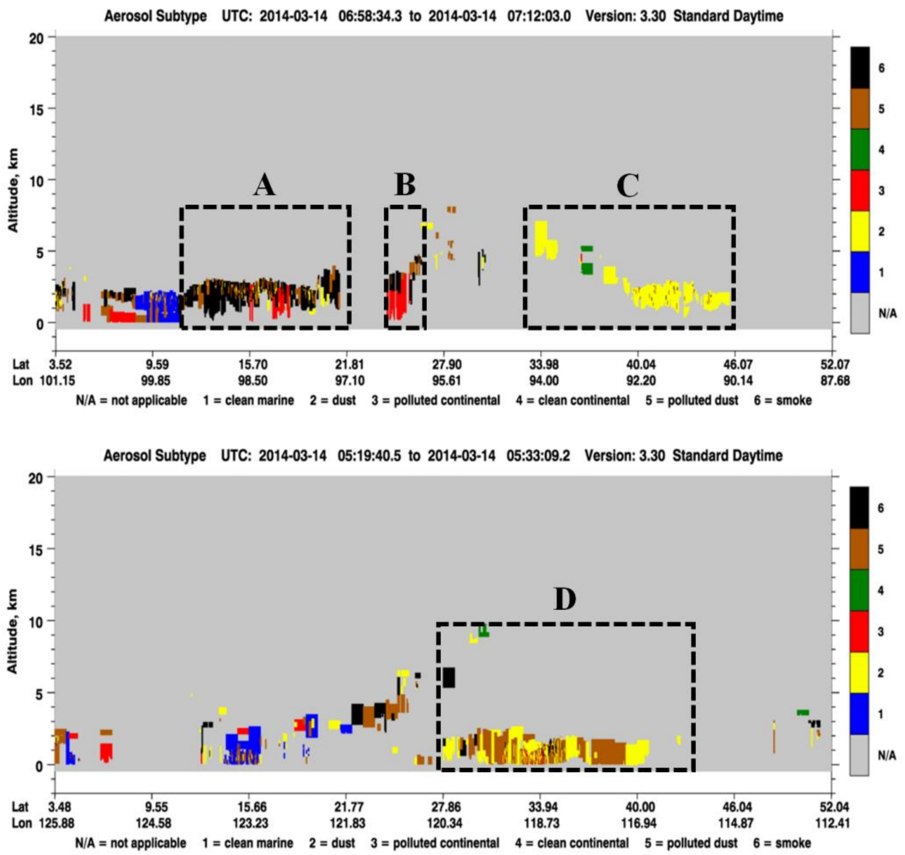

(f) Aerosol type with AOD fraction

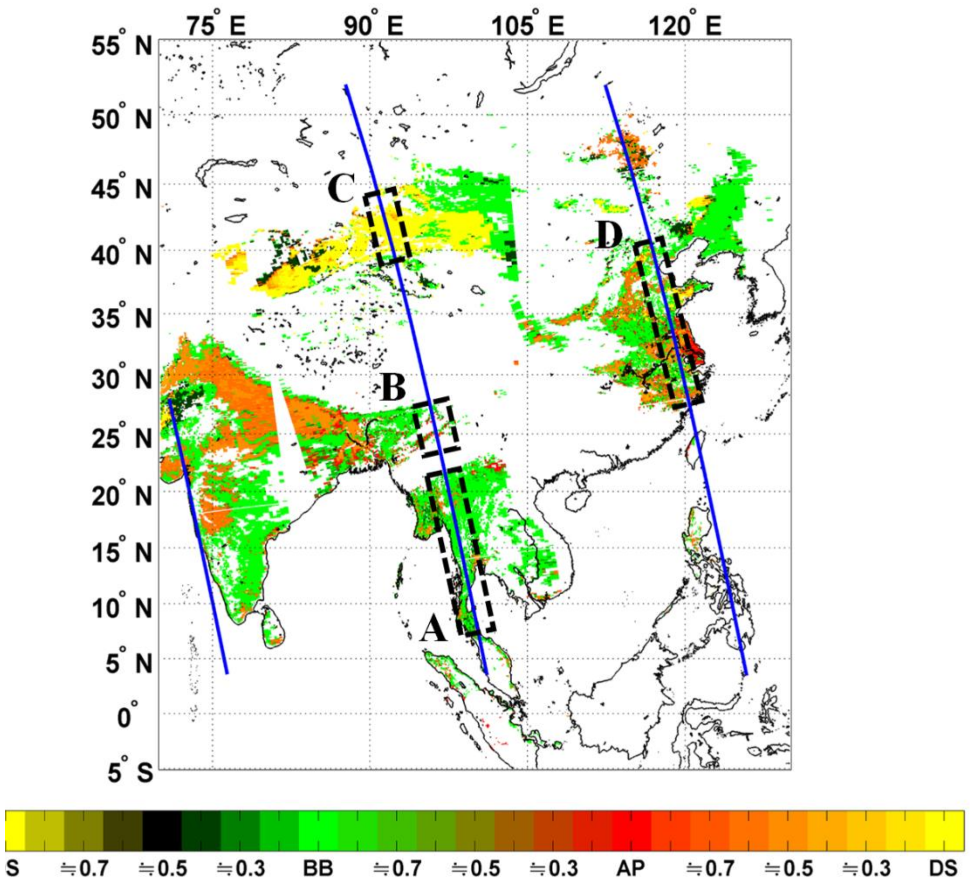

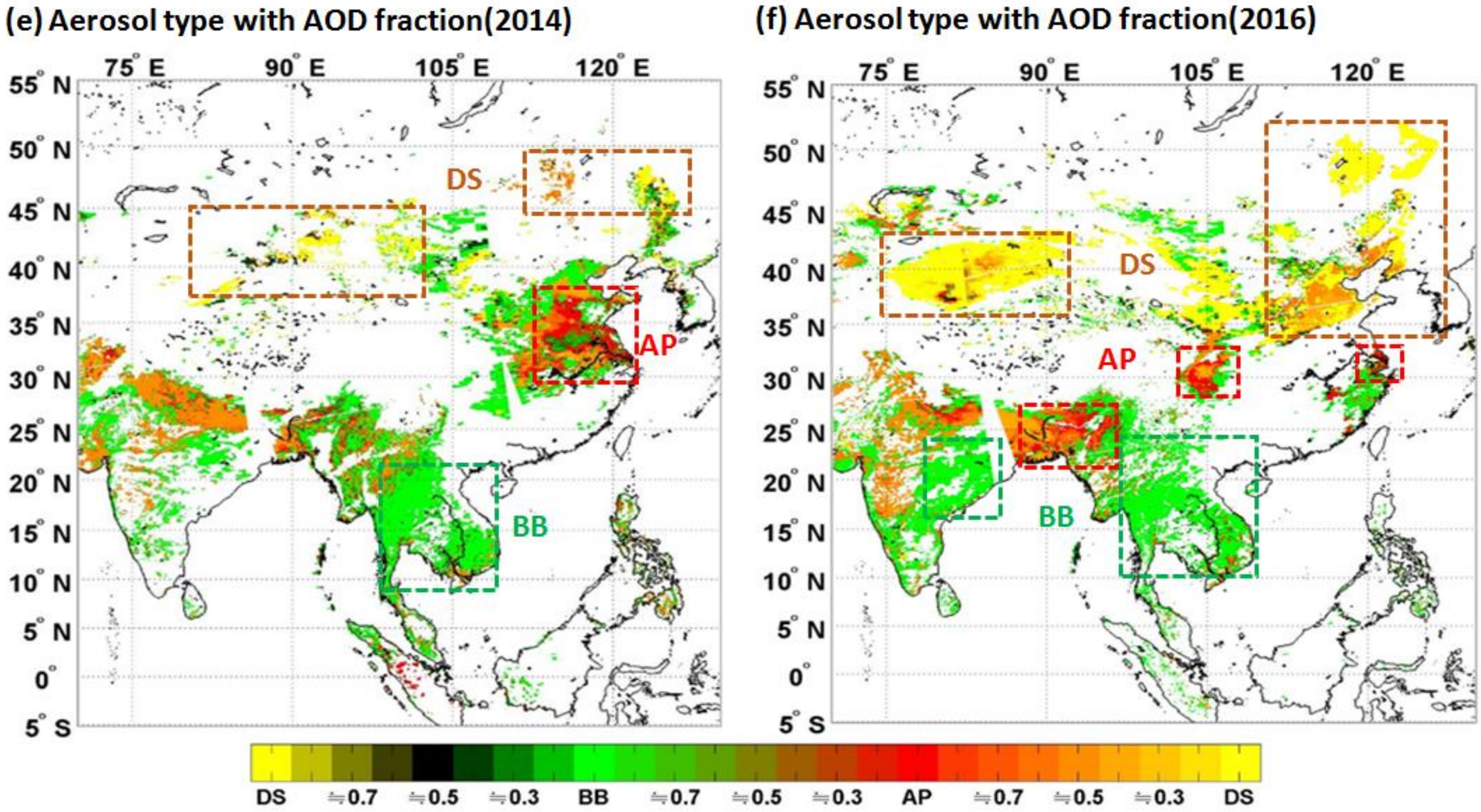
(e) Aerosol type with AOD fraction(2014)
(f) Aerosol type with AOD fraction(2016)
75° E
90° E
105° E
120° E
55° N
50° N
45° N
40° N
35° N
30° N
25° N
20° N
15° N
10° N
5° N
0°
5° S
DS
AP
BB
DS ≒0.7 ≒0.5 ≒0.3 BB ≒0.7 ≒0.5 ≒0.3 AP ≒0.7 ≒0.5 ≒0.3 DS

Validation of NGAI AOD fraction

$$f^{A}_{AOD_{CALIPSO}} = \frac{AOD^{A}_{CALIPSO}}{AOD^{A}_{CALIPSO} + AOD^{B}_{CALIPSO}}$$

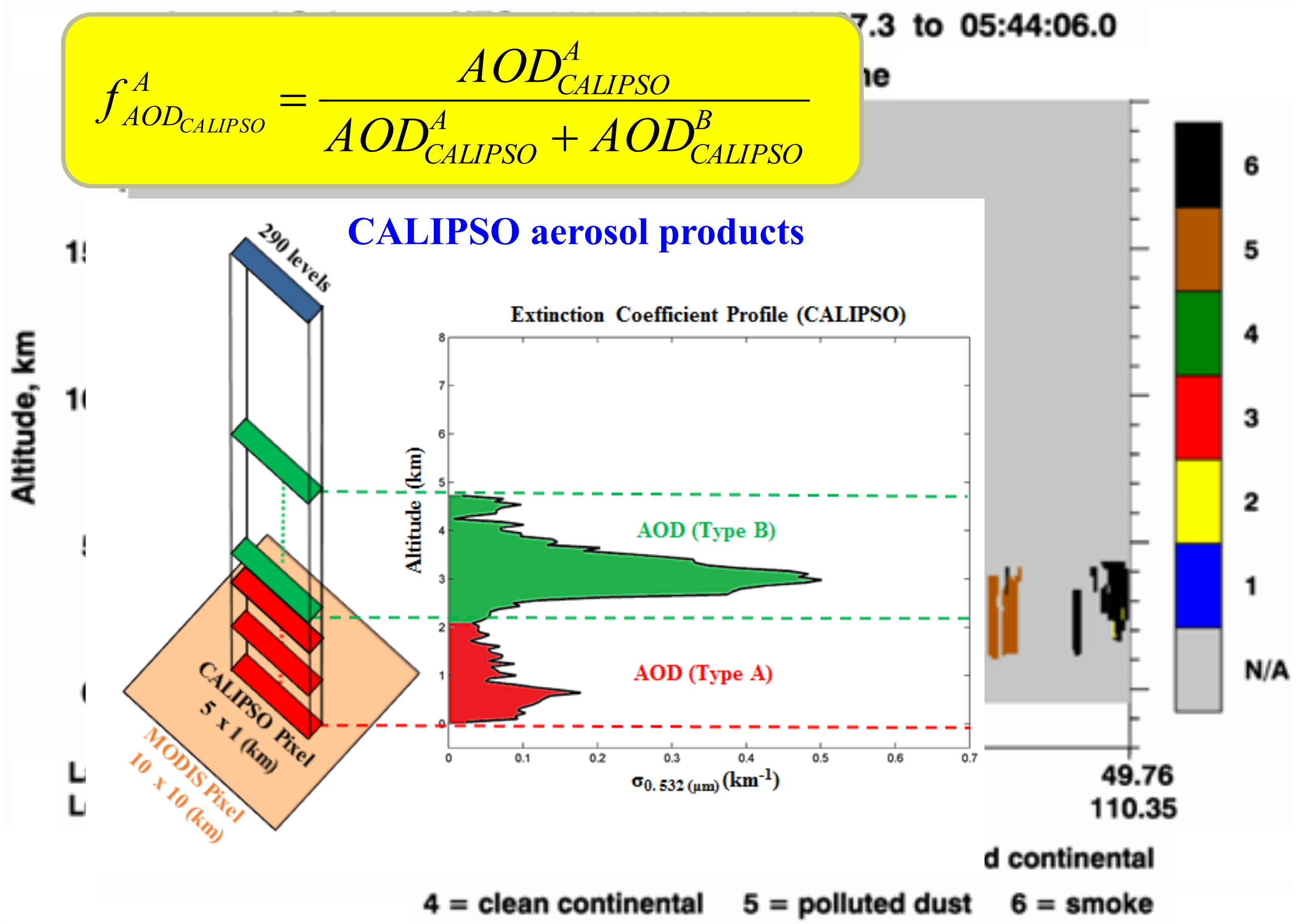

NDAI AOD Fraction Compared with CALIPSO

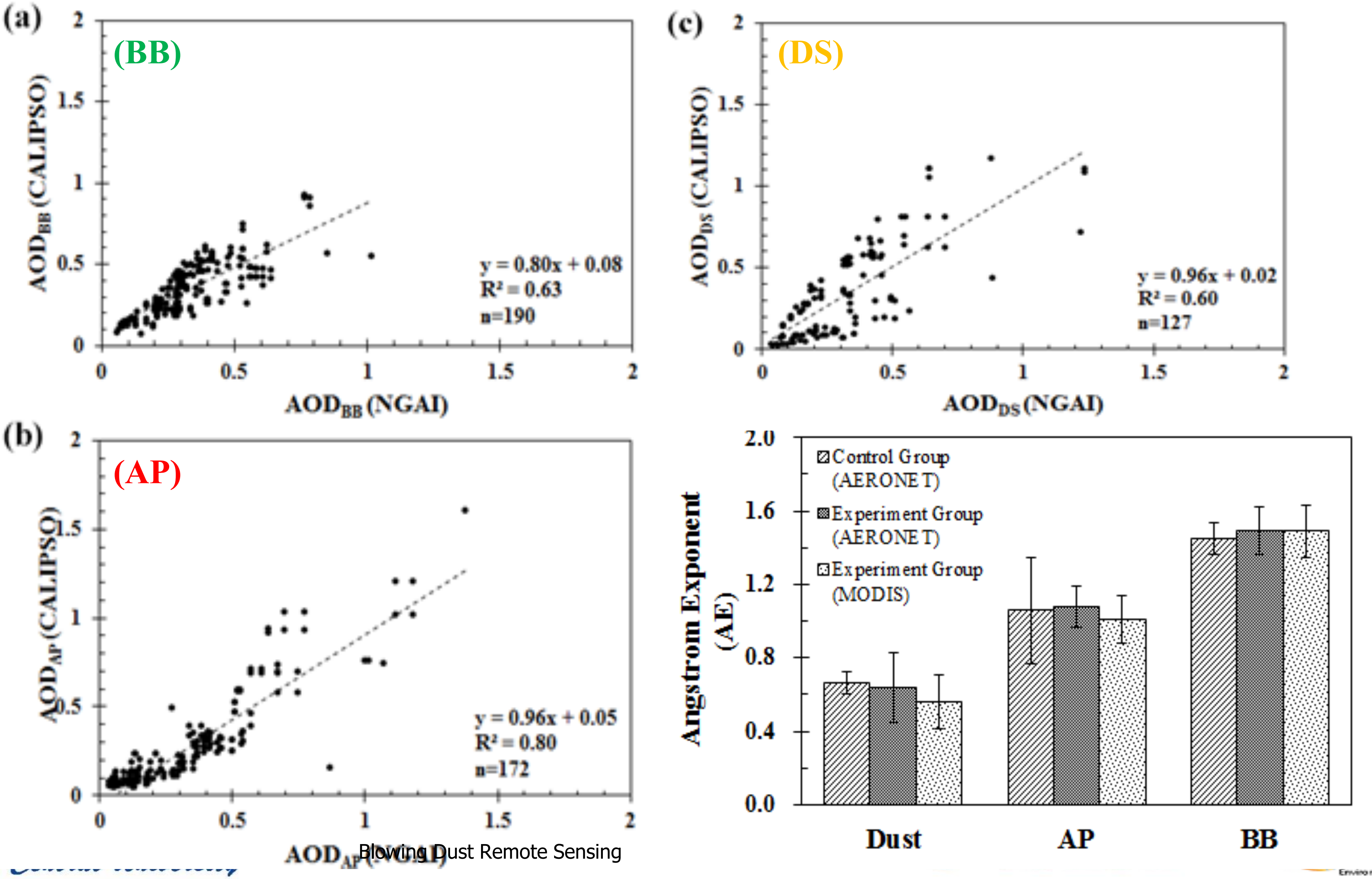

✓ Aerosol Profile Fitting_ Lognormal Dis.

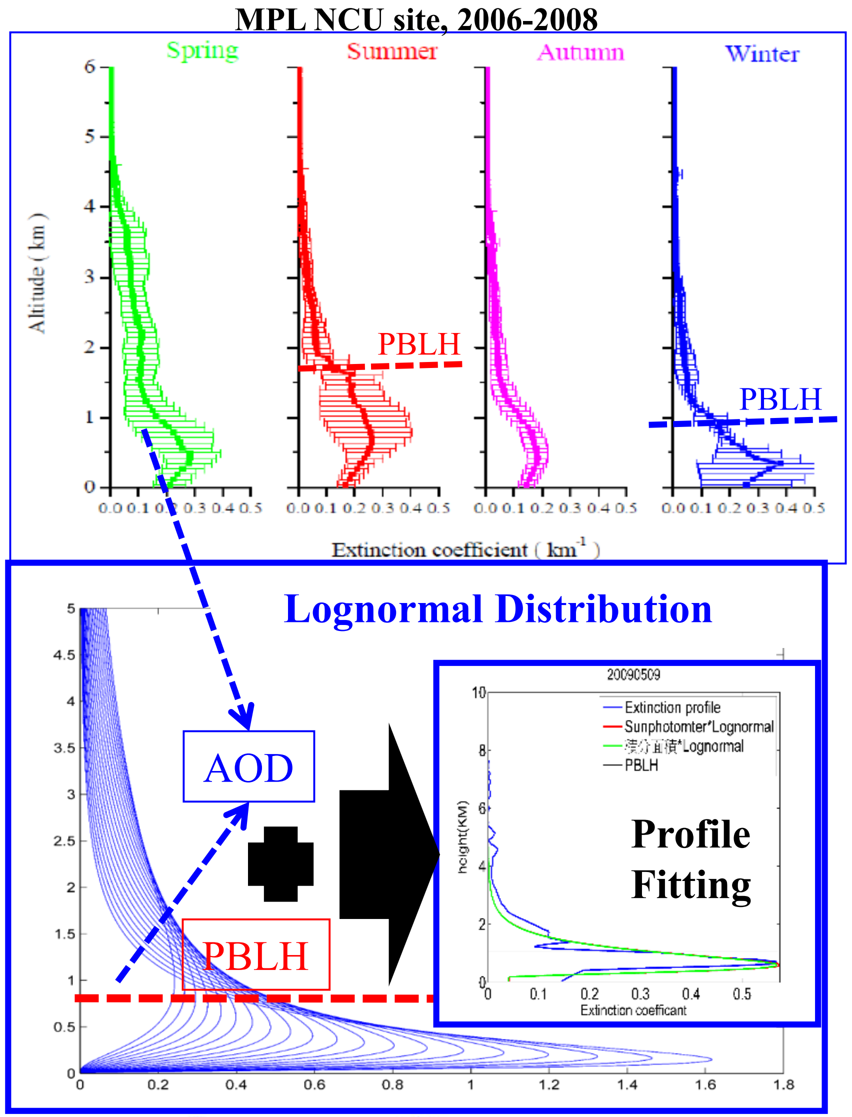

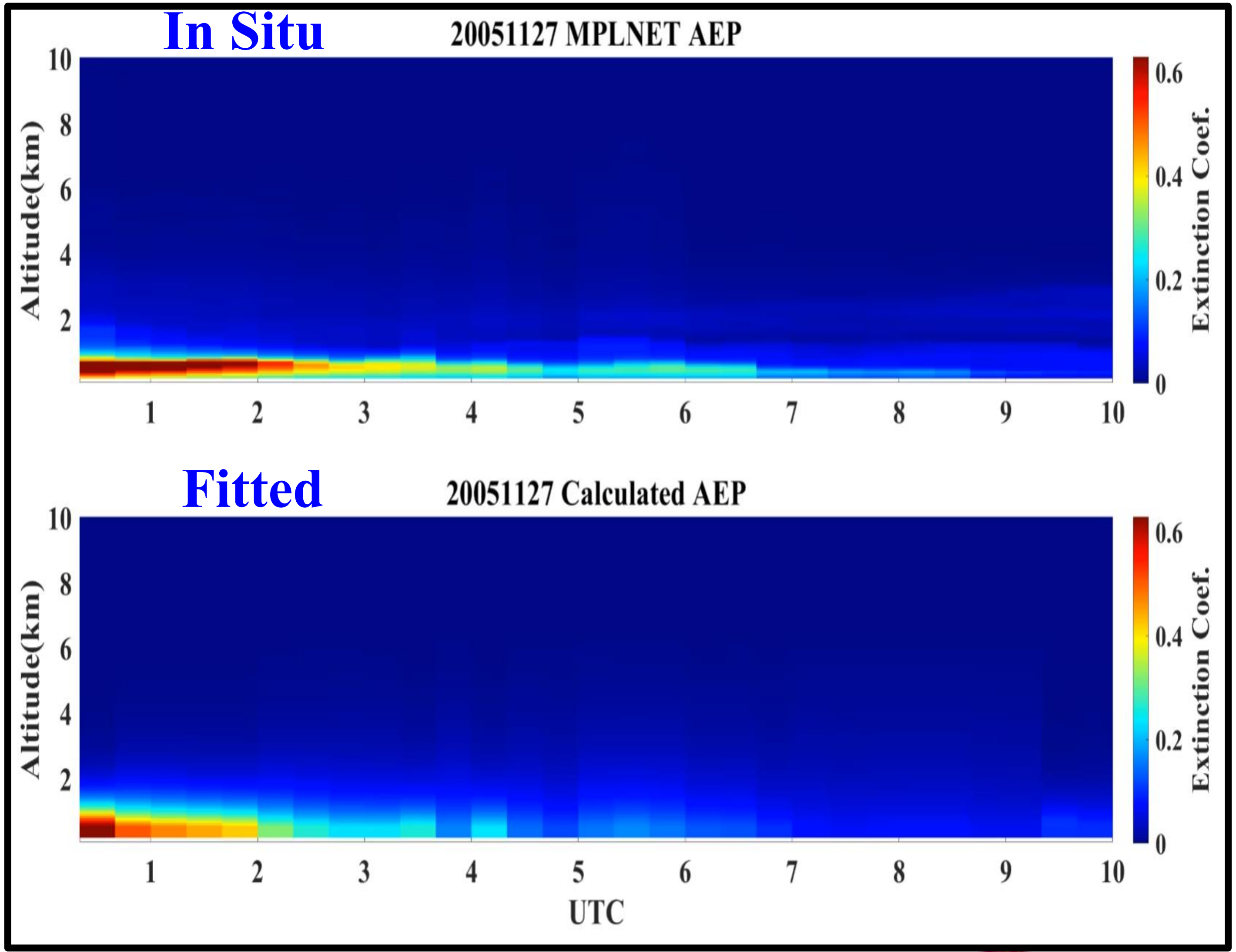

MPL NCU site, 2006-2008

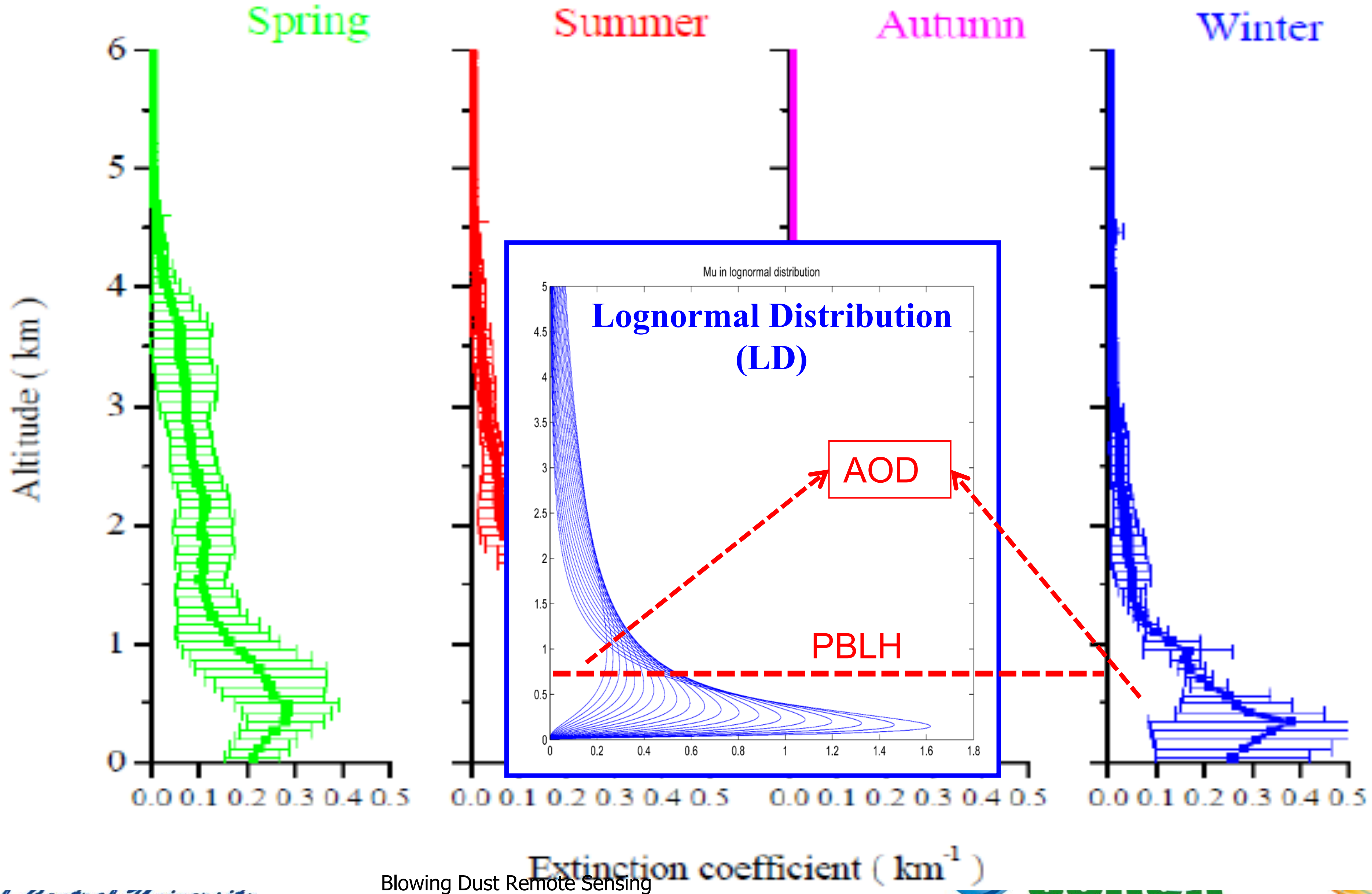

Fitting Test – Lognormal Distribution

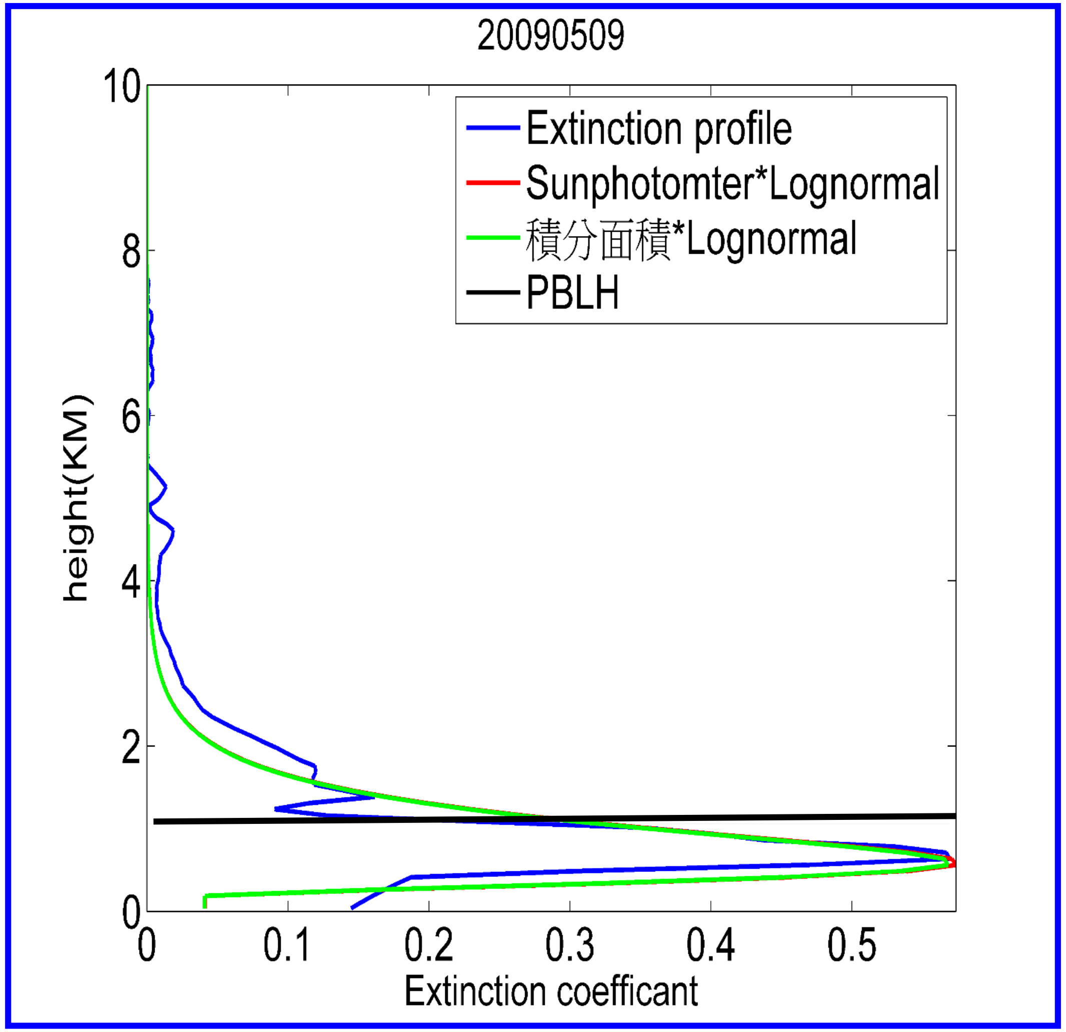

$$f(x\mid\mu,\sigma)=\frac{1}{x\sigma\sqrt{2\pi}}\exp\{\frac{-(\ln x-\mu)^2}{2\sigma^2}\}$$

DATE	20090509
Time(UTC)	129.94~129.98
Mean AOD	0.5392
Mean PBLH(km)	1.0639
μ	-0.2693
σ	0.57
R(2km)	0.8598
R(4km)	0.9252
R(10km)	0.9434
Area under profile	0.534
PBLH-Mode(km)	0.3

Fitting Model – σ and μ of LD (in terms of AOD & PBLH)

- **Profile with single peak from MPL & AERONET at NCU site, 2005~2014**

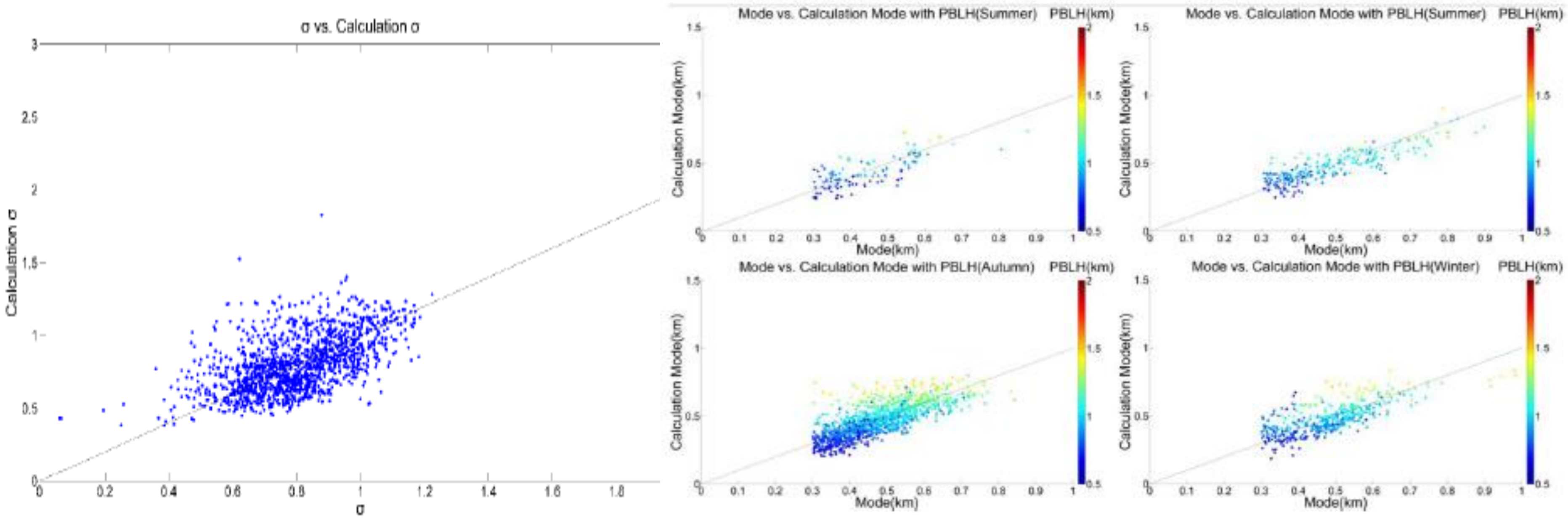

S=3.37	Mean error (%)	Standard deviation(km)	R^2	Case number
Spring	14.6527	0.1201	0.7657	109
Summer	11.7712	0.1516	0.8742	236
Autumn	13.5293	0.1069	0.7654	1139
Winter	14.2241	0.1238	0.7377	432

Results of Aerosol Profiles Fitting

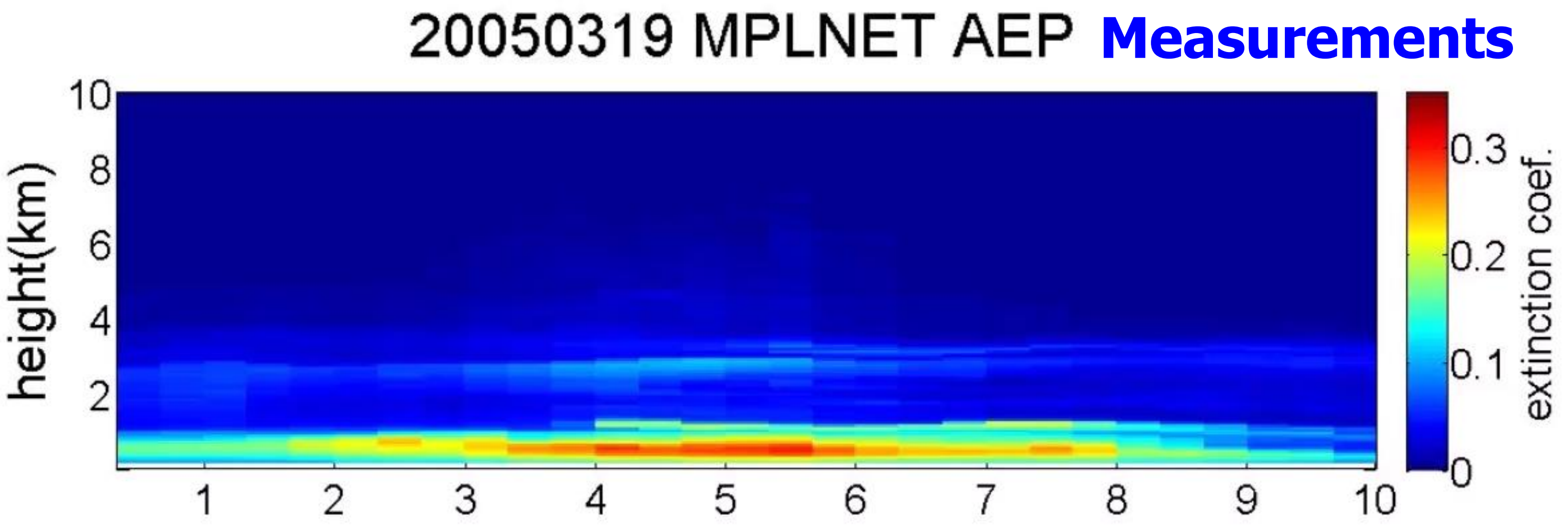

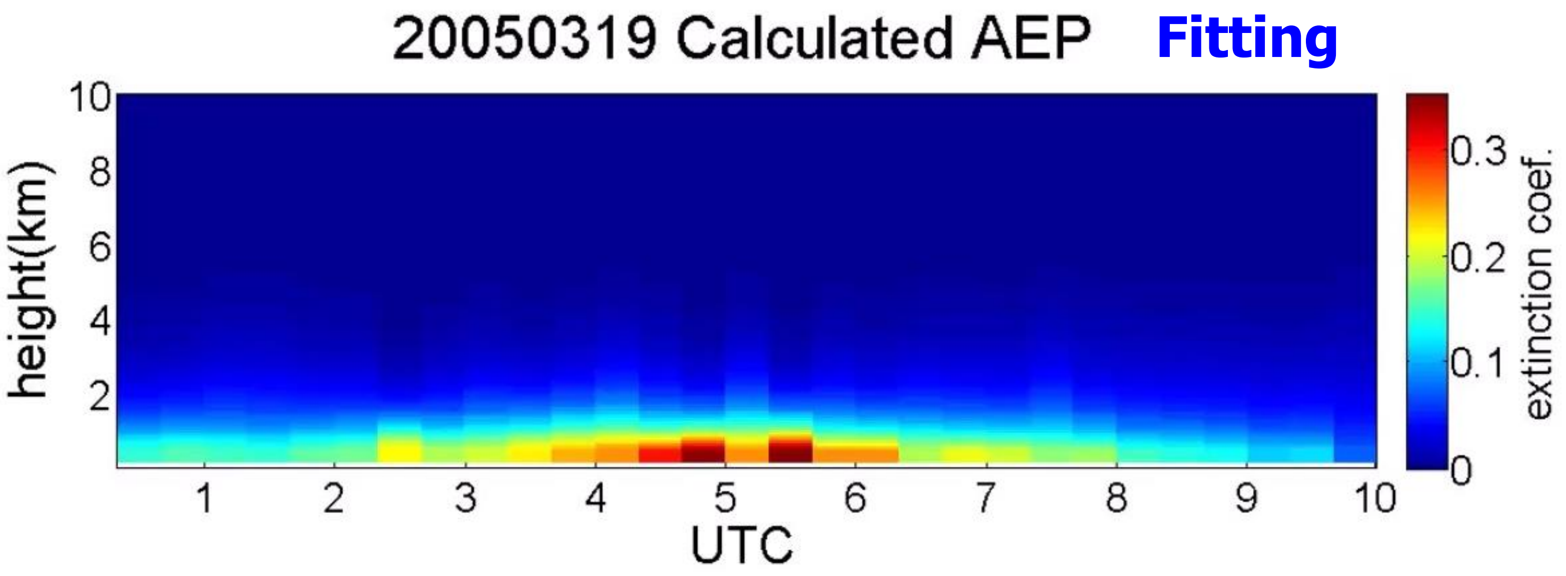

Case Study – MODIS AOD & GEOS-5 FP PBLH

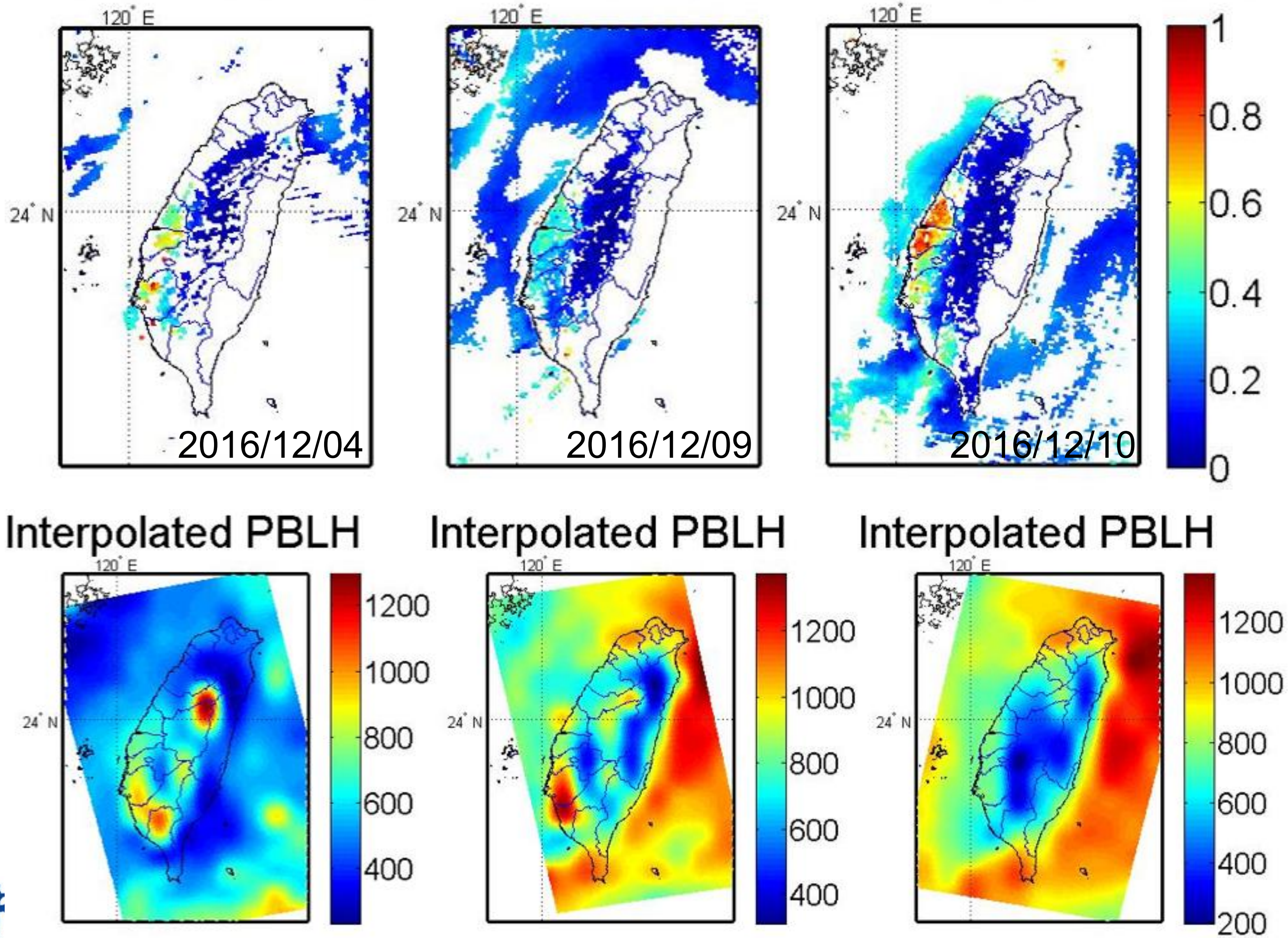

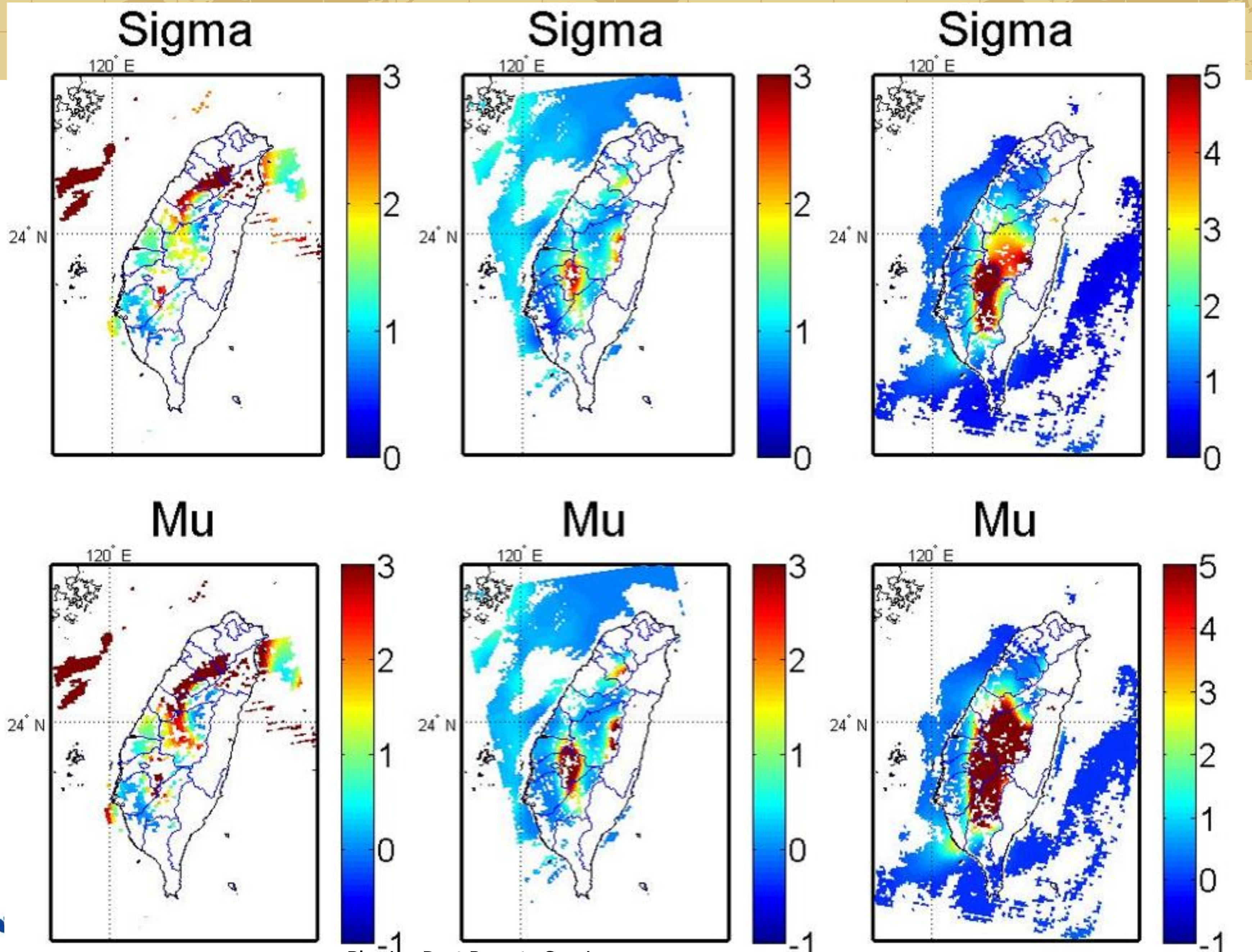
Sigma
120° E
24° N
3
2
1
0
Sigma
120° E
24° N
3
2
1
0
Sigma
120° E
24° N
5
4
3
2
1
0
Mu
120° E
24° N
3
2
1
0
-1
Mu
120° E
24° N
3
2
1
0
-1
Mu
120° E
24° N
5
4
3
2
1
0
-1

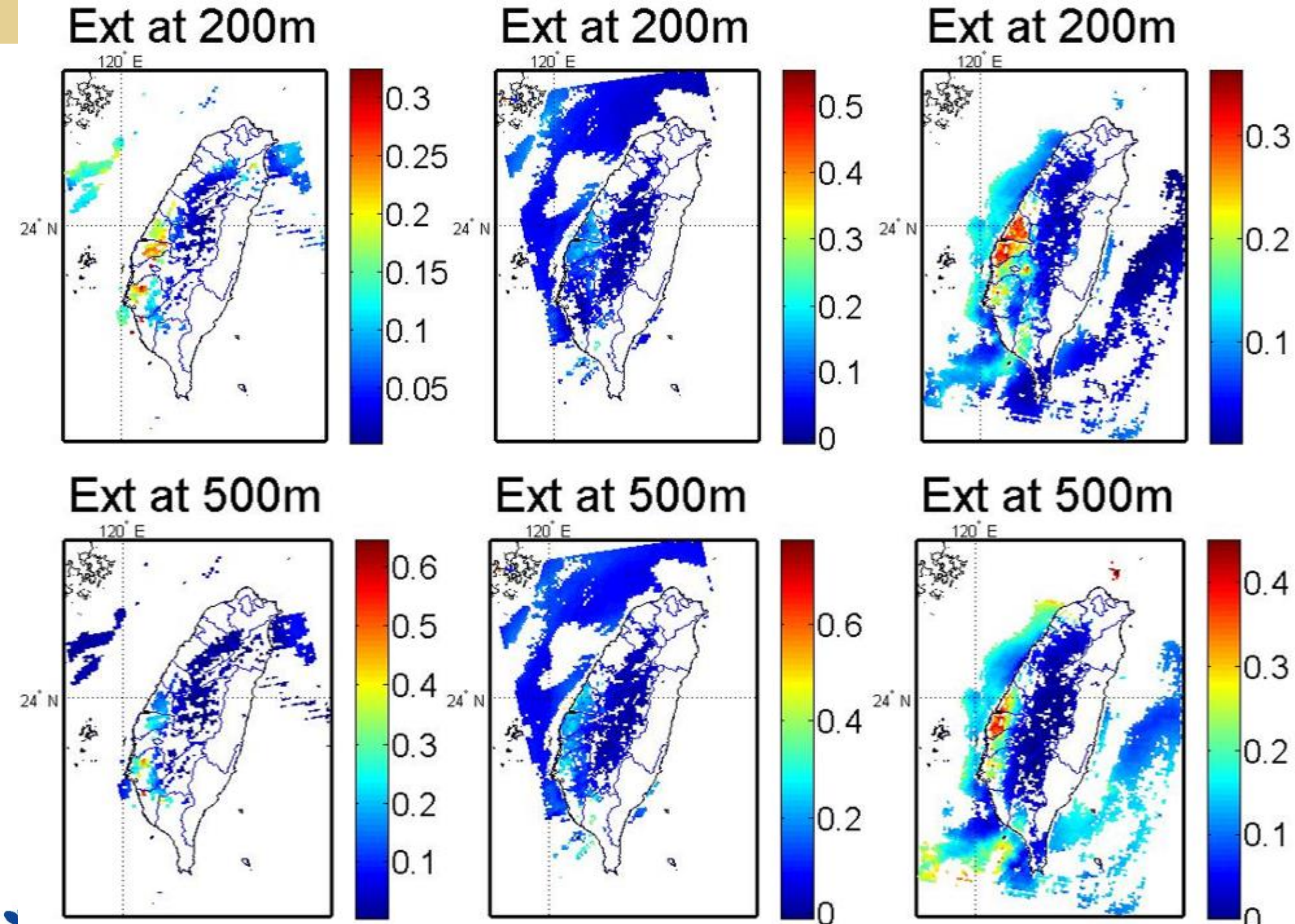
Ext at 200m
Ext at 200m
Ext at 200m
Ext at 500m
Ext at 500m
Ext at 500m
120° E
24° N

3D Extinction

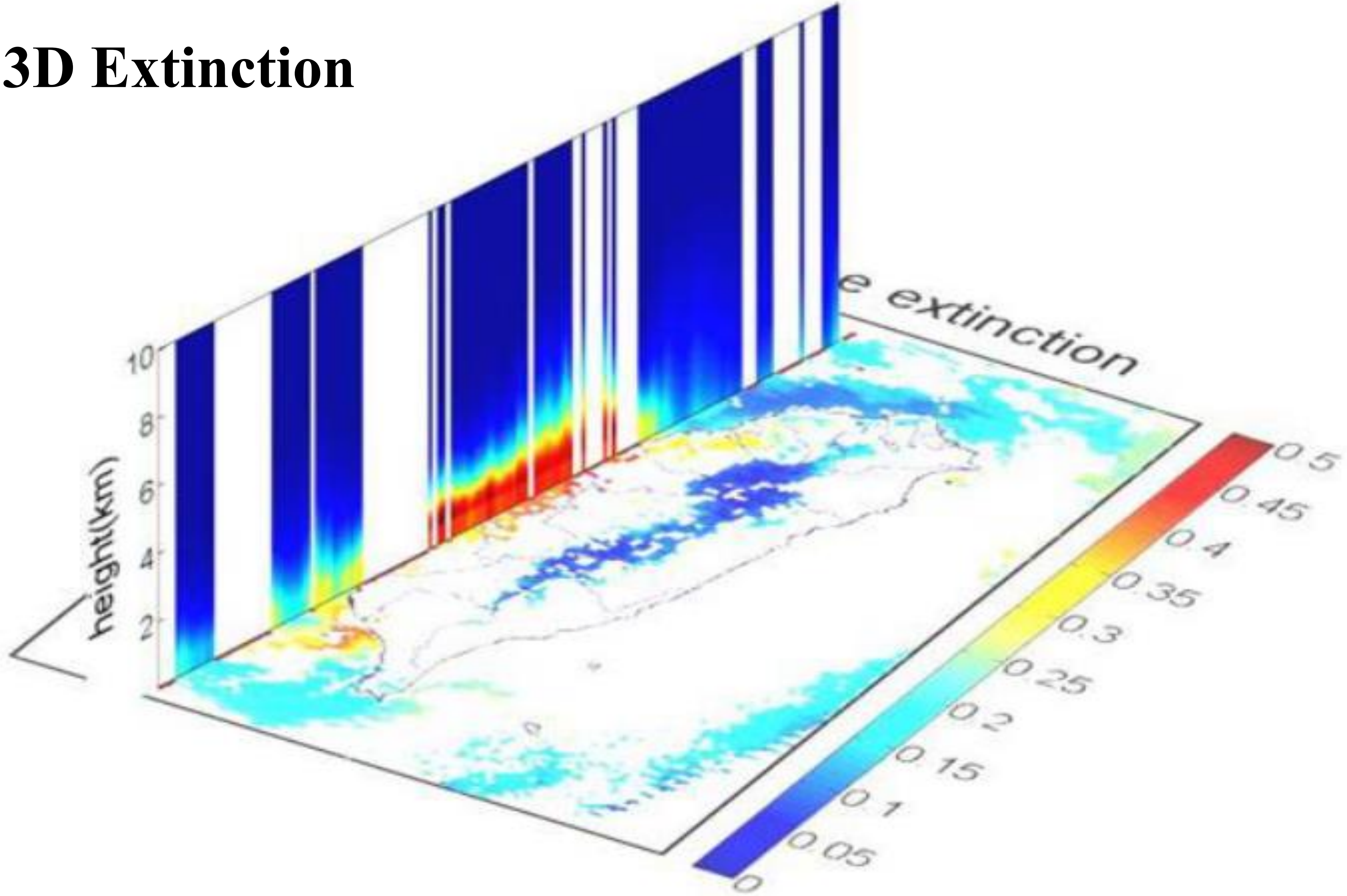

✓ Relationship between AOD & $PM_{2.5}$/ PM_{10}

AOD(440nm) & PM $_{2.5}$

Dust	Relationship	Correlation(R)
AOD & $PM_{2.5}$	$PM_{2.5}$=69.784xAOD+26.043	0.4677
AOD & $PM_{2.5}$	$PM_{2.5}$=35.625xAOD+11.656	0.5616
$\frac{AOD}{f(RH)}$ & $PM_{2.5}$	$PM_{2.5}=66.7\mathrm{x}\frac{AOD}{f(RH)}+7.0329$	0.6248
Anthropogenic Pollutant	Relationship	Correlation(R)
AOD & $PM_{2.5}$	$PM_{2.5}$=23.399xAOD+8.9975	0.6361
AOD & $PM_{2.5}$	$PM_{2.5}$=26.196xAOD+6.2632	0.6160
$\frac{AOD}{f(RH)}$ & $PM_{2.5}$	$PM_{2.5}=73.774\mathrm{x}\frac{AOD}{f(RH)}+10.032$	0.7540
Biomass Burning	Relationship	Correlation(R)
AOD & $PM_{2.5}$	$PM_{2.5}$=35.232xAOD+20.72	0.6727
AOD & $PM_{2.5}$	$PM_{2.5}$=35.84xAOD+11.904	0.7769
$\frac{AOD}{f(RH)}$ & $PM_{2.5}$	$PM_{2.5}=80.953\mathrm{x}\frac{AOD}{f(RH)}+8.4197$	0.8843

AERONET AOD Data

Location	Dates	Parameter	Aerosol type
AOE Baotou(41˚N,110˚E)	2014-2018	AOD (440,675,1020nm) AE (440-870nm)	Dust
Beijing (40˚N,116˚E)	2014-2018	AOD (440,675,1020nm) AE (440-870nm)	Dust
Taipei CWB(25˚N,122˚E)	2014-2018	AOD (440,675,1020nm) AE (440-870nm)	Anthropogenic Pollutants
Chiang Mai (19˚N, 99˚E)	2016-2017	AOD (440,675,1020nm) AE (440-870nm)	Biomass Burning

Data_ Ground based PM Concentration

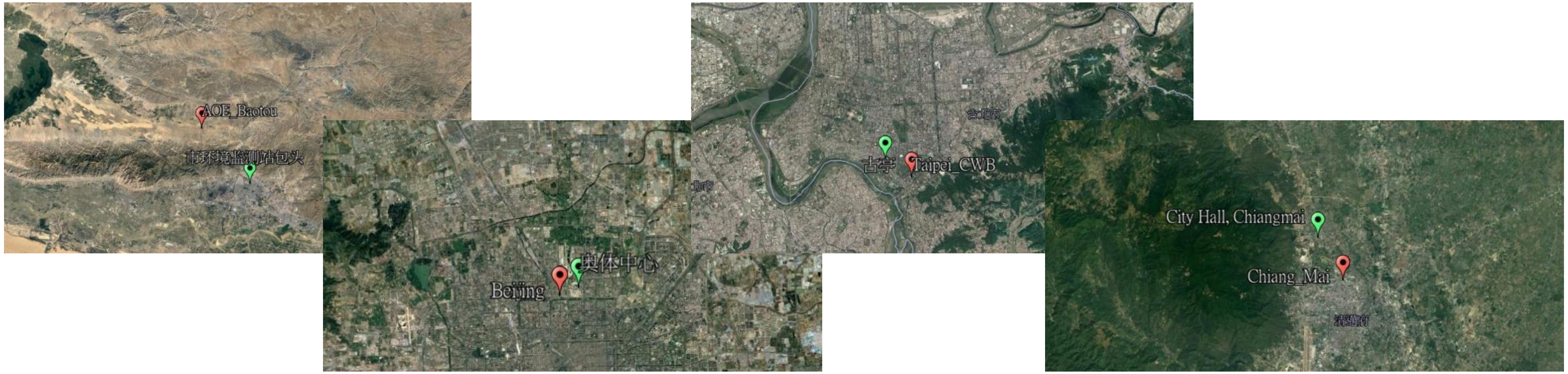

Station	Dates	Data	Corresponding AERONET station
Baotou (China)	2014-2018	PM2.5 / RH	AOE Baotou
Beijing (China)	2014-2018	$PM_{2.5}$ / RH	Beijing
Taipei (Taiwan)	2014-2018	PM2.5 / RH	Taipei CWB
Chiang Mai (Vietnam)	2016-2017	PM2.5 / RH	Chiang Mai

✓ 3-D $PM_{2.5}$ Construction & Near Surface Layer

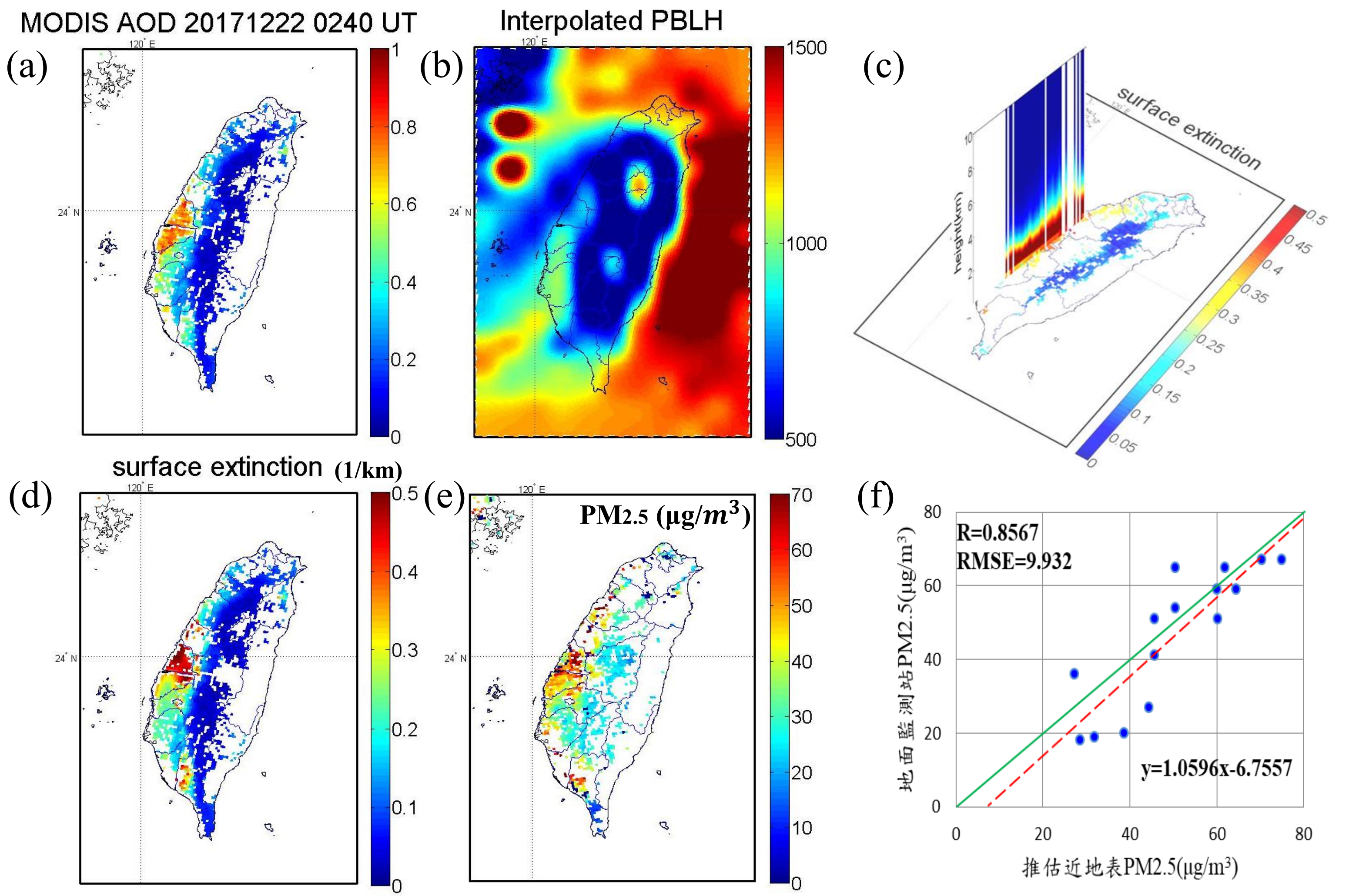

The application of proposed log-normal fitting method to the dataset on December 22, 2017, at 10:30 local time (LT).

✓ High Temporal Resolution Monitor_ Goestationary Satellite

Himawari-8	GOES-16
AHI (Advanced Himawari Imager)	*ABI (Advanced Baseline Imager)*

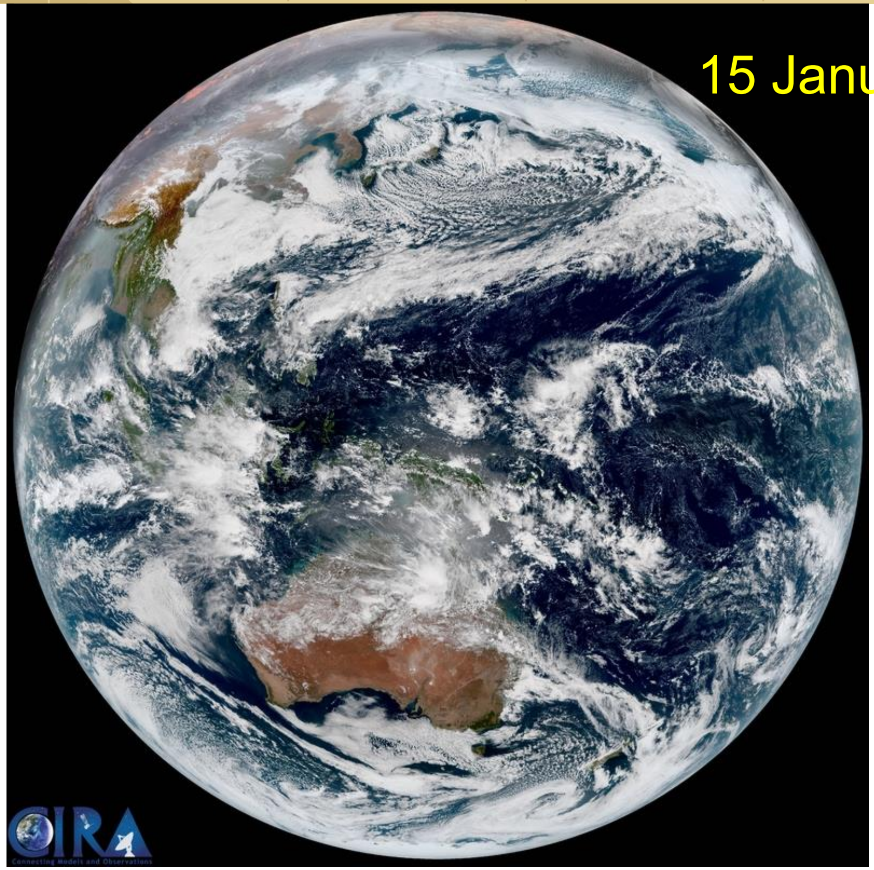

15 January 2017

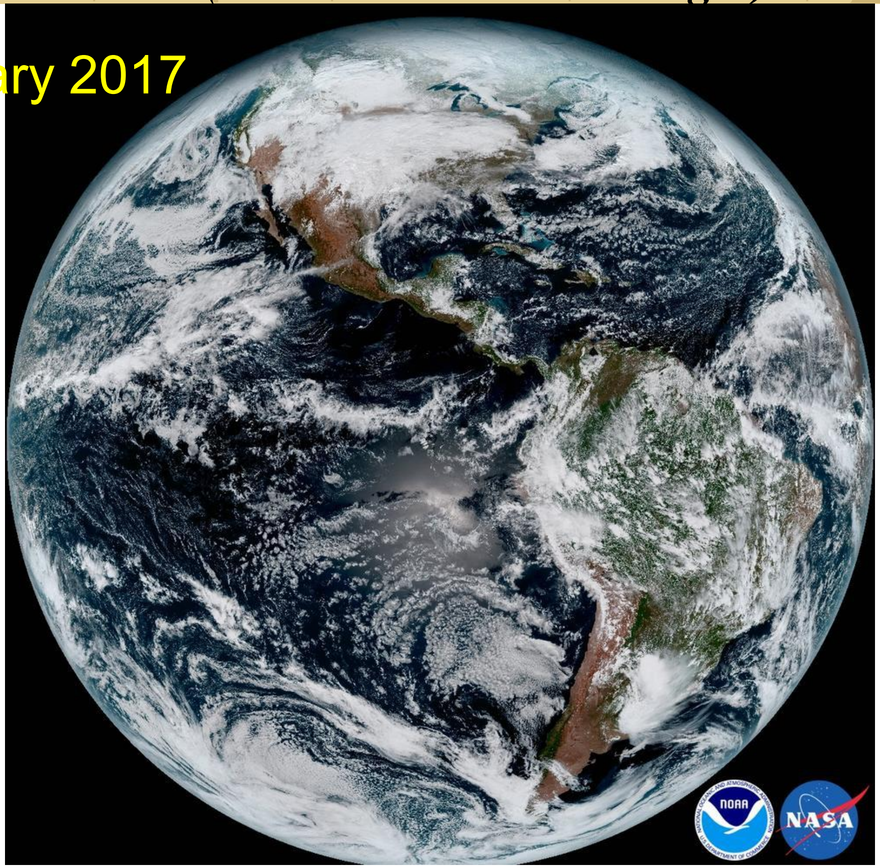

	Himawari-8	GOES-16
Distance:	35,800 km	22,300 mile (35,890 km)
Spectral (μm):	16- 0.46, <u>0.51</u>, 0.64, 0.86, 1.6, 2.3, 3.9, 6.2, 7.0, 7.3, 8.6, 9.6, 10.4, 11.2, 12.3, 13.3	16- 0.47, 0.64, 0.87, <u>1.38</u>, 1.6, 2.3, 3.9, 6.2, 7.0, 7.3, 8.5, 9.6, 10.4, 11.2, 12.3, 13.3
Temporal:	10 min. (or 2.5 min., Japan)	15 min. (or 5 min., ConU.S.)
Spatial:	0.5 – 2 km	0.5 – 2 km

國立中央大學
National Central University

CSRSR

ERSL
Environmental Remote Sensing Laboratory

Every 10 minutes

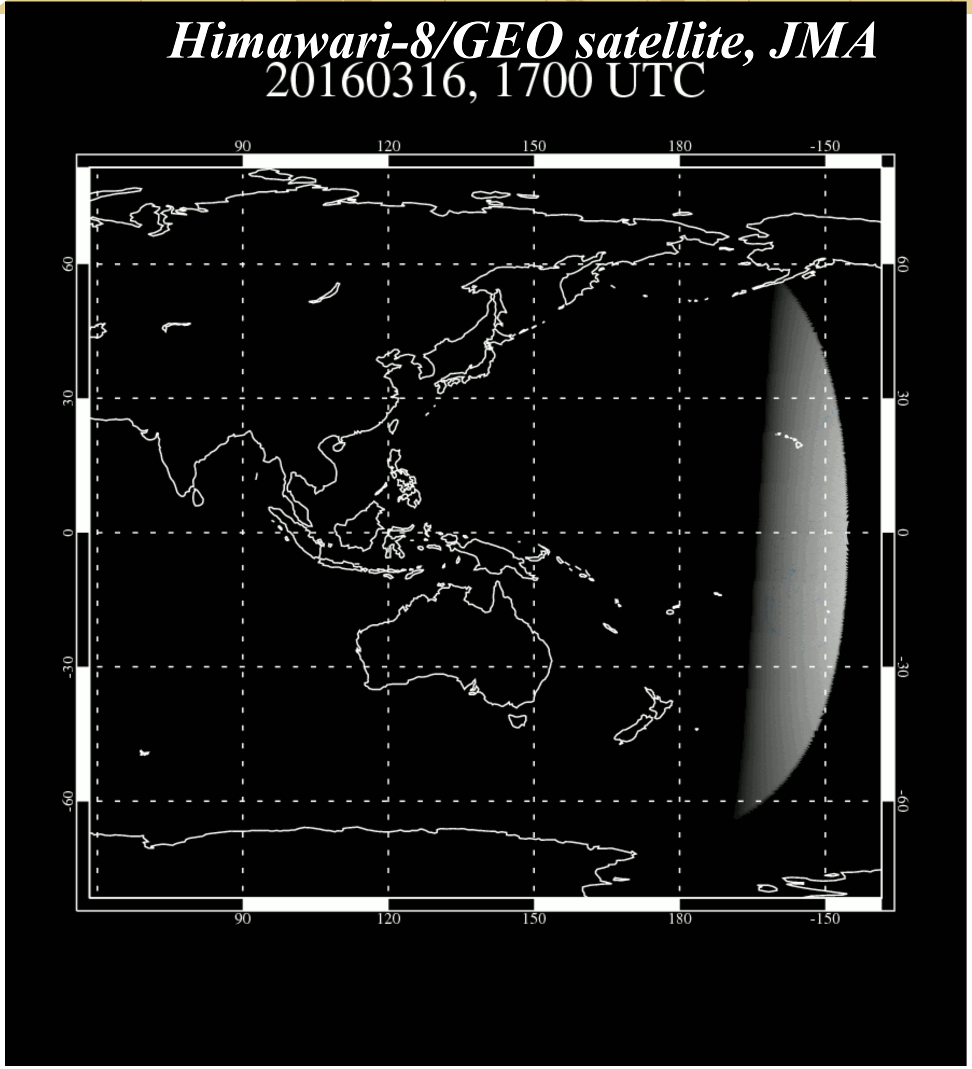

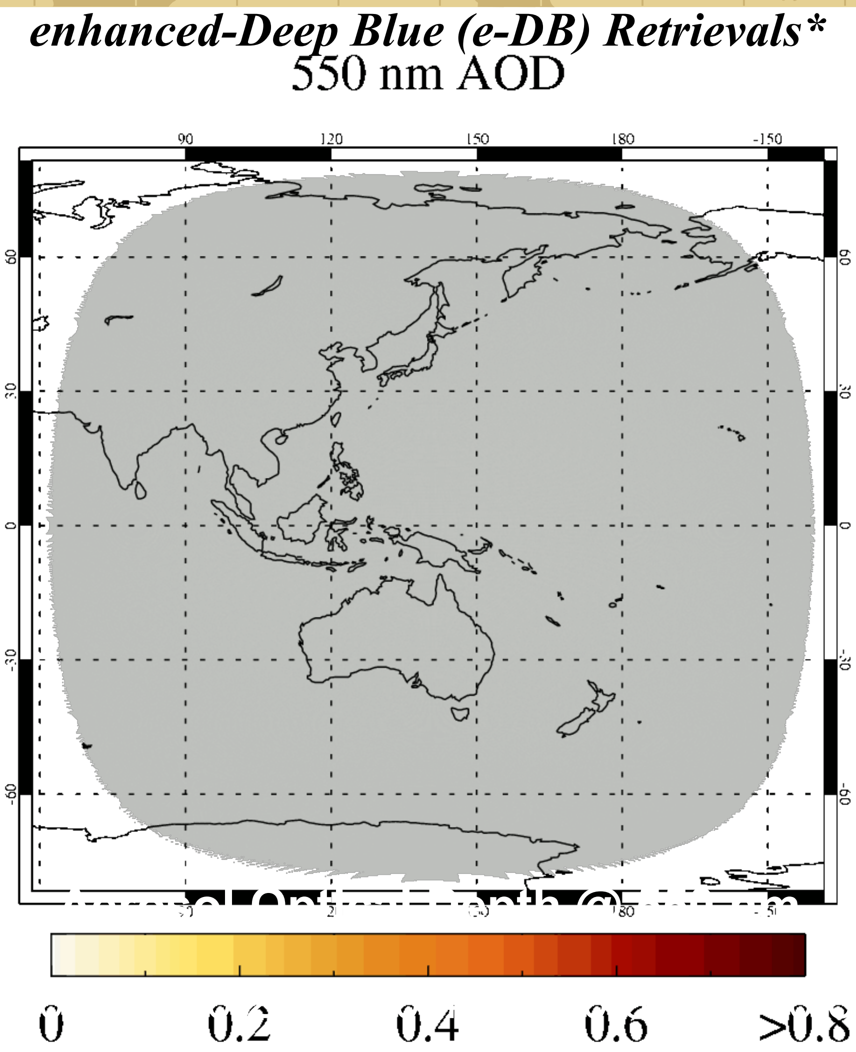

* Hsu, N.C., Jeong, M.-J., Bettenhausen, C., Sayer, A.M., Hansell, R.A., Seftor, C.S., Huang, J., Tsay, S.-C., 2013. Enhanced Deep Blue aerosol retrieval algorithm: The second generation, J. Geophys. Res., 118, 9,296–9,315, doi:10.1002/jgrd.50712.

✓ High Spatiotemporal Resolution Monitor_ Image Fusion

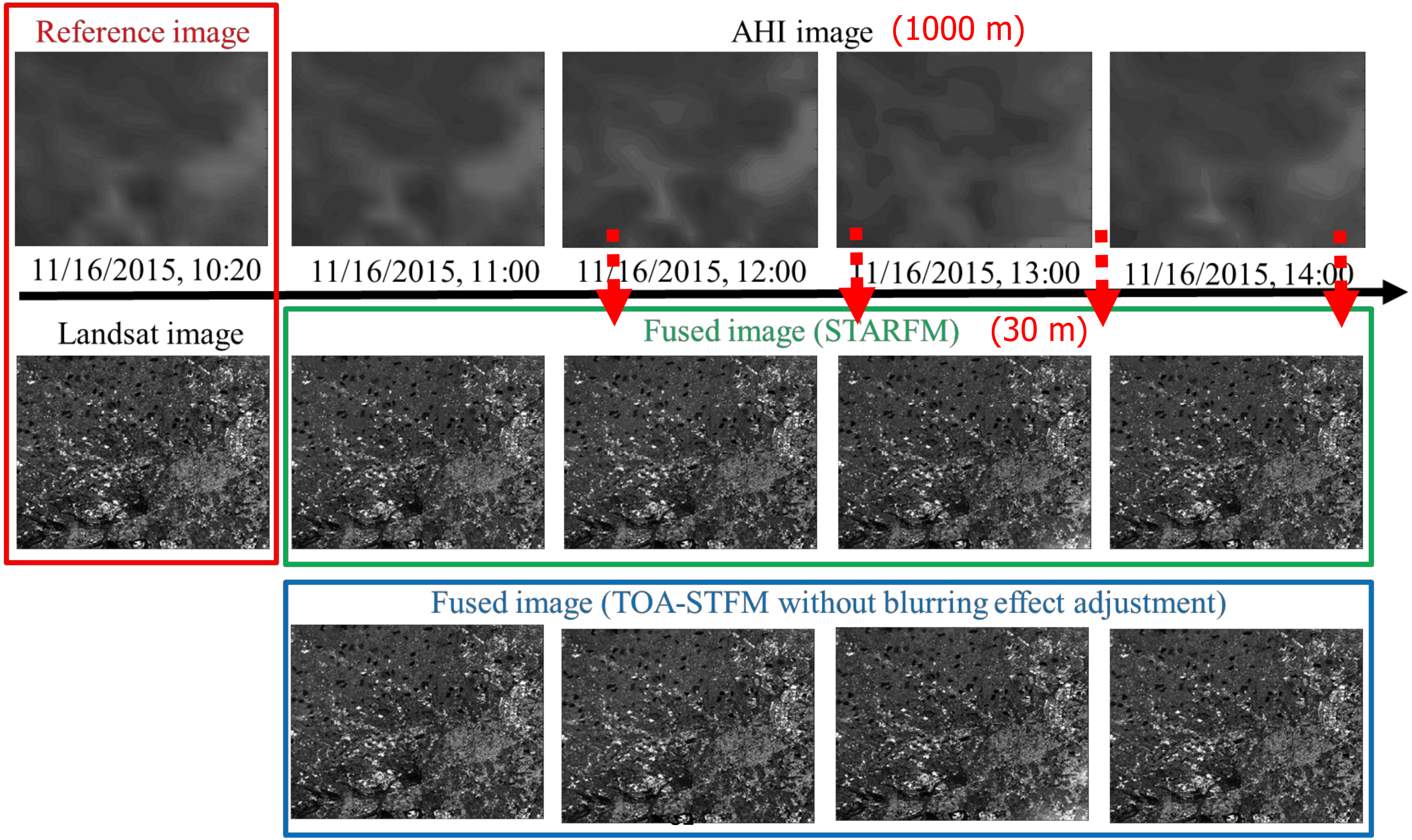

Case Study_ Boimass Burning

H-8 AOD 0220 ~ 0550 UTC 2017.03.04

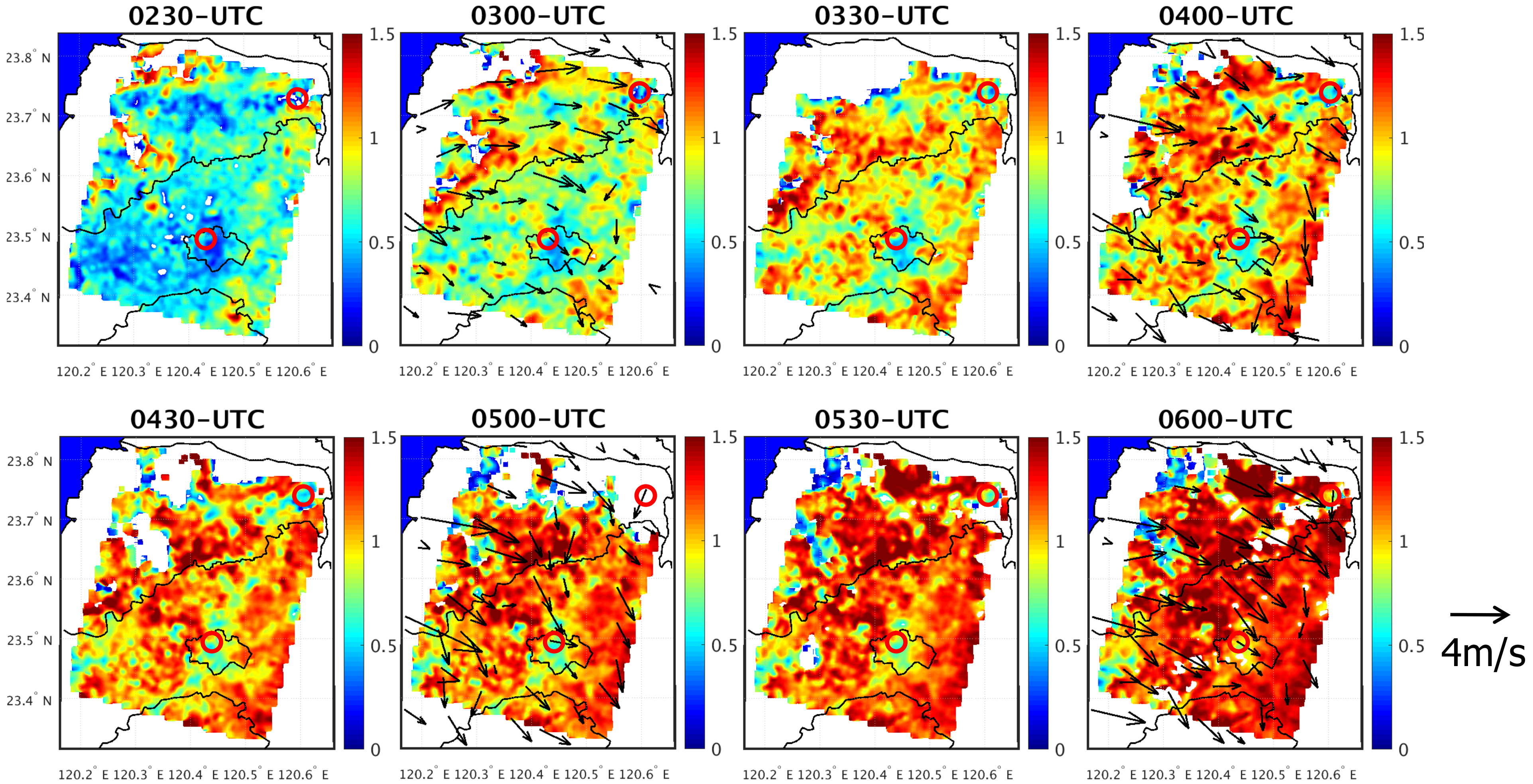

Validate with AERONET AOD

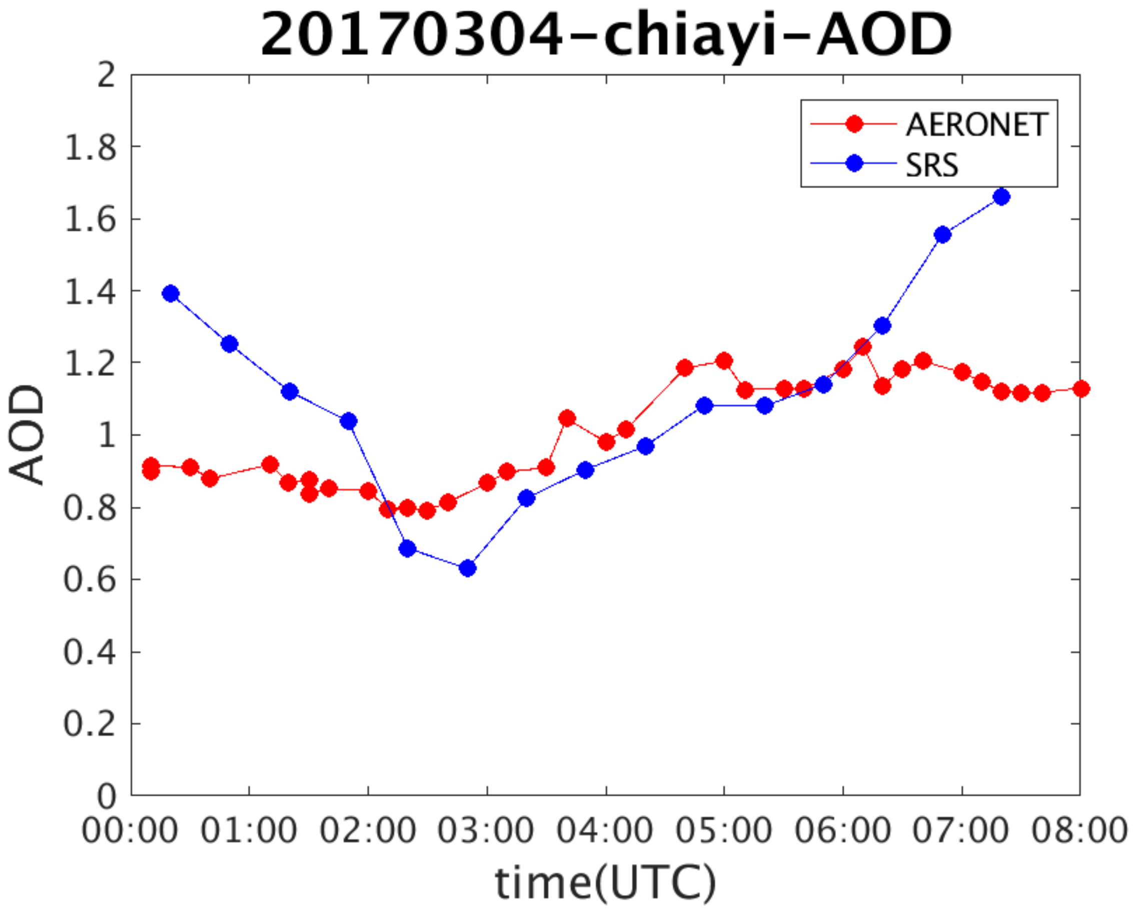

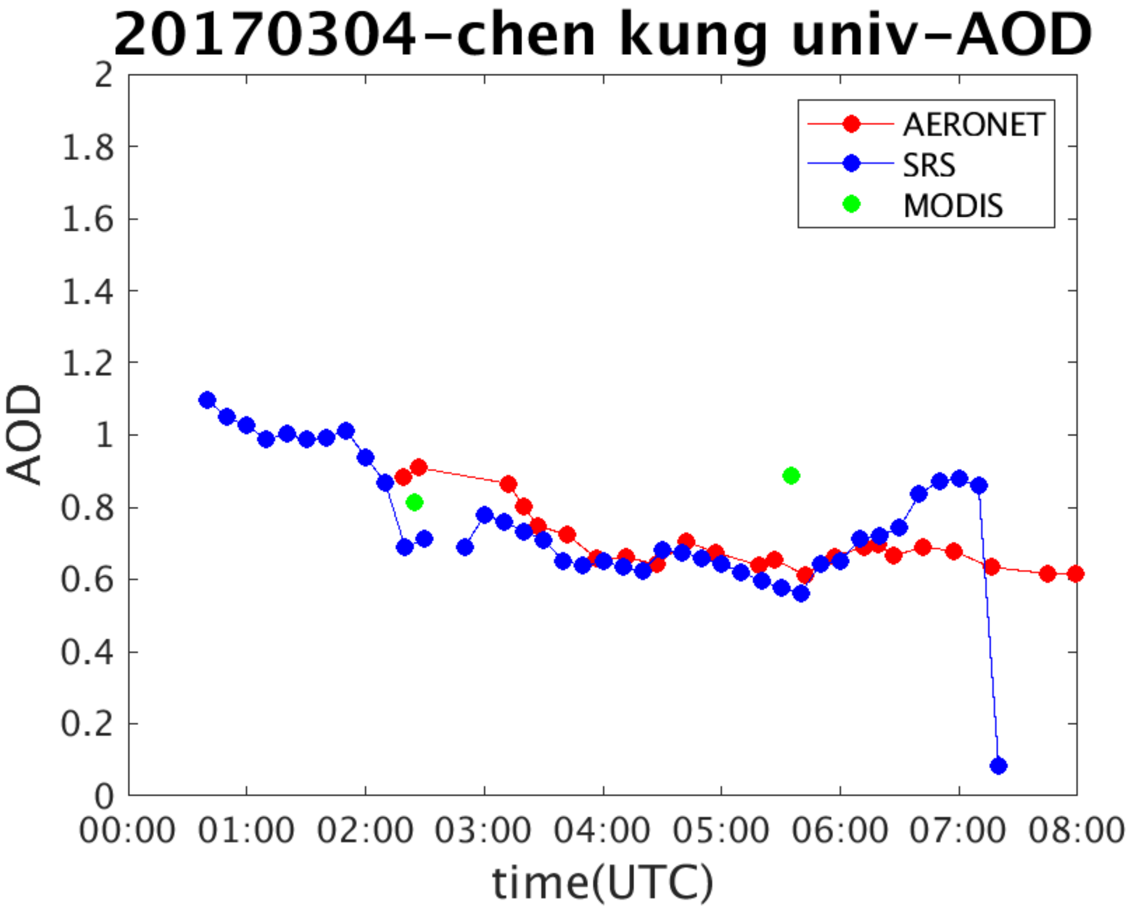

Open Fire Detection and Monitoring

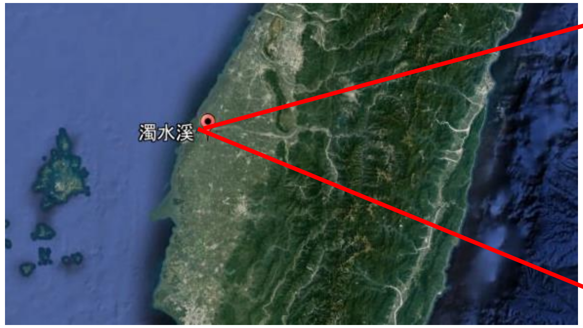

- 22:00 (LCT), 2020.10.18 ~ 18:00 (LCT), 2020.10.19

0800 AOD

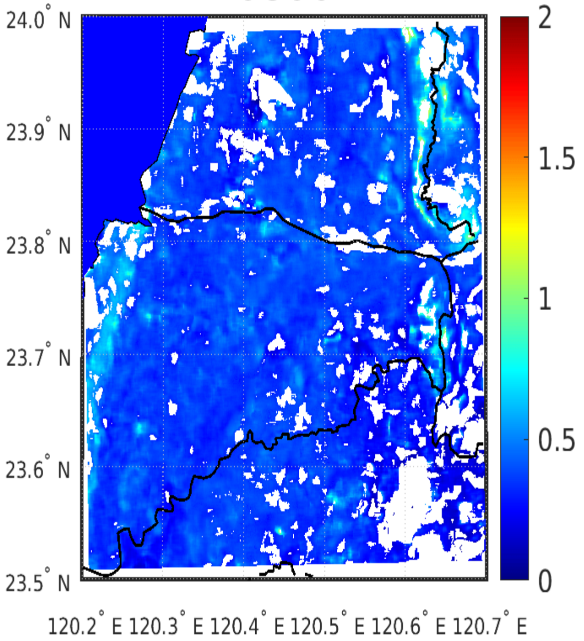

0800 Aerosol Type

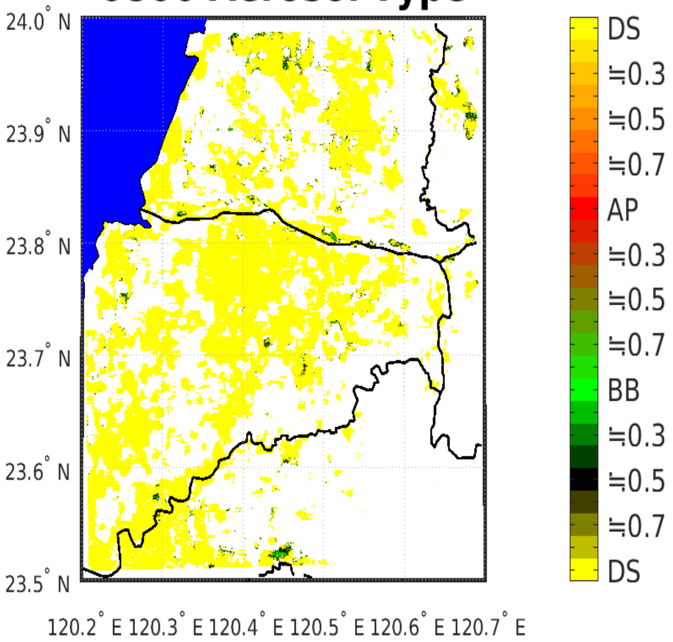

（綠色為生質燃燒，主要為黑炭）

0800 PM2.5

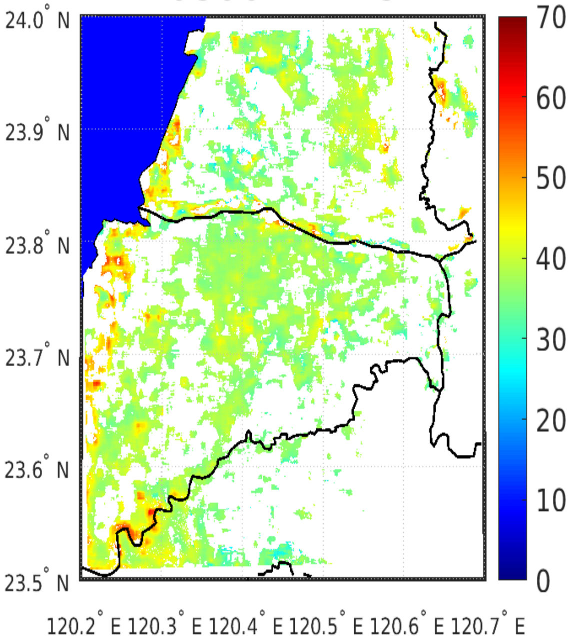

國立中央大學
National Central University

CSRSR

ERSL

✓ Blowing Dust - 2021/01/16

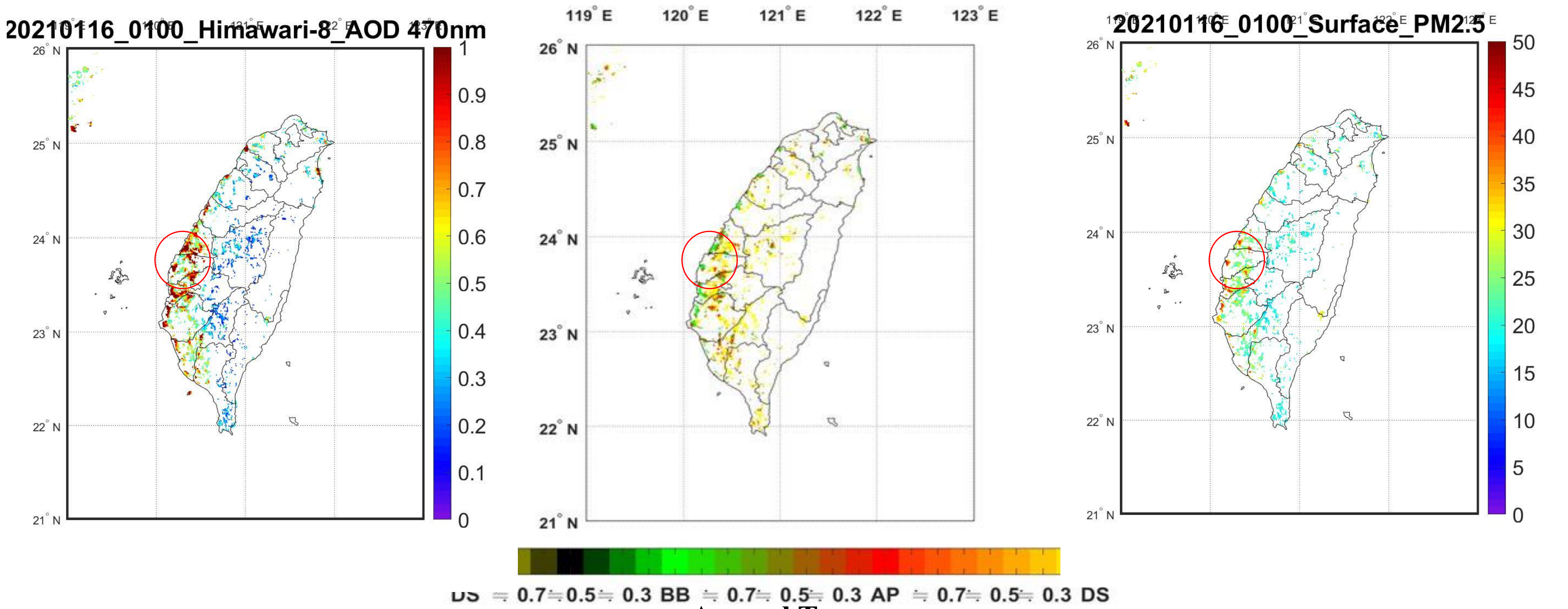

Aerosol Type

✓ Blowing Dust - 2021/02/18

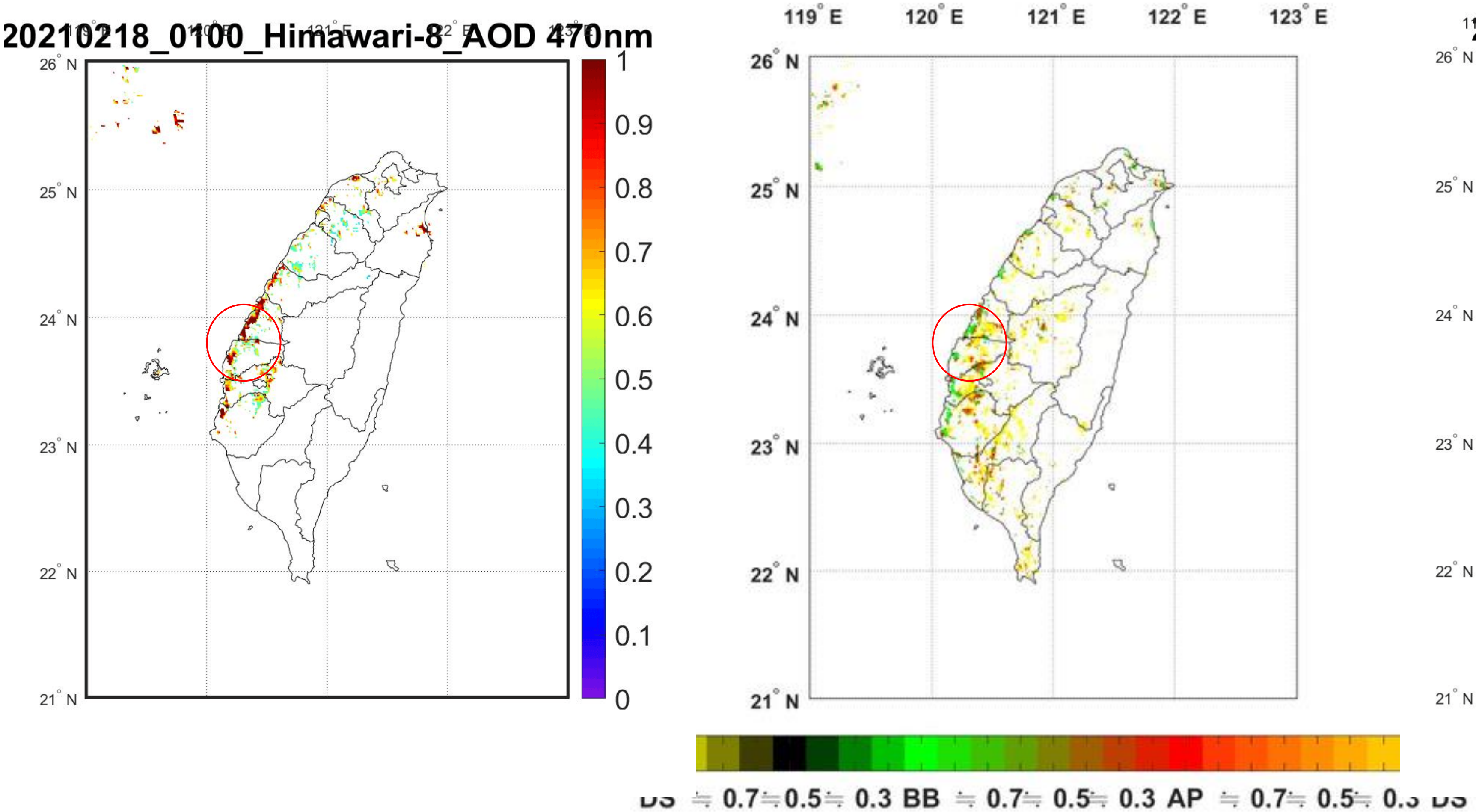

Aerosol Type

✓ Relationship between AOD & PM_{10}

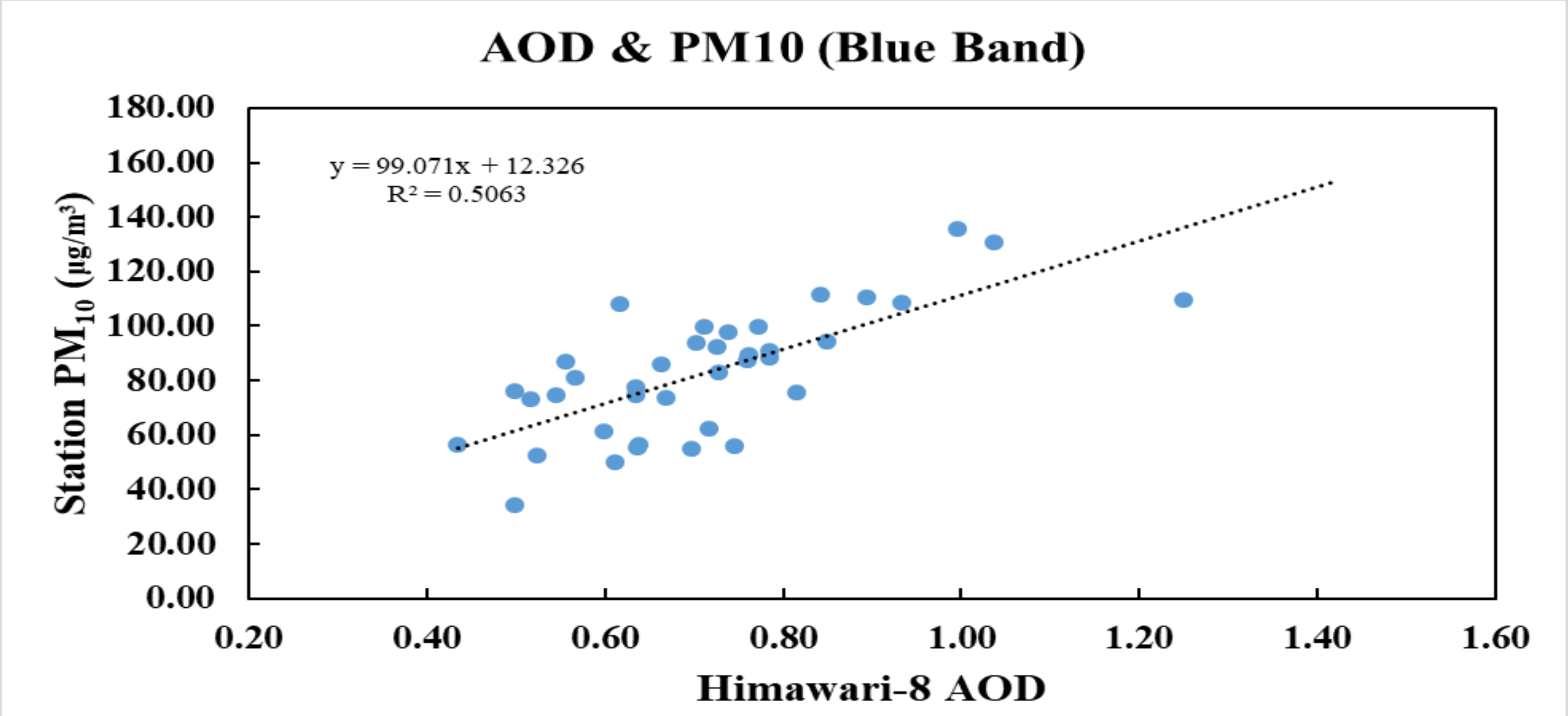

Dust	Relationship	Correlation(R)
AOD_{455nm} & PM_{10}	PM_{10}=99.071xAOD+12.326	0.71
AOD_{510nm} & $PM_{2.5}$	PM_{10}=123.31xAOD+20.082	0.65
AOD_{645nm} & $PM_{2.5}$	PM_{10}=87.441xAOD+34.208	0.43

✓ Discussions

- By considering aerosol type, vertical distribution and water effect, the relationship between AOD & PM would be improved with satellite observations
- The performance of $PM_{2.5}$ retrieval near surface could be reached 0.82 in correlation coefficient compared to in situ measurements
- The results of case studies indicate that high spatiotemporal fused image provides **significant potential for the blowing dust (PM_{10}) detection and monitor in near real-time, and further application to operational**

References

- **Tang-Huang Lin***, Si-Chee Tsay, Wei-Hung Lien, Neng-Huei Lin and Ta-Chih Hsiao, 2021, Spectral derivatives of optical depth for partitioning aerosol type and loading, ***Remote Sensing***, **13(8)**, 1544, https://doi.org/10.3390/rs13081544

- **Tang-Huang Lin***, Kuo-En Chang, Hai-Po Chan, Ta-Chih Hsiao, Neng-Huei Lin , Ming-Tung Chuang and Hung-Yi Yeh, 2020, Potential Approach for Single-Peak Extinction Fitting of Aerosol Profiles Based on In Situ Measurements for the Improvement of Surface $PM_{2.5}$ Retrieval from the Satellite AOD Product, ***Remote Sensing***, **12**, 2174, https://doi.org/10.3390/rs12132174.

- Chih-Yuan Huang, Hsuan-Chi Ho, **Tang-Huang Lin***, 2018, Improving the image fusion procedure for high spatiotemporal aerosol optical depth retrieval: a case study of urban area in Taiwan, ***Journal of Applied Remote Sensing***, 12(4), 042605 (4 September 2018), https://doi.org/10.1117/1.JRS.12.042605.

Thanks for your attention!